

This dissertation has been 62-1751
microfilmed exactly as received

FLEMING, James Replogle, 1934-
AN INVESTIGATION OF THE EFFECT OF HORIZONTAL BARRIERS IN A THERMOGRAVITATIONAL LIQUID THERMAL DIFFUSION COLUMN.

The University of Oklahoma, Ph.D., 1962
Engineering, chemical

University Microfilms, Inc., Ann Arbor, Michigan

THE UNIVERSITY OF OKLAHOMA

GRADUATE COLLEGE

AN INVESTIGATION OF THE EFFECT OF HORIZONTAL BARRIERS IN
A THERMOGRAVITATIONAL LIQUID THERMAL DIFFUSION COLUMN

A DISSERTATION

SUBMITTED TO THE GRADUATE FACULTY

in partial fulfillment of the requirements for the

degree of

DOCTOR OF PHILOSOPHY

BY

JAMES REPLOGLE FLEMING

Norman, Oklahoma

1961

AN INVESTIGATION OF THE EFFECT OF HORIZONTAL BARRIERS IN
A THERMOGRAVITATIONAL LIQUID THERMAL DIFFUSION COLUMN

APPROVED BY

John E. Powers

~~R. L. H. ...~~

Eric Weger

Bernard C. Heston

J. R. ...

DISSERTATION COMMITTEE

ACKNOWLEDGMENT

Although many individuals at the University of Oklahoma contributed to the completion of this investigation, the author wishes to express his especial appreciation to Dr. John E. Powers, who acted as research director throughout the work. His suggestions were most helpful as were the advice and criticism of the other members of the Chemical Engineering Staff.

The author is also particularly indebted to Mr. Frank Maginnis of the Research Instrument Company, Norman, Oklahoma. Mr. Maginnis gave freely of his time during equipment modifications and repairs and was invaluable in his role as a consultant.

The figures prepared by Mr. John Samaska, the typing and proofreading by Ann Fleming and the typing by Jewell Libby are appreciated.

Gratitude is expressed for the financial support received during this investigation from the National Science Foundation and the Celanese Corporation.

TABLE OF CONTENTS

	Page
LIST OF TABLES	vii
LIST OF ILLUSTRATIONS	viii
 Chapter	
I. INTRODUCTION	1
II. HISTORICAL BACKGROUND.....	5
III. THEORETICAL ANALYSES	16
Conventional Theory for the Open Column.....	16
Mathematical Development.....	17
Evaluation of the Constants H and K for the Batch Case.....	24
Evaluation of the Constants H and K for the Continuous Flow Case.....	28
Application of the Transport Equation.....	29
Steady-State Batch Case.....	29
Transient Batch Case.....	39
Continuous Flow Case.....	55
Flow of Fluid Past the Barriers: Evaluation of σ_c	67
Summary.....	72
IV. EQUIPMENT.....	76
Thermogravitational Column and Auxiliary Equip- ments.....	76
Horizontal Barrier Systems.....	89
Apparatus for Determination of Ratio of C-Factors	94
V. EXPERIMENTAL PROCEDURE.....	97
Procedure for Obtaining Plate Spacing.....	98
Procedure for Obtaining Batch-Transient Data..	105
Procedure for Obtaining Continuous Flow Data...	106
Analytical Procedure.....	107
VI. PRESENTATION AND INTERPRETATION OF EXPERIMENTAL RESULTS.....	109

Chapter	Page
Batch Case.....	110
Effect of Number of Barriers.....	110
Effect of Temperature Difference between the Plates.....	115
Effect of Barrier Diameter.....	116
Effect of Plate Spacing.....	117
Transient Batch Case.....	117
Effect of Number of Barriers.....	117
Effect of Temperature Difference between the Plates.....	130
Effect of Barrier Diameter.....	140
Continuous Flow Case.....	145
Effect of Number of Barriers.....	145
Effect of Temperature Difference between the Plates.....	155
Effect of Barrier Diameter.....	160
Summary.....	164
 VII. ADDITIONAL WORK.....	 169
Evaluation of the Thermal Diffusion Coefficient. Column Theory and Operation with Unequal Product Flow Rates ($\sigma_e \neq \sigma_s$).....	169 171
Results of Experimental Work with Plastic Flow Model.....	177
 VIII. CONCLUSIONS.....	 182
 BIBLIOGRAPHY.....	 185
 APPENDICES	
A. COLUMN AND SYSTEM PARAMETERS FOR SETS OF EXPERIMENTAL DATA.....	188
B. TABLES OF EXPERIMENTAL DATA.....	190
C. BARRIER "DRAG" FACTOR DATA.....	201
D. ESTIMATION OF LENGTH CORRECTION FACTOR (l_p).....	203
E. PHYSICAL PROPERTIES OF ETHYL- ALCOHOL-WATER SYSTEM.....	209
F. WORK OF TREACY AND RICH (T6)(T7) WITH HORIZONTAL BARRIERS.....	211

	Page
G. SUMMARY OF EQUATIONS USED TO CALCULATE PREDICTED TRANSIENT CURVES FOR WORK WITH BARRIERS.....	216
H. SAMPLE CALCULATIONS.....	218
I. NOMENCLATURE.....	234
J. LIST OF REFERENCES.....	238

LIST OF TABLES

Table	Page
1. Plate Spacing Measurements Taken for Experimental Sets I, M, Q, and R.....	103
2. Comparison of Batch Separation with Four Horizontal Barriers: Barrier Diameter a Parameter.....	118
3. Column and System Parameters for Sets of Experimental Data.....	189
4. Experimental Batch-Transient Data.....	191
5. Experimental Data for Rate-Separation Curves.....	196
6. Barrier "Drag" Factor Data	202
7. Physical Properties of Ethyl Alcohol-Water System...	210

LIST OF ILLUSTRATIONS

Figure	Page
1. Schematic Diagram of a Center-Feed, Continuous-Flow, Thermogravitational Column.....	18
2. Proposed Model for a Column with Horizontal Barriers: Batch Case.....	33
3. Dimensionless Separation As a Function of Dimensionless Time with Dimensionless Sampling (Flow) Rate As a Parameter.....	43
4. Proposed Model for a Column with Horizontal Barriers: Transient Case.....	46
5. Small Column with End-Feeds: No Bulk Flow.....	48
6. Proposed Model for a Column with Horizontal Barriers: Continuous Feed and Product Withdrawal....	58
7. Small Column (in Enriching Section) with End-Feeds: Continuous Feed and Product Withdrawal.....	60
8. Enriching Section of a Thermogravitational Column with Horizontal Barriers and Continuous Flow.....	62
9. Thermogravitational Thermal Diffusion Column....	77
10. Component of One Transfer Plate with Water Jacket.	79
11. Detail of Thermocouple Installation in a Transfer Plate.....	80
12. Gravity-Flow Feed System.....	82
13. Feed and Product Port Construction.....	83
14. Sample Tap Construction.....	85
15. Control Panel.....	86
16. Cooling and Heating Water Systems.....	88

Figure	Page
17. Barrier Framework with Four Barriers Showing Teflon Spacer Detail.....	90
18. Barrier Framework with Fifty Barriers.....	91
19. Experimental Apparatus for the Determination of the Ratio of Drag Factors.....	96
20. Plate Spacing Measurement.....	99
21. Location of Steel Balls Utilized for Measuring Plate Spacing.....	101
22. Analytical Instruments.....	108
23. Comparison of Experimental Results with Equation (III-54) for Steady-State Batch Case with N Horizontal Barriers.....	111
24. Separation As a Function of Column Length.....	114
25. Comparison with Theory of the Transient Behavior of Columns with Zero and Four Horizontal Barriers.	122
26. Comparison with Theory of the Transient Behavior of Columns with Zero and Two Horizontal Barriers..	125
27. Comparison with Theory of the Transient Behavior of Columns with Zero and Eight Horizontal Barriers....	128
28. Comparison with Theory of the Transient Behavior of Columns with Zero and Sixteen Horizontal Barriers..	129
29. Comparison with Theory of the Transient Behavior of Columns with Zero, Two, Four, Eight, and Sixteen Horizontal Barriers: Higher Temperature Difference.	131
30. Effect of the Temperature Difference between the Plates on the Transient Behavior of a Column with Two Horizontal Barriers.....	133
31. Effect of the Temperature Difference between the Plates on the Transient Behavior of a Column with Four Horizontal Barriers.....	136

Figure	Page
32. Effect of the Temperature Difference between the Plates on the Transient Behavior of a Column with Sixteen Horizontal Barriers.....	138
33. Effect of the Temperature Difference between the Plates on \bar{Q}_c , the Flow Past the Barriers: Transient Data.....	139
34. Effect of the Barrier Diameter on the Transient Behavior of a Column with Four Horizontal Barriers: Higher Temperature Difference.....	143
35. Effect of the Barrier Diameter on the Transient Behavior of a Column with Four Horizontal Barriers: Lower Temperature Difference.....	144
36. Comparison of Rate-Separation Curves for Four Horizontal Barriers with Different Values of \bar{Q}_c , the Flow Past the Barriers.....	147
37. Comparison of Rate-Separation Curves for Columns with Zero and Four Horizontal Barriers.....	149
38. Comparison of Rate-Separation Curves for Columns with Zero and Two Horizontal Barriers.....	151
39. Comparison of Rate-Separation Curves for Columns with Zero and Eight Horizontal Barriers.....	152
40. Comparison of Rate-Separation Curves for Columns with Zero and Sixteen Horizontal Barriers.....	153
41. Comparison of Rate-Separation Curves for Columns with Zero and Fifty Horizontal Barriers.....	154
42. Comparison of Rate-Separation Curves for Columns with Zero, Two, Four, Eight, Sixteen, and Fifty Horizontal Barriers: Higher Temperature Difference.	156
43. Effect of the Temperature Difference between the Plates on the Flow Past the Barriers, \bar{Q}_c : Continuous Flow Data.....	158
44. Effect of the Temperature Difference between the Plates on the Rate-Separation Curve of a Column with Two Horizontal Barriers.....	159

Figure	Page
45. Effect of the Temperature Difference between the Plates on the Rate-Separation Curve of a Column with Four Horizontal Barriers.....	161
46. Effect of the Temperature Difference between the Plates on the Rate-Separation Curve of a Column with Sixteen Horizontal Barriers.....	162
47. Effect of the Barrier Diameter on the Rate-Separation Curve of a Column with Four Horizontal Barriers: Higher Temperature Difference.....	165
48. Effect of the Barrier Diameter on the Rate-Separation Curve of a Column with Four Horizontal Barriers: Lower Temperature Difference.....	166
49. Thermal Diffusion Coefficient, α , for the System Ethyl Alcohol-Water As a Function of the Concentration.....	170
50. Separation As a Function of the Ratio of Product Flow Rates: $Z = 0.887$	175
51. Separation As a Function of the Ratio of Product Flow Rates: $Z = 5.48$	176
52. Separation As a Function of the Ratio of Product Flow Rates: $Z = 0.493$	178
53. Determination of the Ratio of Drag Factors: Graphical Presentation of Experimental Data.....	180
54. Disturbance of Temperature Gradient.....	205
55. Data of Treacy (T6) Compared with Equation (III-54).	214
56. Separation, Δ/Δ_0 , As a Function of Dimensionless Flow, Z	224

AN INVESTIGATION OF THE EFFECT OF HORIZONTAL BARRIERS IN
A THERMOGRAVITATIONAL LIQUID THERMAL DIFFUSION COLUMN

CHAPTER I

INTRODUCTION

In general, a concentration gradient arises when a temperature gradient is applied to an originally uniform mixture. This phenomenon, which is called thermal diffusion, was noted as early as 1856 by Ludwig (L6) and subsequently by Soret (S4) in 1879; since this time, thermal diffusion in liquids or solid solutions has been known as the Ludwig-Soret or the Soret effect.

Two methods of utilizing thermal diffusion for separating mixtures have been developed. One is the static method in which a temperature gradient is applied such that no convection currents arise, and, in addition, there is no bulk flow. In general, a device for the static method consists of a simple container or cell filled with a binary mixture. The bottom of the cell is maintained at some temperature lower than that at the top of the cell, and after a period of time (the time depending on the distance between the top and bottom of the cell and on the binary system used), a concentration difference results between the top and bottom of the cell. The degree of separation in

such a cell is usually small.

Clusius and Dickel (C8) introduced in 1938 a second method for separating mixtures by thermal diffusion. An apparatus utilizing their method multiplies the separation by means of convection currents in a manner similar to the way a counter-current extraction column produces concentration differences many times greater than the difference for a single stage. The apparatus is commonly called a thermogravitational column, or Clusius-Dickel column. These columns can be operated in a batch or continuous manner, where the terms batch and continuous refer, respectively, to the absence or presence of bulk flow through the column.

Since 1938, a great deal of theoretical and experimental work has been done concerning the thermogravitational column, but industry has not yet accepted thermal diffusion as a promising method for separations. Two reasons are given for this hesitancy. First, the absence of a satisfactory kinetic theory of liquids makes it practically impossible to predict accurately the behavior of a given mixture when used in a thermogravitational column. Thus, it becomes necessary to explore experimentally each mixture considered. Second, by nature, thermal diffusion is a thermodynamically irreversible process and requires a relatively large amount of energy for a given separation. Hence, it can be considered only for separations where the more conventional means of separation fail to separate economically.

Since thermal diffusion is intrinsically an expensive process, a column utilizing this method for separations must be designed for maximum efficiency. Considerable work has been done in recent years in an attempt to improve the separation ability of thermal diffusion columns. Various experimental investigators (A2) (B9) (C11) (D4) (L4) (L5) (S1) (S8) (S9) (T6) (T7) (V3) have tried packings, spacers, and baffles as well as other devices in the separation space in an effort to improve column performance. Most of these investigators have found rather startling increases in the separation efficiency when objects were placed in the separation space, but no general experimental agreement has been noted. One problem that hampered these investigations was the lack of an adequate theory to predict column performance when objects were placed in the separation space. Two recent theses have helped fill this void: Lorenz (L4) studied packed column operation and found good agreement between his theory and experimental results; in addition, Boyer (B8) has developed a satisfactory theory to predict column performance when vertical barriers are introduced into the separation space.

The purpose of this work then was to make a theoretical study and experimental investigation of horizontal barriers in a parallel-plate thermogravitational thermal diffusion column. The work was an attempt to supplement the present theory concerning column operation with objects in the separation space and thus had two objectives:

1. Predict, on a theoretical basis, the performance of a thermogravitational column with horizontal barriers in the separation space.
2. Obtain sufficient experimental data to test the adequacy of the theoretical development.

CHAPTER II

HISTORICAL BACKGROUND

The introductory chapter provides only a few references to the literature, most of which pertain to column operation with objects in the separation space. For the reader familiar with the field of thermal diffusion, Chapter I serves as an adequate introduction. However, for the reader less well acquainted with the field, this Chapter on Historical Background has been included. No attempt has been made here to cover thoroughly all facets of thermal diffusion but only to give a representative sampling of some of the work done, with special emphasis on peculiar effects that have been noted. (For a complete historical background, the reader is referred to the thesis by Von Halle (V3) which contains an excellent annotated bibliography.)

The first theory attempting to explain the Soret effect was presented by Van't Hoff (H6) in 1887. His theory tried to account for Soret's observations on the basis of the osmotic pressure of the aqueous solution and predicted that all solutions should give the same steady-state separation providing that the initial concentrations and applied temperature gradients were the same.

Early experiments with aqueous solutions carried out by Berchem (B6), Arrhenius (A3) (A4), Eilert (E1), Wereide (W4), Chipman (C7), and Tanner (T1) showed Van't Hoff's simple theory inadequate. Most of the above experimental work was done with vessels filled with a liquid mixture with heat being supplied to one portion of the solution and heat being removed from another portion. Samples were withdrawn and analyzed after some length of time. Remixing and convection currents plagued these early experiments; hence results were generally inaccurate and not reproducible.

Chapman (C5) effectively summed up the status of the theoretical developments in liquids when he stated that "the prospect of arriving at an even approximately correct theory seems rather remote. This is not only because of the additional difficulties present in every branch of the kinetic theory of liquids as compared with the corresponding theory of gases, but because the theory of thermal diffusion even in gases is unusually complex."

"Though it is depressing thus to dwell on the difficulties which appear to beset the theoretical treatment of the Soret phenomenon, a proper estimation of them may prevent waste of effort on unduly simple methods that are foredoomed to failure."

Thermal diffusion in gases was first predicted theoretically by Enskog (E3) in 1911, and in 1917 he published the derivation of the gas coefficients from Boltzmann's integral equation for the

velocity distribution function. Chapman (C4) predicted the thermal diffusion phenomenon independently in 1916, and with Dootson (C6) he experimentally determined values of the thermal diffusion coefficient, α , for the systems carbon dioxide-hydrogen and sulfur dioxide-hydrogen. Ibbs (I1) confirmed these experimental results in 1921.

All of the early investigators used the static method in their experiments. Mulliken (M2) in 1922 demonstrated that the static method of thermal diffusion could not compete with conventional separation methods. However, although the static, single-stage thermal diffusion experiments were inefficient for separating gas mixtures, experiments of this type remained of great theoretical interest for the study of the nature of intermolecular forces in gases.

Thus it was not until 1938, when Clusius and Dickel (C9) developed their hot-wire thermal diffusion column, that the possibility of using thermal diffusion as a method of separation became really practical. In the Clusius and Dickel column the separation obtainable in the static method is multiplied by a cascading effect brought about by convection currents. This type of column was later refined by Brewer and Bramley (B10), who suggested the use of concentric cylinders rather than the hot-wire type apparatus.

The introduction of the Clusius and Dickel column, commonly called a "thermogravitational column," served to stimulate interest in thermal diffusion, since it transformed what had previously been

essentially a laboratory curiosity into a practical means for effecting difficult separations. Since its inception, the thermogravitational column has been shown to be well suited for producing small amounts of highly enriched gaseous isotopes. Clusius and Dickel (C8) reported the partial separation of the isotopes of neon and of chlorine; Bramley and Brewer (B10), Taylor and Glockler (T2), and Watson (W3) the enrichment of the isotopes of carbon, and others (G8), (G9), (N1), reported enrichment of isotopes of xenon, mercury, and nitrogen, all by thermogravitational means.

Numerous theories have been proposed to explain the behavior of the thermogravitational column. Theoretical papers dealing with the separation of gases were published by Bramley and Brewer (B11), Clusius and Dickel (C10), Furry, Jones, and Onsager (F7), Van der Grinten (G4), and by Waldmann (W1) (W2), all shortly after the thermogravitational column process was disclosed. Debye (D1) presented a theoretical treatment of the problem of separations in the liquid phase in 1939. A detailed theory for gas phase separations was described in German in 1942 by Fleischmann and Jensen (F2), and in the same year, deGroot (G5) published in French a very comprehensive study of thermal diffusion in liquids and solids. This study was also contained in deGroot's thesis (G6) finished in 1945. One of the most successful treatments of column theory was presented by Furry, Jones and Onsager (F7) in 1939, and their theory will be considered later in

this work with horizontal barriers. In addition, Jones and Furry (J8) published an excellent review of column theory in 1946.

In their monograph published in 1952, Grew and Ibbs (G3) comprehensively reviewed the theory and experiments pertaining to the static method in gases. They considered also the static effect in liquids and the thermogravitational column. They concluded that the column theory had not been sufficiently perfected such that separations obtained in thermogravitational columns could be used for the fundamental study of either the gaseous or the liquid state. A theoretical treatment that has been made available recently was written by Abelson, Rosen, and Hoover (A1) and deals with separation of isotopes in liquids.

Although numerous theories have been published, the results are substantially in agreement and differ primarily in the approach used and in the degree of approximation. However, experimental confirmation of the theory has not been entirely satisfactory, and, in general, measurements made in thermogravitational columns agree only in order of magnitude with values calculated from gas theory or obtained through static measurements.

One method that has been employed to test column theory is changing the effective gravitational field causing convective flow. This has been accomplished in two different ways. Tilvis (T5) and Farber and Libby (F1) worked out methods of rotating their columns, thereby

increasing the convective flow. Carr (C2) and Powers (P3) inclined their columns from vertical, thus altering the effective gravitational field. The latter type of investigation was necessarily restricted to a parallel-plate type apparatus.

Sullivan, Ruppel, and Willingham (S8) investigated the effect of rotating one wall of a concentric-cylinder thermogravitational column and found that the hydrodynamic flow pattern obtained increased the separation efficiency of the column. Henke and Stauffer (H3) rotated one cylinder of their concentric-cylinder column in order to create an upward drag at the cold wall and improve column efficiency. Beams (B4) obtained a patent in 1950 on a thermal diffusion device with moving walls; a circular metallic belt formed the walls of the column, and the speed of the belt controlled the rate of convective flow. Apparatuses of this type have been discussed theoretically by Niini (N2) and Ramser (R1).

There are many other facets of thermal diffusion that have been investigated experimentally and considered theoretically.

The approach to steady-state in a thermogravitational column has received attention from numerous investigators. deGroot, Gorter, and Hoogenstraaten (G7) showed that experimental data on transient column behavior obtained with columns of different plate spacings agreed with theory. Powers (P4) (P5) developed equations to correlate the transient behavior of thermal diffusion columns separating

equi-molal binary liquid mixtures under batch conditions (no flow).

Von Halle (V3) considered the approach to steady-state for several types of thermal diffusion columns, again for the batch case.

Hoffman (H7) presented expressions for the concentration in a thermal diffusion column at any time both with and without bulk flow.

Powers and Wilke (P8) did a rather complete study on the effect of flow in a thermogravitational column. Heines, Larson, and Martin (H2) also investigated column operation under continuous flow conditions, and their results are in agreement with Powers and Wilke. Longmire (L3) described the continuous throughput rectification of various organic liquid mixtures in thermogravitational columns and found that, in general, the observed separations were ten percent greater than the theory predicted. Jones (J1) and Jones and Foreman (J8) have published empirical conclusions based on extensive experimental investigation of the continuous separation of liquids. Jones and co-workers have received numerous patents for the continuous separation of liquids by thermal diffusion (J2-5). Frazier (F4)(F5) has obtained a series of patents relating to novel end-feed systems for feeding a group of thermal diffusion columns. In addition, Frazier and co-workers (F6) (G1) (G2) have done a considerable amount of theoretical and experimental work towards developing the end-feed system of columns.

Other experimental work has been reported and can be used to evaluate certain aspects of column theory. Powers and Wilke (P8) conducted studies of column length, temperature difference, and plate spacing as did Heines, Larson, and Martin (H2). Debye and Bueche (D4) and Hirota and Kimura (H5) both report data in substantial agreement with the dependence of plate spacing and column height predicted by theory. Docherty and Ritchie (D5) made an extensive investigation of initial separation rates and their data support the conclusion based on the theory of Debye (D1) that the initial rate of separation is independent of column height. Crownover (C13) studied the effect of column length on the batch separation and transient behavior of a concentric-cylinder column. Vichare (V2) considered the effect of the rate and size of sampling on the transient behavior of a column operated with no bulk flow.

Because only one column and fluid system need be used, one of the most popular and convenient methods for testing column theory has been the use of pressure. Many experimental investigators using pressure (D7) (P2) have been able to correlate their data by using equations of the form predicted by the theory. However, although the theory seems adequate for convective flows in the laminar region, it fails when the convective flow becomes turbulent. The theory predicts decreased separations when the pressure is increased and turbulence occurs, but the separations have been found experimentally

to be equal to or greater than the separations which would be predicted assuming conditions of laminar flow. Drickamer, Mellow, and Tung (D7) attempted to account for an increase in separation with turbulence by developing a semi-empirical modification of the theory. Becker (B5) disagreed with their theory modification for use at low convection rates, but found it satisfactory to correlate his data at high convection rates. In 1953, Hirota and Kobayashi (H4) published data which was in support of Drickamer's modification; however, as pointed out by several authors (P3) (V3), both their theory and use of Drickamer's correlations appear to be in error. Most recently, a paper by Bowring (B7) on the separation of helium isotopes purports to support Drickamer's empirical corrections, but, as noted by Von Halle (V3), the equations actually used to correlate his data were those of Hirota and Kobayashi mentioned above. Thus, the question of turbulence is still the subject of some discussion and has not been — settled completely.

The effect of turbulence is not the only peculiarity in column performance that has been found experimentally. As early as 1939, Brewer and Bramley (B9) (B11) found that the performance of their concentric-cylinder columns was improved when spacers were introduced at intervals in the annular space between the column walls. Brewer and Bramley concluded that the spacers, or baffles, enhanced the separation by inducing swirls in the gas, a conclusion with which

Jones and Furry (J8) disagreed. The work of Donaldson and Watson (D6) in 1951 supported the contentions of Brewer and Bramley, when they reported that by inserting wire turbulence promoters at five centimeter intervals along the column length, the column characteristics were greatly improved. Treacy and Rich (T6) (T7) found that compound baffles of several types gave a six-fold increase in column efficiency. On the other hand, Corbett and Watson (C11) in 1956 examined column performance in the laminar and turbulent regions both with and without spacers, and no significant effect was observed, this being attributed to careful construction of their column. Saxena and Watson (S1) used spacers for centering the hot wire of their column; their results suggested an optimum spacing in that a maximum separation was obtained at a given spacing and fell when the spacers were placed closer or farther apart. The authors felt that the spacers increased the separation only so long as they significantly improved the centering of the hot wire; thereby they agreed with the conclusion of Corbett and Watson.

In further attempts to improve the efficiency of column operation, there have been numerous and varied modifications. Debye (D4) published in 1948 the results of experiments with polymer solutions in which the annular space of the thermogravitational column was packed with glass wool or a similar material to retard the vertical convective flow. A patent was issued to Debye on this process in 1951 (D2). Sullivan, Ruppel, and Willingham (S9) did a more quantitative study

of column performance with various packings and found that the observed separation increased with the density of the packing and that the time required for the separation also increased. Papayanopoulos (P1) devised a packed column with variable heat input similar to the packed column of Sullivan, Ruppel, and Willingham, and claimed that it allowed use of slit widths (distance between the walls) thirteen times wider than conventional columns and that it consumed one-fortieth the energy per unit product. Lorenz (L4) and Lorenz and Emery (L5) developed equations to describe a thermogravitational column with packing, and their equations show increased separations with packing, which is in agreement with observation. Most recently, Boyer (B8) completed a theoretical and experimental investigation of vertical barriers in a parallel-plate thermal diffusion column, and his experimental results are in agreement with his theory.

CHAPTER III

THEORETICAL ANALYSES

As mentioned previously in Chapter II, Furry, Jones, and Onsager (F7) have developed a rather successful theory to explain the performance of a thermogravitational thermal diffusion column with no objects in the separation space (an "open" column); the first part of this chapter on Theoretical Analyses is concerned with a review of this conventional theory without barriers. It is then noted that, although the conventional theory does not predict an increase in the steady-state batch separation when horizontal barriers are placed in the separation space, it was found experimentally that such an increase does occur. An ex post facto line of reasoning is then utilized to develop a modified theory to explain this apparent discrepancy with the conventional theory for the batch case. The modified theory is then expanded to include the transient case and the continuous flow case.

Conventional Theory for the Open Column

In general, a temperature gradient applied to a solution in



a thermogravitational thermal diffusion column brings about two effects: (1) a flux of one component of the solution relative to the other brought about by thermal diffusion (See Figure 1.), and (2) convective currents produced by density differences in the solution near the hot and cold plates. The net result of the two effects is to produce a concentration difference between the two ends of the column. This concentration gradient, in conjunction with the aforementioned convection currents, limits the separation. (The separation is defined as the concentration difference between materials at the top and bottom of the column.)

Mathematical Development

In a binary solution of components 1 and 2, the fluxes of component 1 due to ordinary and thermal diffusion respectively are:

$$J_{x-OD} = -D \frac{\partial C_1}{\partial x} \quad (\text{III-1})$$

$$J_{y-OD} = -D \frac{\partial C_1}{\partial y} \quad (\text{III-2})$$

$$J_{x-TD} = \frac{\alpha D}{T} C_1 C_2 \frac{dT}{dx} \quad (\text{III-3})$$

where

J_{x-OD} is the flux of component 1 in the x-direction due to ordinary diffusion,

J_{y-OD} , the flux of component 1 in the y-direction due to ordinary diffusion,

- D , the ordinary diffusion coefficient,
- $J_x - TD$, the flux of component 1 in the x -direction due to thermal diffusion,
- α , the thermal diffusion coefficient,
- T , the absolute temperature,
- C_1, C_2 , the fractions of components 1 and 2 respectively,
- x , the axis normal to the plates, and
- y , the axis parallel to the plates in the direction of normal convective flow.

It has been assumed implicitly that variations in the direction normal to the x - y plane can be neglected.

Now define $v(x)$ as a function that represents the convective velocity between the plates. A partial differential equation can be obtained by combining Equations (III-1), (III-2), and (III-3) with the above definition for the convective velocity; the resulting equation will describe the fraction, C , in the column as a function of the time, t , and the coordinates x and y . The equation can be simplified considerably by assuming that α and D are constants, that a mean temperature level, \bar{T} , can be used, that the convective velocity function, $v(x)$, is not a function of y , and that end effects are negligible. Equation (III-4) is the equation obtained from Equations (III-1), (III-2), and (III-3) by applying the above assumptions and the condition of continuity:

$$\frac{\partial C_1}{\partial t} = D \left(\frac{\partial^2 C_1}{\partial x^2} + \frac{\partial^2 C_1}{\partial y^2} \right) - \frac{\alpha D}{T} \frac{dT}{dx} \frac{\partial}{\partial x} (C_1 C_2) - v(x) \frac{\partial C_1}{\partial y} \quad (\text{III-4})$$

Equation (III-4) is a partial differential equation of second order in x and y . Furry, Jones, and Onsager (F7) have shown how an ordinary differential equation of first order in y and with constant coefficients can be obtained; the first order, ordinary differential equation that results has become known as the transport equation. Equation (III-4) is first simplified by assuming that steady-state conditions exist ($\partial C_1 / \partial t = 0$) and by assuming that the vertical diffusion term ($D \partial^2 C_1 / \partial y^2$) is negligible in comparison to the mass flow term [$v(x) \partial C_1 / \partial y$]. By further restricting the solution to conditions of laminar flow, the temperature gradient dT/dx can be replaced by $\Delta T / 2\omega$ where ΔT is the temperature difference and 2ω the distance between the plates. With the above assumptions, Equation (III-4) reduces to

$$D \frac{\partial^2 C_1}{\partial x^2} - \frac{\alpha D}{T} \frac{\Delta T}{2\omega} \frac{\partial}{\partial x} (C_1 C_2) - v(x) \frac{\partial C_1}{\partial y} = 0 \quad (\text{III-5})$$

Since there is no accumulation of mass at the plates ($x = \pm \omega$), the mass transferred in (or out) by ordinary diffusion must equal the mass transferred out (or in) by thermal diffusion, and this gives two boundary conditions which Equation (III-5) must satisfy

$$D \frac{\partial C_1}{\partial x} - \frac{\alpha D}{T} \frac{\Delta T}{2\omega} \frac{\partial C_1 C_2}{\partial x} = 0 \quad x = \pm \omega \quad (\text{III-6})$$

Equation (III-5) must also satisfy a material balance made around either end of the column, and this gives a third boundary condition (for the enriching section--see Figure 1)

$$\sigma_e C_e = \rho B_e \int_{-\omega}^{+\omega} C_1 v(x) dx - \rho B_e D \int_{-\omega}^{+\omega} \frac{\partial C_1}{\partial y} dx \quad (\text{III-7})$$

where the subscript e designates the enriching section of the column and where

σ_e is the mass flow rate out of the enriching section,

C_e , the fraction of component 1 in the enriching section product stream,

B_e , the column width in the enriching section, and

ρ , a mean density.

A similar expression can be written for the stripping section of the column

$$-\sigma_s C_s = \rho B_s \int_{-\omega}^{+\omega} C_1 v(x) dx - \rho B_s D \int_{-\omega}^{+\omega} \frac{\partial C_1}{\partial y} dx \quad (\text{III-8})$$

Integration of Equation (III-5) with respect to x yields

$$D \frac{\partial C_1}{\partial x} - \frac{\alpha D}{T} \frac{\Delta T}{2\omega} C_1 C_2 - \int_{-\omega}^{+\omega} v(x) \frac{\partial C_1}{\partial y} dx = f(y) \quad (\text{III-9})$$

From the boundary condition given by Equation (III-6) at $x = -\omega$, it is found that the constant of integration $f(y) = 0$, and rewriting Equation (III-9) yields

$$\frac{\partial C_1}{\partial x} = \frac{a}{T} \frac{\Delta T}{2 \omega} C_1 C_2 + \frac{1}{D} \int_{-\omega}^x v(x) \frac{\partial C_1}{\partial y} dx \quad (\text{III-10})$$

In order to satisfy the conditions at $x = +\omega$, the following relation must hold

$$\int_{-\omega}^{+\omega} v(x) \frac{\partial C_1}{\partial y} dx = 0 \quad (\text{III-11})$$

Moreover, if it is assumed that $\partial C_1 / \partial y$ is independent of x , Equation (III-11) can be satisfied only if

$$\int_{-\omega}^{+\omega} v(x) dx = 0 \quad (\text{III-12})$$

That is, it can be satisfied only for conditions of no bulk flow or batch column operation.

Integration of the second term of Equation (III-7) with respect to the variable x yields

$$\begin{aligned} \sigma_e C_e = \rho B_e \left[C_1 \int_{-\omega}^{+\omega} v(x) dx \right] - \rho B_e \int_{-\omega}^{+\omega} \frac{\partial C_1}{\partial x} \left[\int_{-\omega}^x v(x) dx \right] dx \\ - \rho B_e D \int_{-\omega}^{+\omega} \frac{\partial C_1}{\partial y} dx \end{aligned} \quad (\text{III-13})$$

Substituting in Equation (III-13) the expression for $\partial C_1 / \partial x$ obtained in Equation (III-10) and assuming that $C_1 C_2$ is not a function of x (as well as $\partial C_1 / \partial y$ independent of x):

$$\begin{aligned} \sigma_e C_e = & \overline{C_1} \sigma_e - \overline{C_1 C_2} \frac{\alpha \rho B_e \Delta T}{T 2 \omega} \int_{-\omega}^{+\omega} \left[\int_{-\omega}^x v(x) dx \right] dx \\ & - \frac{\partial \overline{C_1}}{\partial y} \left[\frac{\rho B_e}{D} \int_{-\omega}^{+\omega} \left(\int_{-\omega}^x v(x) dx \right)^2 dx + \rho B_e D \int_{-\omega}^{+\omega} dx \right] \end{aligned} \quad (\text{III-14})$$

where super-bars indicate mean values.

Now defining

$$H \equiv \frac{-\alpha \rho B \Delta T}{T 2 \omega} \int_{-\omega}^{+\omega} \left[\int_{-\omega}^x v(x) dx \right] dx \quad (\text{III-15})$$

$$K_c \equiv \frac{\rho B}{D} \int_{-\omega}^{+\omega} \left[\int_{-\omega}^x v(x) dx \right]^2 dx \quad (\text{III-16})$$

$$K_d = \rho B D \int_{-\omega}^{+\omega} dx \quad (\text{III-17})$$

and

$$K \equiv K_c + K_d \quad (\text{III-18})$$

Equation (III-14) can be written

$$\sigma_e (C_e - \bar{C}_1) = \bar{C}_1 \bar{C}_2 H_e - \frac{\partial \bar{C}_1}{\partial y} (K_{C_e} + K_{d_e}) \quad (\text{III-19})$$

or, utilizing Equation (III-18)

$$\sigma_e (C_e - \bar{C}_1) = \bar{C}_1 \bar{C}_2 H_e - \frac{\partial \bar{C}_1}{\partial y} K_e \quad (\text{III-20})$$

An additional term, K_p , is sometimes included in Equation (III-18) in an attempt to account for the effects of parasitic remixing in a column. Unfortunately, K_p can only be evaluated empirically, but the work of previous investigators (B8) (P3) for the same binary system, ethyl alcohol-water, has shown that K_p is negligible in comparison to K_C for the column dimensions and temperatures used in this work with horizontal barriers. Therefore, K_p will be assumed negligible throughout this work.

It will be shown in subsequent sections of this chapter how Equation (III-20) can be utilized for several different cases of column operation. First, however, the evaluation of the constants H and K will be considered.

Evaluation of the Constants H and K for the Batch Case

Upon examination of Equations (III-15) and (III-16), it can be seen that the problem of evaluating the constants H and K_C becomes primarily one of obtaining an expression for the velocity distribution,

$v(x)$. The Navier-Stokes equation is the usual convenient starting point for the derivation of the velocity distribution, and with suitable boundary conditions the equation yields

$$-\frac{dP}{dy} + \frac{\eta}{g_c} \frac{d^2 v(x)}{dx^2} - \frac{\rho g}{g_c} = 0 \quad (\text{III-21})$$

Rewriting Equation (III-21) yields

$$\frac{d^2 v(x)}{dx^2} - \frac{\rho g}{\eta} - \frac{dP}{dy} \frac{g_c}{\eta} = 0 \quad (\text{III-22})$$

Differentiating Equation (III-22) with respect to x gives

$$\frac{d^3 v(x)}{dx^3} - \frac{g}{\eta} \frac{\partial \rho}{\partial x} - \frac{g_c}{\eta} \frac{\partial}{\partial x} \left(\frac{dP}{dy} \right) = 0 \quad (\text{III-23})$$

Now

$$\frac{\partial \rho}{\partial x} = \frac{\partial \rho}{\partial T} \frac{dT}{dx} + \boxed{\frac{\partial \rho}{\partial C_1} \frac{dC_1}{dx}} \quad (\text{III-24})$$

The enclosed term above is the so-called "forgotten effect," or effect of concentration on the density gradient. Numerous authors (B8) (L3) (P3) (V3) have pointed out that neglecting this term is not always a good approximation and can lead to appreciable error, particularly in cases of large plate spacings. deGroot (G7) determined a mean value of $\partial C_1 / \partial x$ to use in Equation (III-24):

$$\overline{\frac{\partial C_1}{\partial x}} = \frac{0.3 \alpha \Delta T}{\bar{T} (2\omega)} \quad (\text{III-25})$$

Although Equation (III-25) can be used to improve the interpretation of column data in some cases, use of Equations (III-24) and (III-25) shows that the forgotten effect can be neglected for the binary system and column conditions considered in this work:

$$\frac{\partial \rho}{\partial x} = \frac{\partial \rho}{\partial T} \frac{dT}{dx} + \frac{\partial \rho}{\partial C_1} \frac{dC_1}{dx} \quad (\text{III-24})$$

$$= (7.8 \times 10^{-4} \frac{\text{gram}}{\text{cm}^3 \cdot ^\circ\text{K}}) \left(\frac{26.7^\circ\text{C}}{.0792\text{cm}} \right) + 1300 \times 10^{-4}$$

$$\times \frac{(0.3)(0.51)(26.7)}{(322)(0.0792)} \quad (\text{III-26})$$

$$= (7.8 \times 10^{-4}) (337) + (1300 \times 10^{-4}) (0.16)$$

Thus, the contribution by the temperature effect to $\partial \rho / \partial x$ is more than twelve times greater than the contribution by the forgotten effect.

Therefore, neglecting the enclosed term in Equation (III-24) and defining

$$\beta_T = - \frac{\partial \rho}{\partial T} \quad (\text{III-27})$$

$$\frac{dT}{dx} = \frac{\Delta T}{2 \omega} \quad (\text{III-28})$$

Equation (III-24) becomes

$$\frac{\partial P}{\partial x} = -\beta_T \frac{\Delta T}{2 \omega}$$

(III-29)

Equation (III-23) can now be written (since dP/dy is not a function of x)

$$\frac{d^3 v(x)}{dx^3} + \frac{\beta_T g \Delta T}{2 \omega \eta} = 0$$

(III-30)

Equation (III-30) is readily integrated and the constants of integration evaluated through use of the boundary conditions

$$v(x) = 0 \quad \text{at } x = +\omega$$

(III-31)

$$v(x) = 0 \quad \text{at } x = -\omega$$

(III-32)

and as before

$$\int_{-\omega}^{+\omega} v(x) dx = 0$$

(III-12)

From the above, one arrives at Equation (III-33):

$$v(x) = \frac{-\beta_T g \Delta T}{12 \omega \eta} (x^3 - \omega^2 x)$$

(III-33)

If the expression for the velocity distribution, Equation (III-33), is substituted in Equations (III-15) and (III-16) and the integrations

carried out, the resulting expressions for H and K_c are

$$H = \frac{\alpha \beta_T \rho g (2\omega)^3 B (\Delta T)^2}{6! \eta \bar{T}} \quad (\text{III-34})$$

$$K_c = \frac{\beta_T^2 \rho g^2 (2\omega)^7 B (\Delta T)^2}{9! D \eta^2} \quad (\text{III-35})$$

Finally, integration of Equation (III-17) yields

$$K_d = 2 \omega \rho B D \quad (\text{III-36})$$

Evaluation of the Constants H and K for the Continuous Flow Case

For mass flow through the column, in general, the expressions for H and K from the batch case are used even though the assumed velocity distribution, $v(x)$, is distorted by the addition of bulk flow. This is the most common method of handling the flow case and has been successful in many instances.

There have been some attempts to derive an expression for the velocity distribution, $v(x)$, for the flow case and subsequently to integrate this new velocity distribution in Equations (III-15) and (III-16) in order to arrive at expressions for H and K_c for the case of flow. However, in doing so, an incompatibility with an earlier assumption is met, namely, that $\partial C_1 / \partial y$ is independent of x [in Equations (III-12) and (III-14)], and the resulting expressions for H and K are invalid.

In an attempt to avoid this difficulty, Powers (P3) assumed that $\partial C_1/\partial y$ was not independent of x but varied linearly; that is,

$$\frac{\partial C_1}{\partial y} = (1 + \gamma x) f(y) \quad (\text{III-37})$$

This assumption made it possible to include a bulk flow rate term in the velocity distribution and hence to improve on the equations for the continuous flow case. However, as pointed out by Hoffman (H7), this assumption is not entirely satisfactory in that it fails to satisfy the condition

$$\frac{\partial}{\partial x} \left(\frac{\partial C_1}{\partial y} \right) = 0 \quad \text{at } x = \frac{1}{\omega} \quad (\text{III-38})$$

Hoffman stated that the function representing $\partial C_1/\partial y$ cannot be a polynomial of finite length, nor can it be a constant. Hoffman did not present an expression for $\partial C_1/\partial y$ but assumed that such a function would be of the form

$$\frac{\partial C_1}{\partial y} = f(y) \cdot \sum_{n=0}^{\infty} a_n \left(\frac{x}{\omega} \right)^n \quad (\text{III-39})$$

Application of the Transport Equation

Steady-State Batch Case

For the case with no bulk flow through the column, ($\sigma_e=0$), Equation (III-20) becomes

$$0 = \overline{C_1 C_2} H_e - \frac{\partial \overline{C_1}}{\partial y} K_e$$

(III-40)

Now if only concentrated solutions are considered ($0.3 < C_1 < 0.7$ weight fraction), Equation (III-40) can be simplified by assuming that $\overline{C_1 C_2} = 0.25$, and the resulting expression can be integrated to give

$$(C_e - C_F) = \Delta_e = \frac{H_e L_e}{4 K_e}$$

(III-41)

Equation (III-41) then gives the separation, Δ_e , for the enriching section of a column. A similar expression is found for the stripping section of the column, and the total steady-state batch separation, Δ_0 , is then

$$\Delta_0 = \Delta_e + \Delta_s \tag{III-42}$$

$$\Delta_0 = \frac{HL}{4K} \tag{III-43}$$

where the subscript indicates the absence of bulk flow, and L is the total column length ($L = L_e + L_s$). In Equation (III-43) it has been assumed that $H = H_e = H_s$ and $K = K_e = K_s$.

The ultimate, steady-state batch separation in a thermogravitational thermal diffusion column depends on the quotient of

two velocities: the velocity in the vertical direction brought about by the internal convective circulation, and the velocity of a given molecule in the horizontal direction resulting from thermal diffusion. The insertion of horizontal barriers into the separation space should not affect the velocity in the vertical direction since the internal circulation (or velocity) is independent of column length (See Equations (III-33) and (III-44).), and similarly the velocity in the horizontal direction should not be affected except in the immediate region around each barrier. Therefore, as a first approximation, one would predict from conventional theory that the addition of horizontal barriers in the separation space should, at best, not affect the batch steady-state separation. If an effective length is considered, then the barriers would tend to reduce the batch separation.

However, numerous experimental runs with barriers showed that the use of horizontal barriers in a column significantly increased the batch steady-state separation over the batch separation in the same column with no barriers. (See Figure 23.) In addition, Treacy and Rich (T6) (T7) have done experimental work with horizontal barriers in a concentric-cylinder column for the separation of a gaseous mixture of nitrogen and methane. Their data also show increased steady-state batch separations when barriers are introduced into the separation space. (The data of Treacy and Rich are presented and discussed in Appendix F.) Thus, a type of ex post facto

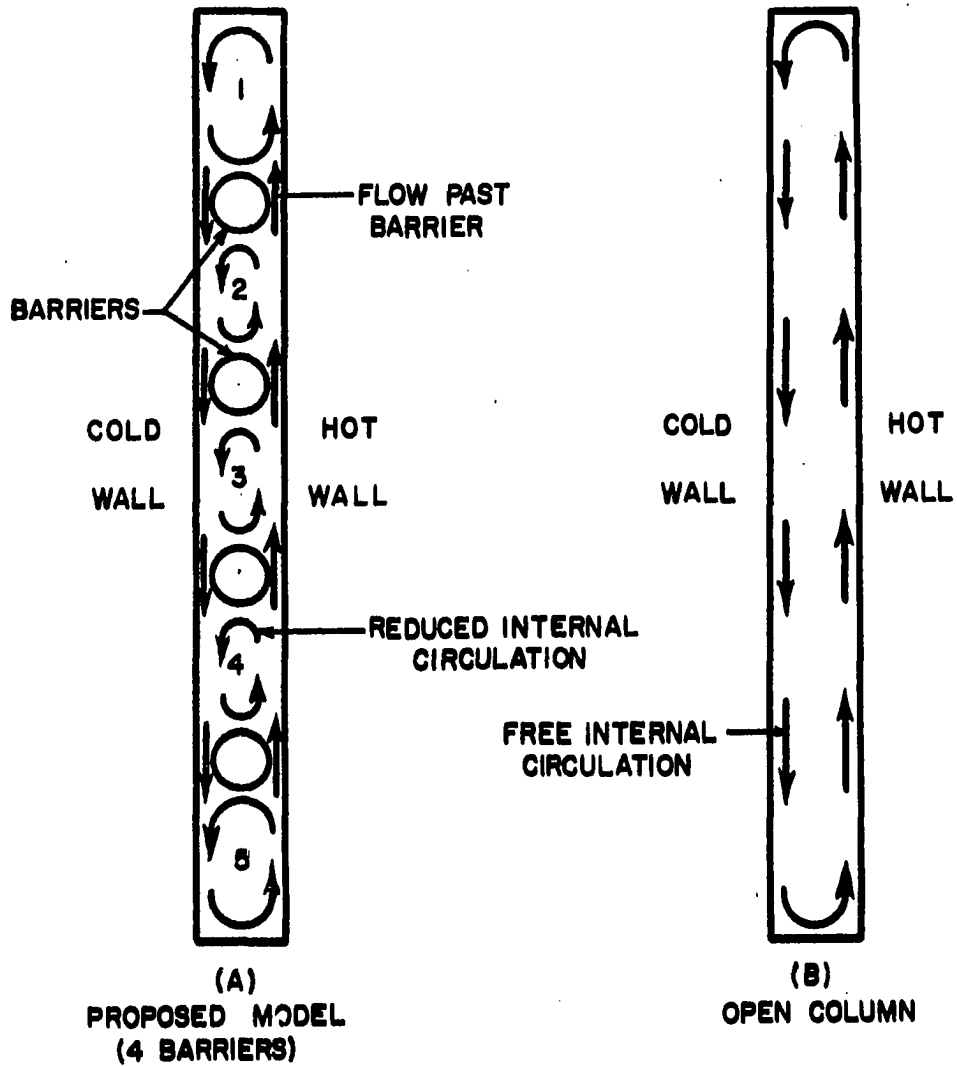
reasoning must be utilized in order to explain this apparent conflict with conventional theory.

As pointed out previously, the steady-state batch separation depends on the quotient of two velocities: the velocity in the vertical direction brought about by the internal circulation, and the velocity of a given molecule in the horizontal direction resulting from thermal diffusion. Now if the magnitude of the convective velocity were reduced relative to the horizontal flux, the horizontal flux would become more important and consequently increase the separation under batch conditions. In view of this and the experimental results with horizontal barriers, a model is suggested to explain the increased batch separations when horizontal barriers are introduced into the separation space.

Figure 2 shows the proposed model for a column with four equally-spaced horizontal barriers. The circulations in each of the five sections of the column (numbered 1 through 5 in the Figure) are equal, but are somewhat smaller than the free circulation in the open column (open column meaning no objects in the separation space). The reduced circulation can be explained by a "turn-around" effect at the ends of each of the five small sections shown in Figure 2. At the ends, part of the circulating fluid flows past the barriers whereas the majority of the fluid is "turned around" and flows back the opposite side of the column. During this turn around, there is a

Figure 2

Proposed Model for a Column with Horizontal
Barriers: Batch Case



NOTE: NOT TO SCALE

small loss of momentum, and the magnitude of the circulation is reduced slightly. The relative amount of fluid that flows past the barriers is thought to be dependent on the barrier diameter to plate spacing ratio and also proportional to the magnitude of the internal circulation. This flow past the barriers will be discussed in more detail later in this chapter.

With the above model, Equation (III-33) can be modified to account for the introduction of horizontal barriers:

$$\text{No Barriers: } v(x) = \frac{\beta T g \Delta T}{12 \omega \eta} (x^3 - \omega^2 x) \quad (\text{III-33})$$

$$\text{N Barriers: } v(x) = \frac{\beta T g \Delta T}{12 \omega \eta} (x^3 - \omega^2 x) \frac{1}{(1 + bN)} \quad (\text{III-44})$$

where

N is the number of horizontal barriers, and

b is an empirical constant.

The above modification follows from the fact that the momentum loss should be proportional to the number of barriers, and hence the convective velocity inversely proportional to the number of barriers.

Now if the velocity distribution given by Equation (III-44) is substituted in Equations (III-15) and (III-16) and the integrations

carried out, the resulting expressions for H^N and K_c^N , K_d^N and K^N are

$$H^N = \frac{\alpha \beta_T \rho g (2\omega)^3 B (\Delta T)^2}{6! \eta \bar{T} (1 + bN)} \quad (\text{III-45})$$

$$K_c^N = \frac{\beta_T^2 \rho g^2 (2\omega)^7 B (\Delta T)^2}{9! D \eta^2 (1 + bN)^2} \quad (\text{III-46})$$

$$K_d^N = 2 \omega \rho B D \quad (\text{III-47})$$

$$K^N = K_c^N + K_d^N \quad (\text{III-48})$$

where the remixing term, K_p , has again been neglected.

Finally, recalling Equation (III-43), and assuming that H^N and K^N are the same for each of the $(N + 1)$ small columns, the expression for the steady-state batch separation with N horizontal barriers is

$$\Delta_0^N = \frac{H^N L}{4K^N} \quad (\text{III-49})$$

where the superscript indicates the number of horizontal barriers in the separation space, the subscript indicates the bulk flow rate as before, and L is the total column length.

A quick calculation shows that K_d^N is negligible in comparison to K_c^N for the column dimensions and system being considered in this work:

$$K_d^N = 2 \omega \rho B D \quad (\text{III-47})$$

$$K_d^N = (.0792 \text{ cm}) (.912 \frac{\text{gram}}{\text{cm}^3}) (9.21 \text{ cm})$$

$$(1.07 \times 10^{-5} \frac{\text{cm}^2}{\text{sec}}) (60 \frac{\text{sec}}{\text{min}})$$

$$K_d^N = .00043 \frac{\text{gram-cm}}{\text{min}}$$

Since values of K_c^N are in the range from one to ten for this work with barriers, it is apparent that K_d^N can be neglected. Therefore, Equation (III-49) can be written simply

$$\Delta_o^N = \frac{H^N L}{4K_c^N} \quad (\text{III-50})$$

Substituting for the H and K's in Equations (III-43) and (III-50) yields

$$\Delta_o^0 \text{ (No Barriers)} = \frac{126^a D \eta L}{\beta_T g (2\omega)^4 T} \quad (\text{III-51})$$

and

$$\Delta_o^N \text{ (N Barriers)} = \frac{126^a D \eta L (1 + bN)}{\beta_T g (2\omega)^4 T} \quad (\text{III-52})$$

However, one additional effect, a length correction, must be included in Equation (III-52) before a satisfactory expression for the ratio of the batch separations can be obtained. The barriers create a zone of essentially constant temperature between the plates. This is because the stainless steel barriers have a much higher thermal conductivity than that of the surrounding alcohol-water solution (by a factor of about forty). This area of constant temperature disturbs the linear temperature gradient between the plates and reduces the separation in the region of disturbance. In addition, the "turn-around" effect mentioned previously necessitates still another length correction. This correction arises from the fact that a finite length is needed for the velocity distribution to be re-established as part of the fluid flowing by convection reverses its direction of flow. That is, in each of the $(N + 1)$ small columns created by the N barriers, (See Figure 2.) there is a convective flow of fluid, up at the hot plate and down at the cold plate. Near the top and bottom of each small column, a portion of the convective stream reverses its direction of flow: part of the stream moving upwards at the hot plate reverses direction and moves downwards at the cold plate, and vice-versa. (Recall that part of the convective stream flows past the barrier.)

The length correction then is composed of the sum of the above two effects: the disturbance of the linear temperature gradient

created by the barriers, and the length necessary to re-establish the velocity distribution at the ends of each of the small columns. The two effects can be combined into a single term, which shall be designated l_r , and defined as the length of the disturbance created by a single horizontal barrier. Introducing l_r in Equation (III-52) gives

$$\Delta_o^N = \frac{126 \alpha D \eta (L - Nl_r) (1 + bN)}{\beta_T g (2\omega)^4 T} \quad (\text{III-53})$$

where $(L - Nl_r)$ is an "effective length" term.

Dividing Equation (III-53) by Equation (III-51) shows that the ratio of the batch separation obtainable with N barriers to the steady-state batch separation obtainable in the open column is simply

$$\frac{\Delta_o^N}{\Delta_o^0} = (1 + bN) \left(\frac{L - Nl_r}{L} \right) \quad (\text{III-54})$$

An attempt was made on a semi-theoretical basis to estimate the magnitude of l_r . (See Appendix D.) A value of seven plate spacings per barrier ($l_r = 0.55$ cm) was obtained for a length correction factor for the binary system and column conditions considered in this work. Although this value of the length correction factor is certainly not exact, it gives one an order of magnitude value which can be used to calculate batch separations from Equation (III-54).

Transient Batch Case

Equation (III-4) was derived earlier by combining the basic rate equation, Equation (III-1), Fick's law, an expression describing the convective velocity, $v(x)$, and the continuity conditions:

$$\frac{\partial C_1}{\partial t} = D \left(\frac{\partial^2 C_1}{\partial x^2} + \frac{\partial^2 C_1}{\partial y^2} \right) - \frac{\alpha D}{T} \frac{dT}{dx} \frac{\partial}{\partial x} (C_1 C_2) - v(x) \frac{\partial C_1}{\partial y} \quad (\text{III-4})$$

As pointed out previously, the nonlinearity of Equation (III-4) makes it difficult to obtain a rigorous solution. However, by following the procedure developed by Furry, Jones, and Onsager (F7) the right-hand side of Equation (III-4) was reduced to a function of y alone; the resulting equation was Equation (III-20). Furry, Jones and Onsager obtained a somewhat more general transport equation than Equation (III-20), and for the batch case it can be written

$$\tau_1 = H \overline{C_1 C_2} - K \frac{\partial C_1}{\partial y} \quad (\text{III-55})$$

where τ_1 is the net amount of one component which passes through a cross-section normal to the walls of the thermogravitational column. Powers (P4) (P5) has pointed out that Equation (III-55) can be used to study the transient behavior of a thermal diffusion column by combining it with the continuity conditions (for a differential length of column) from which one gets

$$\mu \frac{\partial \bar{C}_1}{\partial t} = \frac{\partial^2 \bar{C}_1}{\partial y^2} K - \frac{\partial(\bar{C}_1 \bar{C}_2)}{\partial y} H$$

(III-56)

where μ is the amount of solution per unit length of column.

$$\mu = 2\omega B\rho$$

(III-57)

Von Halle (V3) has obtained a general solution to an equation of the same form as Equation (III-56). In addition, Powers has presented a restricted solution of Equation (III-56). Powers' restricted solution will be presented here because it applies to the restricted experimental region investigated ($\bar{C}_1 \bar{C}_2 = 0.25$), and because the final equation is much simpler than Von Halle's general solution.

In order to obtain an analytical solution for Equation (III-56), Powers considered only the case in which a constant average value of the product of concentrations, $\bar{C}_1 \bar{C}_2$, could be used. Therefore, assume $\bar{C}_1 \bar{C}_2 = 0.25$ and Equation (III-56) reduces to

$$\mu \frac{\partial \bar{C}_1}{\partial t} = K \frac{\partial^2 \bar{C}_1}{\partial y^2}$$

(III-58)

Equation (III-58) is readily solved by separation of variables and subsequent expansion in a Fourier series subject to the following boundary conditions:

- (1) The composition at every point in the column is known at the beginning. That is, at $t = 0$, the composition is uniform and equal to C_F throughout the column. Mathematically

$$C = C_F \quad \text{for all } y \text{ at } t = 0 \quad (\text{III-59})$$

- (2) The ends of the column ($y = \pm L$) are impervious to flow; hence, the flux described by Equation (III-55) is zero at the ends of the column. In mathematical terms

$$\frac{\partial C_1}{\partial y} = \frac{H}{K} \overline{C_1 C_2} \quad \text{at } y = \pm L \text{ for all } t \quad (\text{III-60})$$

- (3) Assume that the column is symmetrical about $y = 0$ (the vertical center of the column) and that the composition does not change at this point; that is,

$$C = C_F \quad \text{at } y = 0 \quad \text{for all } t \quad (\text{III-61})$$

Applying these boundary conditions, the solution of Equation (III-58) is

$$\Delta = C_e - C_s = \frac{\overline{C_1 C_2} H L}{K} \left[1 - \frac{8}{\pi^2} \sum_{n=0}^{\infty} \frac{e^{-\frac{(2n+1)^2 \pi^2 K t}{L^2 \mu}}}{(2n+1)^2} \right] \quad (\text{III-62})$$

where L is the total length of the column, and, as before, the subscripts e and s refer to the enriching and stripping sections respectively. At steady-state ($t = \infty$)

$$\Delta_{\infty} = \frac{\overline{C_1 C_2} H L}{K} \quad (\text{III-63})$$

so that

$$\frac{\Delta}{\Delta_{\infty}} = \left[1 - \frac{8}{\pi^2} \sum_{n=0}^{\infty} \frac{e^{-\frac{(2n+1)^2 \pi^2 K t}{L^2 \mu}}}{(2n+1)^2} \right] = f(\xi) \quad (\text{III-64})$$

where ξ is a dimensionless time quantity defined by

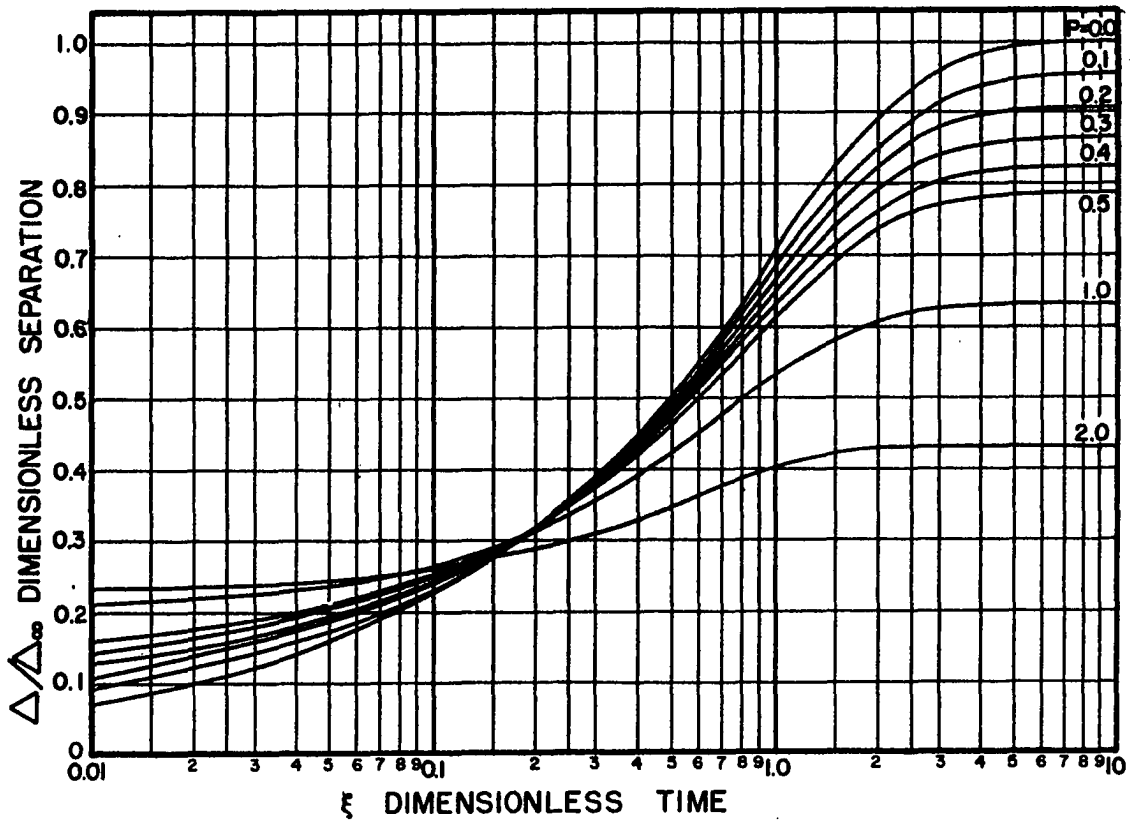
$$\xi = \frac{\pi^2 K t}{L^2 \mu} \quad (\text{III-65})$$

Figure 3 gives Δ / Δ_{∞} as a function of the dimensionless time factor, ξ , and the curve for $P = 0$ is the curve given by Equation (III-64).

Hoffman (H7) has treated the general case of the approach to equilibrium in columns with continuous bulk flow. In addition, Vichare (V2) recently has completed an investigation of the effect of the rate of sampling on the transient behavior of a thermogravitational column (without reservoirs). Heretofore it has been assumed implicitly that sampling (necessary to determine column performance as a function of time) did not affect the transient behavior of a column. However, it is apparent that sampling does indeed impose a bulk flow

Figure 3

Dimensionless Separation As a Function of Dimensionless Time with Dimensionless Sampling (Flow) Rate As a Parameter



on the column, and certainly frequent sampling would alter the transient behavior of a column. In order to approximate the magnitude of the error introduced by sampling, Vichare assumed that the intermittent sampling effectively imposed a small but continuous bulk flow, σ , on the column where σ is the total mass of sample collected divided by the total time of the transient run. In other words, a column with continuous feed and product drawoffs of σ should give the same transient behavior as a column where sampling is done at periodic, short intervals, the total masses withdrawn at the end of the transient run being equal.

Vichare presented his results with a dimensionless flow, P , as the parameter:

$$P = \frac{\sigma L}{K} \quad (\text{III-66})$$

where

σ is the mass flow per unit time,

L , the total column length, and

K , the constant defined by Equations (III-18), (III-35), and (III-36).

For the true batch case, $\sigma = P = 0$. As P increases, the deviation from the true batch case increases, and for values of P greater than one-tenth, the deviation becomes appreciable. (See Figure 3.)

The transient behavior of a column with no bulk flow and with no objects in the separation space can be predicted through use

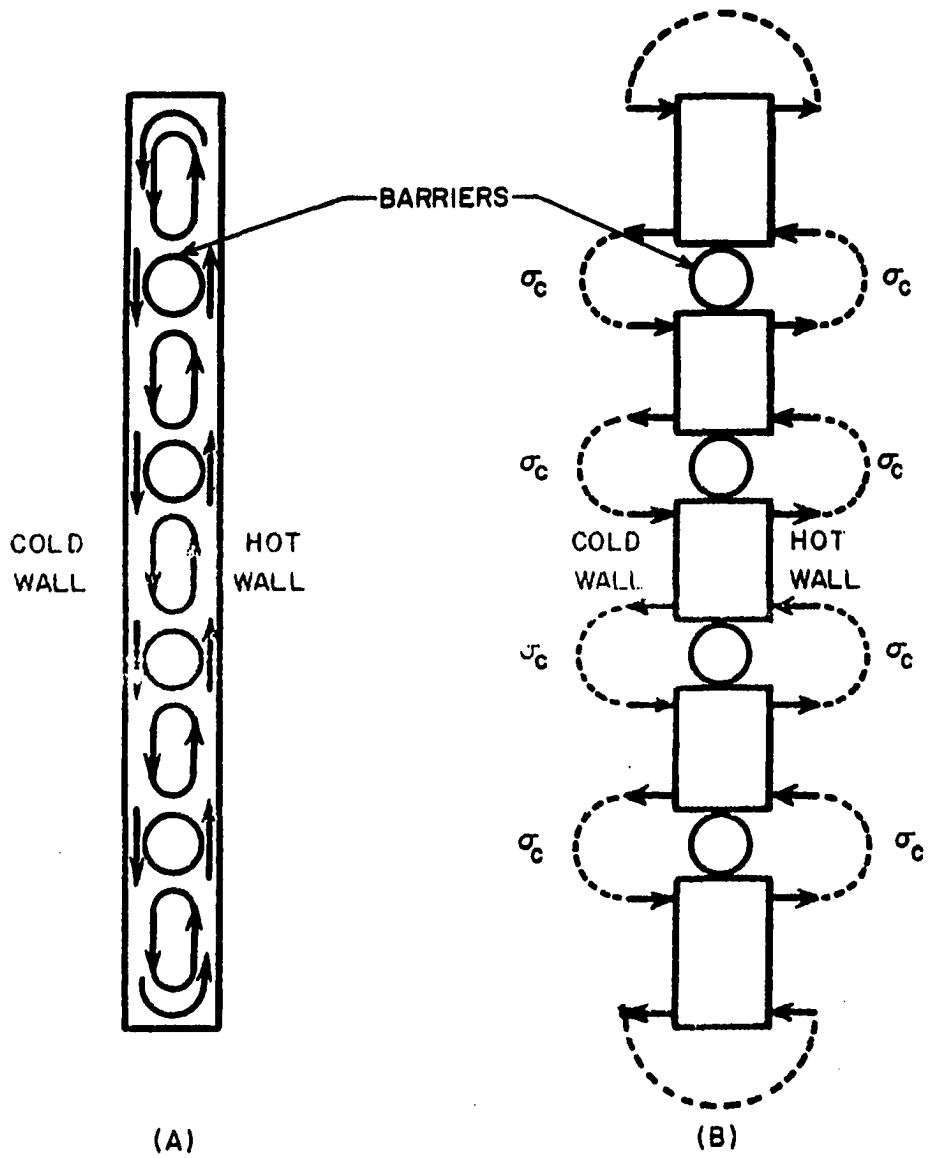
of Equation (III-64). It can be seen from this Equation [or Equation (III-65)] that the time required to reach a given separation in the open column is proportional to the square of the column length.

Consider now Figure 4A. The first part of the Figure shows a column with four equally-spaced horizontal barriers. The second part of the Figure shows an analogous case; that is, a column with four equally-spaced barriers is analogous to five smaller columns interconnected by the streams σ_c . The streams σ_c are all equal, and are caused by the convective circulation forcing fluid past the barriers.

Now consider each of the small columns shown in Figure 4B. Recall that for the conditions existing in these small columns (small separations in which the product $\overline{C_1 C_2} = 0.25$), the time to reach equilibrium is proportional to the square of the column length. [See Equation (III-65).] Thus, each small column will reach equilibrium twenty-five times faster than a similar column five times as long. Assume then that each of the small columns reaches equilibrium instantaneously, and that there is communication between the columns via the equal streams, σ_c . Further, assume symmetry about the x-axis; that is, the separation will equal $2(C_e - C_F)$. At time zero, the columns are all filled with feed solution, C_F . At time zero plus, all of the small columns will have reached their equilibrium separation (because of the assumption of instantaneous equilibrium) and, in fact, the separation, which shall be designated Δ_B , will be

Figure 4

Proposed Model for a Column with Horizontal
Barriers: Transient Case



the same for each of the columns above the center column and twice as large as the separation in the center column, which shall be designated Δ_L . This is simply because the batch separation is proportional to column length, and the columns above the center column are twice as long as the column cut by the x-axis.

Notice that the top of any of the small columns in Figure 4B is enriched in a given component while the bottom of the same column is stripped of the component. Therefore, enriched material is carried upwards and stripped material is carried downwards by the streams σ_c . Thus, as time passes, there will be a net transfer of one component up the column and of the other component down the column, so that, although the separation remains constant for each of the small columns, the average concentration changes. Therefore, the concentration difference between any two columns, one above the x-axis and one below, must change with time.

Consider now any column, n, in the enriching section with end-feeds such as the one shown in Figure 5. A material balance around the column gives

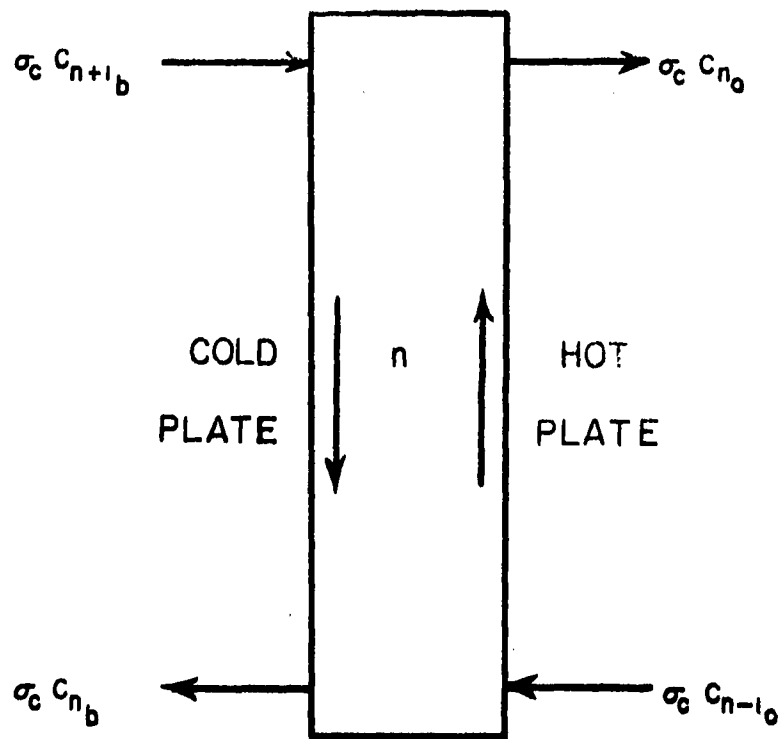
$$\rho \quad V \frac{d\bar{C}_n}{dt} = \sigma_c (C_{n+1_b} + C_{n-1_o} - C_{n_o} - C_{n_b}) \quad (\text{III-67})$$

where

ρ is the mean density of the fluid in column n,

Figure 5

Small Column with End-Feeds: No Bulk Flow



$$\Delta_B = C_{n_0} - C_{n_b}$$

AVERAGE CONCENTRATION IN
COLUMN = \bar{C}_n

V , the volume of any column n ,

\bar{C}_n , the average concentration of component 1 in column n ,

C_{n+1b} , the concentration of component 1 in the stream leaving the bottom of column $(n + 1)$,

C_{n-1o} , the concentration of component 1 in the stream leaving the top of column $(n-1)$, and

C_{no} , C_{nb} , the concentrations of component 1 in the streams leaving the top and bottom of column n .

Since the separation in the small column has been assumed not a function of time:

$$C_{no} = \bar{C}_n + \frac{\Delta_B}{2} = \bar{C}_n + \frac{\Delta_\infty^N}{2(N+1)} \quad (\text{III-68})$$

$$C_{no} = C_{nb} + \frac{\Delta_\infty^N}{(N+1)} \quad (\text{III-69})$$

$$C_{n+1o} = C_{n+1b} + \frac{\Delta_\infty^N}{(N+1)} \quad (\text{III-70})$$

where Δ_∞^N is the steady-state batch separation for the column with N equally-spaced barriers. Substituting Equations (III-69) and (III-70) in Equation (III-67) yields

$$\frac{d\bar{C}_n}{dt} = \frac{\sigma_c}{\rho V} (C_{n+1o} + C_{n-1o} - 2C_{no}) \quad (\text{III-71})$$

Define $R \equiv \sigma_c / \rho V$ and substitute in Equation (III-71)

$$\frac{d\bar{C}_n}{dt} = R (C_{n+1} + C_{n-1} - 2C_n)$$

(III-72)

where the subscripts have been dropped since all concentrations refer to the stream leaving the top of a column. Equation (III-72) then describes the transient behavior of column n in the enriching section as a function of the overhead concentrations in columns $(n + 1)$ and $(n - 1)$. Equation (III-72) is valid for only one point (the top) in the column, but since experimental measurements were made at this point, this is the point of interest. It should be pointed out again that symmetry about the x -axis has been assumed; consequently, an expression similar to Equation (III-72) can be written for any column n in the stripping section (below the point of symmetry).

There are two columns above and two columns below the point of symmetry (the x -axis), however, which do not satisfy Equation (III-72): the uppermost (or bottom-most) column which has no streams entering or leaving one end, and the center column (cut by the x -axis) which is but one-half as long as the other columns. For the uppermost column a material balance yields

$$\frac{d\bar{C}_{N+1}}{dt} = R \left[C_N - C_{N+1} + \frac{\Delta_{\infty}^N}{(N+1)} \right]$$

(III-73)

and for the center column

$$C_1 = C_F + \frac{\Delta_{\infty}^N}{2(N+1)}$$

(III-74)

where

C_F is the concentration of component 1 at the point of symmetry where the concentration does not change with time, and

C_1 is the concentration of component 1 in the stream leaving the top of the center column. The columns are numbered from the center column up.

In order to solve the above equations, it is convenient to remove them from the time domain by use of the Laplace transformation. The Laplace transform of Equation (III-72) is

$$C_n(s) = \frac{R}{s + 2R} \left[C_{n+1}(s) + C_{n-1}(s) + \frac{\Delta_\infty^N}{2R(N+1)} \right] + \frac{C_F}{s + 2R} \quad (\text{III-75})$$

Similarly, the transform of Equation (III-73) is

$$C_{n+1}(s) = \frac{R}{s + R} \left[C_n(s) + \frac{\Delta_\infty^N(s+2R)}{2Rs(N+1)} \right] + \frac{C_F}{s + R} \quad (\text{III-76})$$

and of Equation (III-74) simply

$$C_1(s) = \frac{C_F}{s} + \frac{\Delta_\infty^N}{2s(N+1)} \quad (\text{III-77})$$

Thus, for any number of equally-spaced horizontal barriers, N , a system of equations will result consisting of $(N-2)/2$ equations of the type given by Equation (III-75), one equation of the type given by Equation (III-76), and one equation of the type given by Equation (III-77). It is comparatively easy to solve the system of equations

for small N , but the problem becomes progressively more difficult as N gets larger. The problem essentially is one of finding the inverse transform of the solved system of equations. The inverse of the solution places it again in the time domain and gives the desired time-dependent solution. In general, finding the inverse transform entails finding the roots of a $(N/2)$ th order polynomial where N is again the number of barriers. Values of N of zero, two, four, eight, sixteen, and fifty were considered in the transient run with barriers. For $N = 0$, the system of equations is simply

$$C_1(s) = \frac{C_F}{s} + \frac{\Delta_{\infty}^{N=0}}{2s} \quad (\text{III-78})$$

and inverting gives

$$(C_1 - C_F) = \frac{\Delta_{\infty}^{N=0}}{2} \quad (\text{III-79})$$

or, since $(C_1 - C_F) = \frac{\Delta}{2}$,

$$\frac{\Delta}{\Delta_{\infty}^{N=0}} = 1.0 \quad (\text{III-80})$$

which arises from the fact that instantaneous equilibrium was assumed.

For $N = 2$, the system of equations is

$$C_2(s) = \frac{R}{s+R} \left[C_1(s) + \frac{\Delta_{\infty}^{N=2} (s+2R)}{6Rs} \right] + \frac{C_F}{s+R}$$

(III-81)

$$C_1(s) = \frac{C_F}{s} + \frac{\Delta_{\infty}^{N=2}}{6s}$$

(III-82)

Combining Equations (III-81) and (III-82) yields

$$\left[C_2(s) - \frac{C_F}{s} \right] = \frac{\Delta_{\infty}^{N=2}}{6s} \left[\frac{(s+3R)}{(s+R)} \right]$$

(III-83)

and the inverse of Equation (III-83) yields

$$\frac{\Delta}{\Delta_{\infty}^{N=2}} = \frac{2}{3} (1 - e^{-Rt}) + \frac{1}{3}$$

(III-84)

For $t = 0$, $\Delta/\Delta_{\infty}^{N=2} = \frac{1}{3}$, which results from the assumption of instantaneous equilibrium in the small columns.

For four barriers, the system of equations yields a polynomial of second order (in the denominator) and a quadratic solution gives the roots for the inverse solution. (See Appendix H.) The eight barrier and sixteen barrier cases give fourth and eighth order polynomials, and the polynomial roots were obtained by multiple trial and error in this work. For really large values of N , the trial and error method of obtaining roots is cumbersome, and a computer is necessary.

It should be pointed out that it is unnecessary that N be an even number as implicitly assumed. If an odd number of barriers are equally-spaced, however, one barrier would fall on the x -axis, and all $(N + 1)$ columns formed by the N barriers (N odd) would be of equal length. Consequently, the case with N equally-spaced barriers (N odd) would yield a system of $\left(\frac{N - 1}{2}\right)$ equations of the type given by Equation (III-75), and one equation of the type given by Equation (III-76). For $N = 1$,

$$C_1(s) = \frac{R}{s + R} \left[\frac{C_F}{s} + \Delta_{\infty}^{N=1} \frac{(s + 2R)}{4Rs} \right] + \frac{C_F}{s + R} \quad (\text{III-85})$$

and the inverse yields

$$\frac{\Delta}{\Delta_{\infty}^{N=1}} = \frac{1}{2} + \frac{1}{2} (1 - e^{-Rt}) \quad (\text{III-86})$$

The calculation for $N = 3$ can be found in Appendix H.

The cases for $N = 0$ and $N = 1$ emphasize the error introduced by assuming instantaneous equilibrium in the small columns. However, the magnitude of the error introduced by this assumption can be approximated. Recall that the relaxation time in the $(N + 1)$ small columns is proportional to the square of the column length. The transient behavior of the columns can then be calculated using Equation (III-65) where $L^N = L/(N + 1)$ and where K is given by Equation (III-35). For $N = 0$, Equation (III-65) would then describe the transient behavior of the column directly. For other values of

N, Equation (III-65) can be used to introduce a correction, the magnitude of the correction depending on the magnitude of L^N .

This correction will be discussed again in Chapter VI.

Furthermore, it should be pointed out that it is not necessary that the barriers be equally-spaced in the column as assumed. However, there is no apparent advantage to spacing them otherwise, and the theoretical development becomes somewhat more involved mathematically since the separation, Δ_B , would not be the same for each small column.

Continuous Flow Case

Under conditions of continuous flow, feed is added to the center of the column and overhead and bottom products removed continuously from the ends of the column. In almost any conceivable industrial application, the flow case is the one of primary interest, since no appreciable amount of product can be obtained under batch conditions.

Now consider Equation (III-20) again. Although Jones and Furry (J8) have obtained a general solution to this form of the transport equation, a simplifying approximation can be made for the binary system investigated in connection with this work with barriers. The liquid mixtures were in the concentration range $0.3 < C_1 < 0.7$ weight fraction, and thus the product $\overline{Q C_2}$ can be approximated by $\overline{C_1 C_2} = 0.25$. With this simplification, Equation (III-20) reduces to

$$\sigma_e (C_e - \bar{C}_1) = \frac{H_e}{4} - \frac{\partial C_1}{\partial y} K_e \quad (\text{III-87})$$

Integration of Equation (III-87) over the length of the enriching section, L_e , yields

$$(C_e - \bar{C}_1) = \frac{H_e}{4\sigma_e} \left(1 - e^{-\frac{\sigma_e L_e}{K_e}}\right) \quad (\text{III-88})$$

Since \bar{C}_1 is the mean concentration of component 1 at the feed point, $\bar{C}_1 = C_F$, and Equation (III-88) can be written

$$(C_e - C_F) = \frac{H_e}{4\sigma_e} \left(1 - e^{-\frac{\sigma_e L_e}{K_e}}\right) \quad (\text{III-89})$$

An analogous procedure is followed for the stripping section of the column and the result is

$$(C_F - C_s) = \frac{H_s}{4\sigma_s} \left(1 - e^{-\frac{\sigma_s L_s}{K_s}}\right) \quad (\text{III-90})$$

The total separation in a column, enriching minus stripping composition, is given by

$$\Delta = C_e - C_s = \frac{H_e}{4\sigma_e} \left(1 - e^{-\frac{\sigma_e L_e}{K_e}}\right) + \frac{H_s}{4\sigma_s} \left(1 - e^{-\frac{\sigma_s L_s}{K_s}}\right) \quad (\text{III-91})$$

Equation (III-91) can be reduced if it is assumed that $H_e = H_s = H$, $K_e = K_s = K$, $\sigma_e = \sigma_s = \sigma$, and $L_e = L_s = \frac{L}{2}$, and the resulting equation is

$$\Delta = \frac{H}{2\sigma} \left(1 - e^{-\frac{\sigma L}{2K}} \right) \quad (\text{III-92})$$

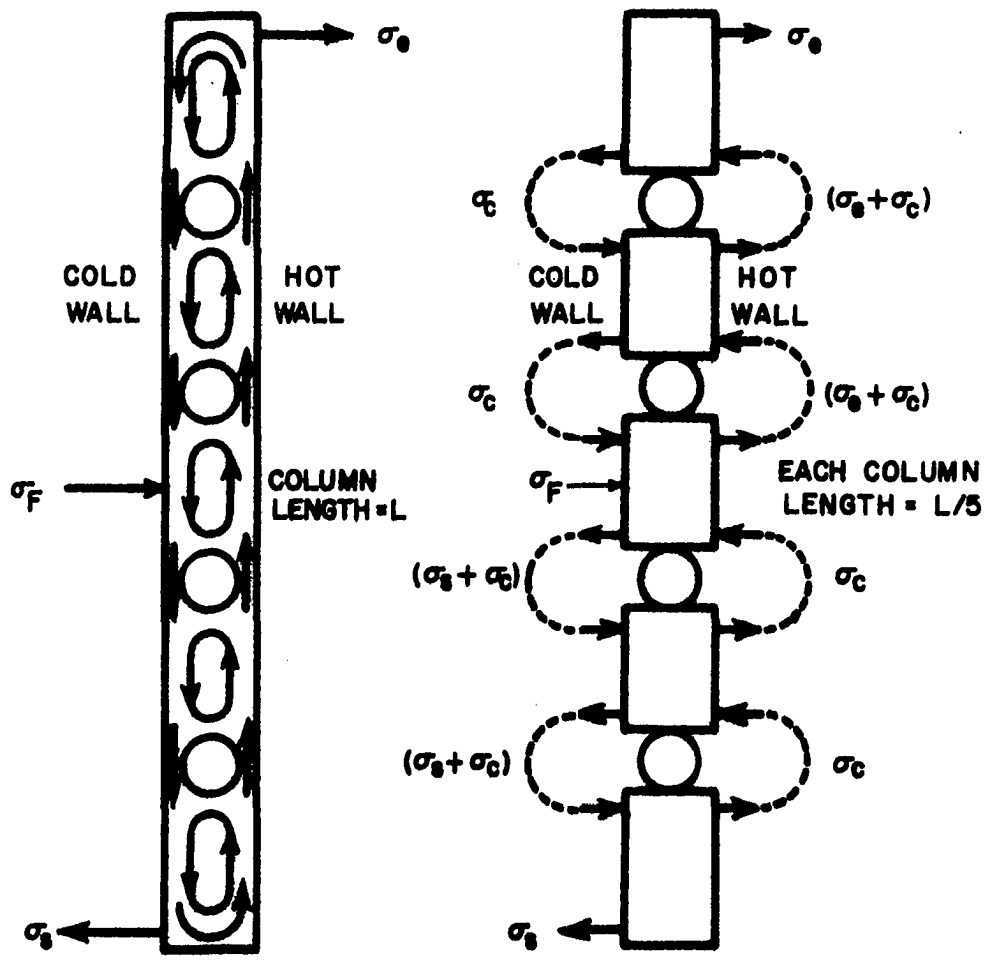
As noted previously, the constants H and K are from the batch case and are given by Equations (III-34) through (III-36).

Now consider the case of a column with N equally-spaced horizontal barriers. Figure 6 shows a situation similar to that in the previous section on the transient behavior of a column under batch conditions. As in the batch case, it is assumed that a column with N equally-spaced barriers performs effectively in the same manner as the sum of the separations given by the (N + 1) small columns. For the flow case, in addition to the flow, σ_c , brought about by the convective circulation, there is a bulk flow of σ_e grams/min through each column above the feed point and a flow of σ_s grams/min through each column below the feed point. That is, in contrast to the batch case, in the flow case each column has a net bulk flow of fluid passing through it. A material balance immediately makes this obvious since mass is continuously removed from overhead at a rate, σ_e , and removed from the bottom at a rate, σ_s . Therefore, the feed, σ_F , must equal ($\sigma_e + \sigma_s$).

It is assumed that σ_e joins the stream σ_c flowing upward near the hot plate in the enriching section, and that σ_s joins the stream σ_c flowing downward near the cool plate in the stripping

Figure 6

Proposed Model for a Column with Horizontal Barriers:
Continuous Feed and Product Withdrawal



section. In other words, it is assumed that the bulk flow does not oppose the convective flow. It is further assumed that the addition of bulk flow does not alter the velocity distribution, $v(x)$, for the batch case [defined by Equation (III-44)]. A similar assumption originally was made by Jones and Furry (J8), and it has been proven satisfactory except for high flow rates. (P3)

The concentration difference between the overhead and bottom streams leaving each of the small columns with end-feeds (See Figure 7.) is given by a modification of Equation (III-89) for the enriching section of the column:

$$(C_{n_o} - C_{n_b}) = \frac{H_e^N}{4 \sigma_e} \left[1 - e^{-\frac{\sigma_e L}{K_e^N (N+1)}} \right] \quad (\text{III-93})$$

where

C_{n_o} is the concentration of component 1 in the overhead stream from column n ,

C_{n_b} , the concentration of component 1 in the bottom stream from column n ,

σ_e , the bulk flow rate, and

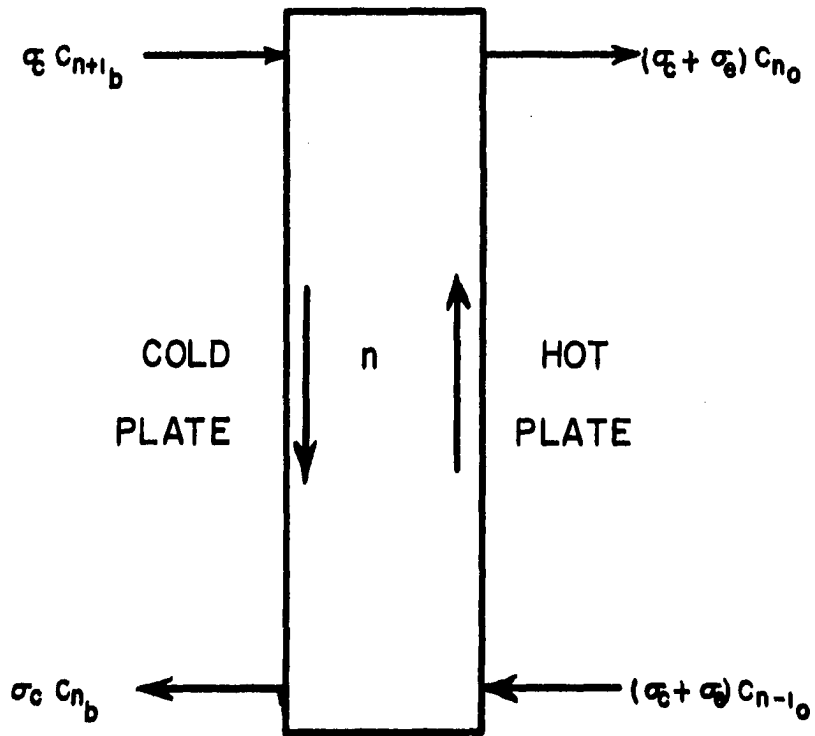
L , the total length of the column containing N horizontal barriers. The length of the small column, n , is given by $L/(N + 1)$. Finally,

H_e^N is the constant defined by Equation (III-45), and

K_e^N , the constant defined by Equation (III-46). Both of the latter constants are for the batch case.

Figure 7

Small Column (in Enriching Section) with End-Feeds:
Continuous Feed and Product Withdrawal



Thus, if the composition leaving the bottom of a small column is known, then the overhead composition can be calculated from Equation (III-92). Notice that the composition is flow-rate dependent; that is, the concentration difference between the overhead and bottom exit streams depends on the magnitude of the bulk flow rate, σ_e (or σ_s).

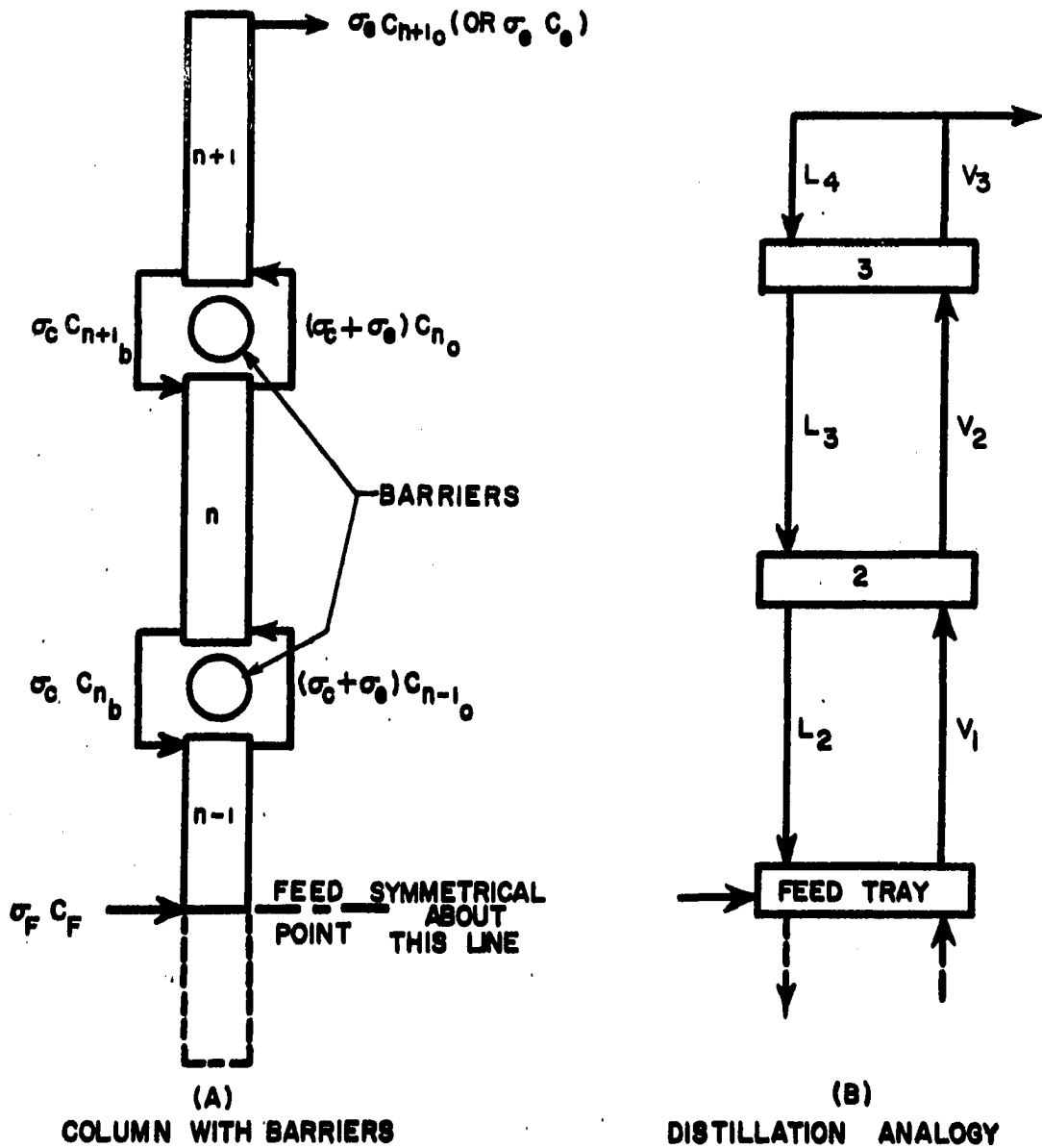
Consider now Figure 8A which shows the enriching section of a column with four equally-spaced horizontal barriers. The usual assumption of symmetry about the feed-point requires a modification of Equation (III-93) for the feed column since it is but one-half as long as the other columns (again assuming that the barriers are equally-spaced). With this modification for length, the equation expressing the concentration difference between the feed and the overhead exit stream from the feed column is

$$(C_{n-1O} - C_F) = \frac{H_e^N}{4 \sigma_e} \left[1 - e^{-\frac{\sigma_e L}{2K_e^N (N+1)}} \right] \quad (\text{III-94})$$

Thus, a calculation can be made from column to column much in the same manner as a plate to plate calculation in a distillation column. (See Figure 8B.) Equations (III-93) and (III-94) give relationships between the overhead and bottom streams leaving a column whereas a vapor-liquid equilibrium condition gives this relationship on a distillation tray. Material balances can then be made around the

Figure 8

Enriching Section of a Thermogravitational Column with Horizontal Barriers and Continuous Flow



small columns or around the individual distillation trays in order to obtain a sufficient number of relationships to solve for all unknowns.

Following this procedure of a column to column calculation, equations can be written relating the overhead and bottom streams leaving each of the columns in the enriching section shown in Figure 8A:

$$(C_e - C_{n+1b}) = \frac{H_e^N}{4\sigma_e} \left[1 - e^{-\frac{\sigma_e L}{K_e^N(N+1)}} \right] \quad (\text{III-95})$$

$$(C_{n_o} - C_{nb}) = \frac{H_e^N}{4\sigma_e} \left[1 - e^{-\frac{\sigma_e L}{K_e^N(N+1)}} \right] \quad (\text{III-96})$$

$$(C_{n-1_o} - C_F) = \frac{H_e^N}{4\sigma_e} \left[1 - e^{-\frac{\sigma_e L}{2K_e^N(N+1)}} \right] \quad (\text{III-97})$$

The above expressions give three equations but five unknowns: C_e , C_{n+1b} , C_{n_o} , C_{nb} , and C_{n-1_o} . Material balances made around each of the columns above the feed column yield two other equations:

$$\text{Mass In} = \text{Mass Out}$$

$$(\sigma_c + \sigma_e) C_{n_o} = \sigma_c C_{n+1b} + \sigma_e C_e \quad (\text{III-98})$$

$$\sigma_c C_{n+1b} + (\sigma_c + \sigma_e) C_{n-1o} = \sigma_c C_{nb} + (\sigma_c + \sigma_e) C_{no} \quad (\text{III-99})$$

The system of equations is solved by beginning with Equations (III-95) and (III-98) and solving for $(C_e - C_{n_o})$. Equation (III-96) is then used in conjunction with Equation (III-99) to solve for $(C_e - C_{n-1_o})$ and finally Equation (III-97) is used to find $(C_e - C_F)$. The result is

$$\Delta_e = (C_e - C_F) = \left(\frac{\sigma_c}{\sigma_c + \sigma_e} \right) \frac{H_e^N}{4\sigma_e} \left[1 - e^{-\frac{\sigma_e L}{K_e^N(N+1)}} \right] + \left(\frac{\sigma_c}{\sigma_c + \sigma_e} \right)^2 \times \frac{H_e^N}{4\sigma_e} \left[1 - e^{-\frac{\sigma_e L}{K_e^N(N+1)}} \right] + \frac{H_e^N}{4\sigma_e} \left[1 - e^{-\frac{\sigma_e L}{2K_e^N(N+1)}} \right] \quad (\text{III-100})$$

Defining

$$\zeta_e = \frac{\sigma_c}{\sigma_c + \sigma_e} \quad (\text{III-101})$$

$$\Delta_{B_e} = \frac{H_e^N}{4\sigma_e} \left[1 - e^{-\frac{\sigma_e L}{K_e^N(N+1)}} \right] \quad (\text{III-102})$$

$$\Delta_{L_e} = \frac{H_e^N}{4\sigma_e} \left[1 - e^{-\frac{\sigma_e L}{2K_e^N(N+1)}} \right] \quad (\text{III-103})$$

Equation (III-100) can be written

$$\Delta_e = \Delta_{B_e} (\zeta_e + \zeta_e^2) + \Delta_{L_e} \quad (\text{III-104})$$

which gives the separation in the enriching section of a column with four equally-spaced horizontal barriers.

A similar expression can be written for the stripping portion of the column:

$$\Delta_s = \Delta_{B_s} (\zeta_s + \zeta_s^2) + \Delta_{L_s} \quad (\text{III-105})$$

where

$$\zeta_s = \frac{\sigma_c}{\sigma_c + \sigma_s} \quad (\text{III-106})$$

$$\Delta_{B_s} = \frac{H_s^N}{4\sigma_s} \left[1 - e^{-\frac{\sigma_s L}{K_s^N(N+1)}} \right] \quad (\text{III-107})$$

and

$$\Delta_{L_s} = \frac{H_s^N}{4\sigma_s} \left[1 - e^{-\frac{\sigma_s L}{2K_s^N(N+1)}} \right] \quad (\text{III-108})$$

Finally, the total separation Δ^N is given by

$$\Delta^N = \Delta_e + \Delta_s$$

and for $N = 4$ the total separation is given by

$$\Delta^{N=4} = \Delta_{B_e} (\zeta_e + \zeta_e^2) + \Delta_{L_e} + \Delta_{B_s} (\zeta_s + \zeta_s^2) + \Delta_{L_s} \quad (\text{III-109})$$

Equation (III-109) can be simplified by assuming that $\Delta_{B_e} = \Delta_{B_s} = \Delta_B$ and $\Delta_{L_e} = \Delta_{L_s} = \Delta_L$ which yields

$$\Delta^{N=4} = 2 [\Delta_B (\zeta + \zeta^2) + \Delta_L] \quad (III-110)$$

Thus, Equation (III-110) gives the separation obtainable in a column with four equally-spaced horizontal barriers, with bulk flow rate $\sigma_e = \sigma_s$ and with convective flow past the barriers, σ_c . The expression for the separation given by N equally-spaced barriers follows easily and is

$$\Delta^N = 2 [\Delta_L + \Delta_B \sum_{n=1}^{\frac{N}{2}} \zeta^n] \quad (III-111)$$

where

$$\zeta = \frac{\sigma_c}{\sigma + \sigma_c} \quad (III-112)$$

and

$$\Delta_B = \frac{H^N}{4\sigma} \left[1 - e^{-\frac{\sigma L}{KN(N+1)}} \right] \quad (III-113)$$

$$\Delta_L = \frac{H^N}{4\sigma} \left[1 - e^{-\frac{\sigma L}{2K^N(N+1)}} \right] \quad (III-114)$$

Once again it should be pointed out that there is no reason the barriers should be equally-spaced in the column. However, as before, the general expression for N barriers is simplified by assuming the barriers equally-spaced, and there seems to be no advantage gained by an unequal spacing.

It has also been assumed in Equation (III-111) that N is again an even interger. If an odd number of equally-spaced barriers are used, one barrier will fall at the feed-point, and hence all (N + 1) columns are of the same length. Thus, there is no need to treat the feed column differently, and the case with N odd gives simply.

$$\Delta^N = 2 \left[\Delta_B \sum_{n=0}^{\frac{N-1}{2}} \zeta^n \right]$$

(III-115)

Flow of Fluid Past the Barriers: Evaluation of σ_c

The term for flow of fluid past the barriers, σ_c , is an important quantity in this work with horizontal barriers as can be seen by examining the equations describing the transient behavior of a column with barriers [Equations (III-75) and (III-76)] and also the equation describing the rate-separation curve for a column with barriers [Equation (III-111) in conjunction with Equation (III-112)]. Evaluation of this term, σ_c , must thus be considered.

It was felt that for conditions of laminar flow, the flow past the barriers should be proportional to the magnitude of the internal convective circulation. The flow should also be a function of the distance between the plates, or the barrier diameter to plate spacing ratio. Thus,

$$\sigma_c \propto \frac{(\text{Barrier Diameter})}{\text{Plate Spacing}} \times (\text{Convective Circulation}) \quad (\text{III-116})$$

or rewriting

$$\sigma_c = C (\text{Convective Circulation}) \quad (\text{III-117})$$

where the coefficient, C , is dependent on the barrier diameter to plate spacing ratio. The convective circulation can be obtained easily. In obtaining an expression for the circulation, it is convenient to consider an average value of the velocity over one-half the distance between the plates rather than a velocity distribution as a function of x . (The average velocity over the entire plate spacing is zero.) In the vicinity of the barrier, this velocity distribution as a function of x has little meaning, and hence the average velocity is more realistic. Therefore,

$$\text{Average velocity, } \bar{v} = \frac{1}{\omega} \int_0^{\omega} \frac{-\beta T g \Delta T}{12 \omega \eta} \frac{(x^3 - \omega^2 x)}{1 + bN} dx \quad (\text{III-118})$$

$$\bar{v} = \frac{\beta_T g \omega^2 \Delta T}{48\eta (1 + bN)} \quad (\text{III-119})$$

Finally, the circulation in mass per unit time is

$$\begin{aligned} \text{Circulation, grams per minute} &= \bar{v} \frac{\text{cm}}{\text{sec}} \times \\ \omega \text{ cm} \times B \text{ cm} \times \bar{\rho} \frac{\text{gram}}{\text{cm}^3} \times 60 \frac{\text{sec}}{\text{min}} \end{aligned} \quad (\text{III-120})$$

$$\text{Circulation} = \frac{5 \beta_T \rho g (2\omega)^3 B \Delta T}{32 \eta (1 + bN)} \quad (\text{III-121})$$

The convective circulation can thus be calculated from Equation (III-121), and the problem of obtaining a value for σ_c in Equation (III-117) becomes one of evaluating the coefficient, C. Rather than attempt to calculate a value for C (which might not be possible anyway), it was decided to obtain an empirical value of C for one particular barrier diameter to plate spacing ratio, and then experimentally determine values of C for other barrier diameter to plate spacing ratios by use of a model flow apparatus. (The plastic model is described in Chapter IV.) The theory behind the model is as follows.

For laminar flow, the drag imparted by a body on a flowing fluid is proportional to the flow past the body, and the drag is given by (H8)

$$F_D = a u \eta L_x \phi \left(\frac{L}{L'} \right) \quad (\text{III-122})$$

where

F_D is the drag or resistance of a single barrier,

a , a proportionality constant,

u , the bulk stream velocity,

η , the fluid viscosity,

L_x , the linear magnitude associated with the body (or barrier) parallel to the direction of motion, and

$\phi \left(\frac{L}{L'} \right)$, a dimensionless "shape ratio" function.

The quantity composed of the two constants, $a \phi \left(\frac{L}{L'} \right)$, is

dependent on the relative ratio of the barrier diameter to the distance between the plates and must be determined experimentally except in special cases, for example, when the plates are so far from the barriers as to not disturb the flow. In this case, it could be evaluated simply as a fluid streaming about a right circular cylinder. Combining these two constants, Equation (III-122) can be written

$$F_D = \frac{C u \eta d}{g_c} \quad (\text{III-123})$$

where

C is the coefficient or "drag factor" in this case,

d, the diameter of the barrier, and
 g_c , a dimensional constant.

In order to determine the cylinder drag, pressure drop measurements were taken as a function of the mass flow of fluid through the above-mentioned plastic flow apparatus. The drag force of the plates is given by (C12)

$$-\frac{dP}{dL} = \frac{12 u \eta}{g_c (2\omega)^2} \quad (\text{III-124})$$

where

$\frac{dP}{dL}$ is the pressure drop per unit length,

u, the average stream velocity, and

2ω , the distance between the plates.

The drag force was subtracted from the total pressure drop to give the cylinder drag.

The average stream velocity, u, was calculated by dividing the volumetric flow rate by the cross-sectional area of flow. This is one inadequacy that the plastic model has in that the average stream velocity used in Equations (III-123) and (III-124) is not the same as the velocity distribution existing between the hot and cold plates in a thermogravitational column. However, only the ratio of drag factors at the two cylinder diameter to plate spacing ratios was desired, not the absolute values, and it was felt that any error

incurred in using the average stream velocity, u , should be nearly the same for both of the cylinder diameters considered.

Results of the experimental work with the plastic flow model are found in Chapter VII.

Summary

The conventional thermogravitational thermal diffusion column theory developed by Furry, Jones, and Onsager has been reviewed in this chapter. The conventional theory does not predict an increase in the steady-state batch separation when horizontal barriers are introduced into the separation space, but it was found experimentally in this work, and in the work of Treacy and Rich with gases, that such an increase does occur. Thus, an ex post facto approach was used to modify the conventional theory. The modification is essentially a "correction" introduced to account for the loss of momentum by the circulating fluid in the vicinity of the barriers. The correction is the b -term introduced in Equation (III-44). The magnitude of b is small ($b = 0.035$ for this work), and thus the increase in the steady-state batch separation for a single barrier is small. The batch separation in a column with N equally-spaced horizontal barriers can be predicted by Equation (III-53)

$$\Delta_o^N = \frac{126 \alpha D \eta (L - Nl_r)(1 + bN)}{\beta_T g (2 \omega)^4 \bar{T}} \quad \text{(III-53)}$$

The effective length term $(L - Nl_r)$ in Equation (III-53) accounts for disturbances introduced by the barriers. These disturbances consist of (1) the disturbance of the linear temperature gradient between the plates in the region surrounding the barrier and (2) the disturbance of the velocity distribution near the ends of each of the $(N + 1)$ small columns created by the N barriers. The length correction, l_r , is seven plate spacings per barrier ($l_r = 0.55$ cm).

The batch, transient behavior of the series of $(N + 1)$ small columns formed by the barriers can be predicted by $\frac{(N - 2)}{2}$ equations of the type

$$C_n(s) = \frac{R}{s + 2R} \left[C_{n+1}(s) + C_{n-1}(s) + \frac{\Delta_{\infty}^N}{2R(N+1)} \right] + \frac{C_F}{s + 2R} \quad (\text{III-75})$$

one equation of the type

$$C_{n+1}(s) = \frac{R}{s + R} \left[C_n(s) + \frac{\Delta_{\infty}^N (s+2R)}{2Rs(N+1)} \right] + \frac{C_F}{s + R} \quad (\text{III-76})$$

and one equation of the type

$$C_1(s) = \frac{C_F}{s} + \frac{\Delta_{\infty}^N}{2s(N+1)} \quad (\text{III-77})$$

The above equations (in Laplace transform form) for the transient case were derived assuming an even number of equally-spaced barriers and assuming instantaneous equilibrium in each of the small

columns. Other equations are presented for the case when N is odd. Recalling that instantaneous equilibrium was assumed in the small columns, it is pointed out that correction is necessary when the time to equilibrium in the small columns becomes large enough to introduce an appreciable error (when N is small).

The continuous flow case was treated by again assuming that a column with N barriers performs in the same manner as the sum of the separations given by the $(N + 1)$ small columns. A rate-separation curve can be predicted by use of Equation (III-111)

$$\Delta^N = 2 \left[\Delta_L + \Delta_B \sum_{n=1}^N \zeta^n \right] \quad (\text{III-111})$$

where

$$\zeta = \frac{\sigma_c}{\sigma_c + \sigma} \quad (\text{III-112})$$

$$\Delta_B = \frac{H^N}{4\sigma} \left[1 - e^{-\frac{\sigma_L}{K^N(N+1)}} \right] \quad (\text{III-113})$$

and

$$\Delta_L = \frac{H^N}{4\sigma} \left[1 - e^{-\frac{\sigma_L}{2K^N(N+1)}} \right] \quad (\text{III-114})$$

The term R in Equations (III-75) and (III-76) and ζ in Equation (III-112) both contain the quantity σ_c , the flow past the barriers. It was felt that σ_c should be a function of the barrier

diameter to plate spacing ratio and proportional to the magnitude of the convective circulation. Values of σ_c can be obtained by use of Equation (III-117)

$$\sigma_c = C \cdot (\text{Convective Circulation}) \quad (\text{III-117})$$

if values of C are known for different barrier diameter to plate spacing ratios. [The convective velocity can be calculated from Equation (III-121).]

CHAPTER IV

EQUIPMENT

Chapter III presents a theoretical development from which the performance of a thermogravitational thermal diffusion column with horizontal barriers can be predicted. In order to test this theoretical development, it was necessary to obtain experimental data. The thermogravitational column used to acquire the data, the horizontal barrier systems, and the auxiliary equipment used in conjunction with the column are described in detail in this chapter. In addition, a description is given of the plastic model utilized to experimentally determine the ratio of C-values.

Thermogravitational Column and Auxiliary Equipment

The thermogravitational thermal diffusion column used in this work was of parallel-plate design as opposed to a concentric-cylinder type column. (See Figure 9.) The plates were fabricated from three-eighths inch 304 stainless steel plate and were approximately sixty inches long and six inches wide. The plates were ground flat on an industrial grinder and polished to a mirror-like finish with successively finer grades of emery paper (320-400-600).

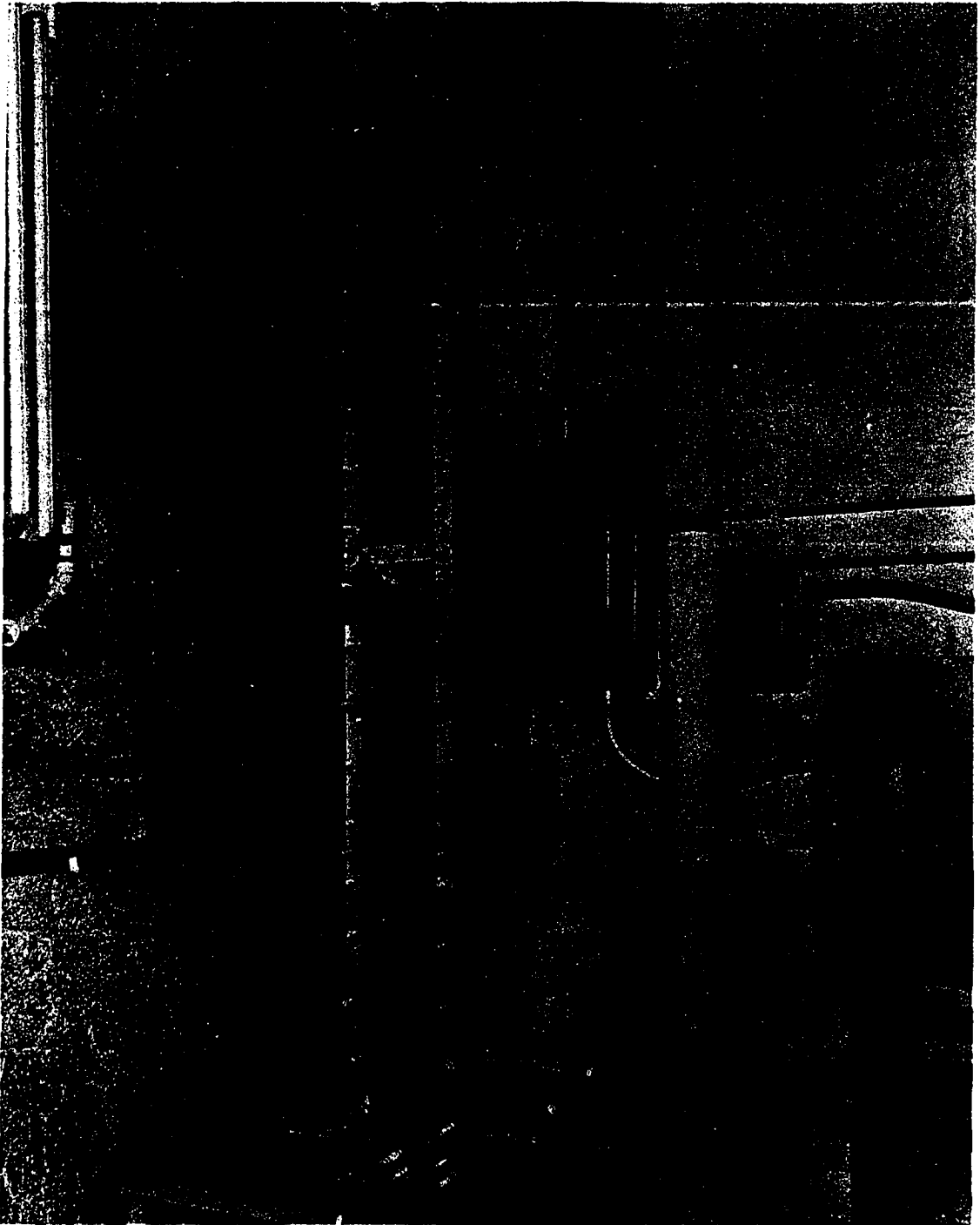


Figure 9

Thermogravitational Thermal Diffusion Column

One plate was heated by hot water and the other plate cooled by water which was colder than the hot water. The water jackets for the plates were formed by placing a rectangle fabricated from one-inch-square cadmium-plated steel bar behind each plate. (See Figure 10.) These rectangles served a dual purpose in that they added a considerable degree of rigidity to the plates as well as defining the water jacket volume. The final plate completing the water jacket was cut from one-eighth inch steel sheet and cadmium-plated to hinder corrosion. Each plate assembly (hot and cold) was bolted together with thirty-four bolts around its periphery and torqued to 100 inch-lbs. These thirty-four bolts remained in place at all times. In addition, eighteen bolts were used to bolt the two plate assemblies together, and these acted also to seal the water jackets. The water jacket gasket material was nylon-filled neoprene one inch wide and 0.015 inch thick. The material and thickness used for the water jacket gaskets were found to be critical because of leakage. Gasket surfaces were machined smooth to facilitate sealing.

Each plate had two copper-constantan thermocouples, one silver-soldered approximately midway between the feed inlet and overhead product outlet and the other approximately midway between the feed inlet and bottom product outlet. (See Figure 11 for thermocouple details.)

Figure 10

Components of One Transfer Plate with Water Jacket

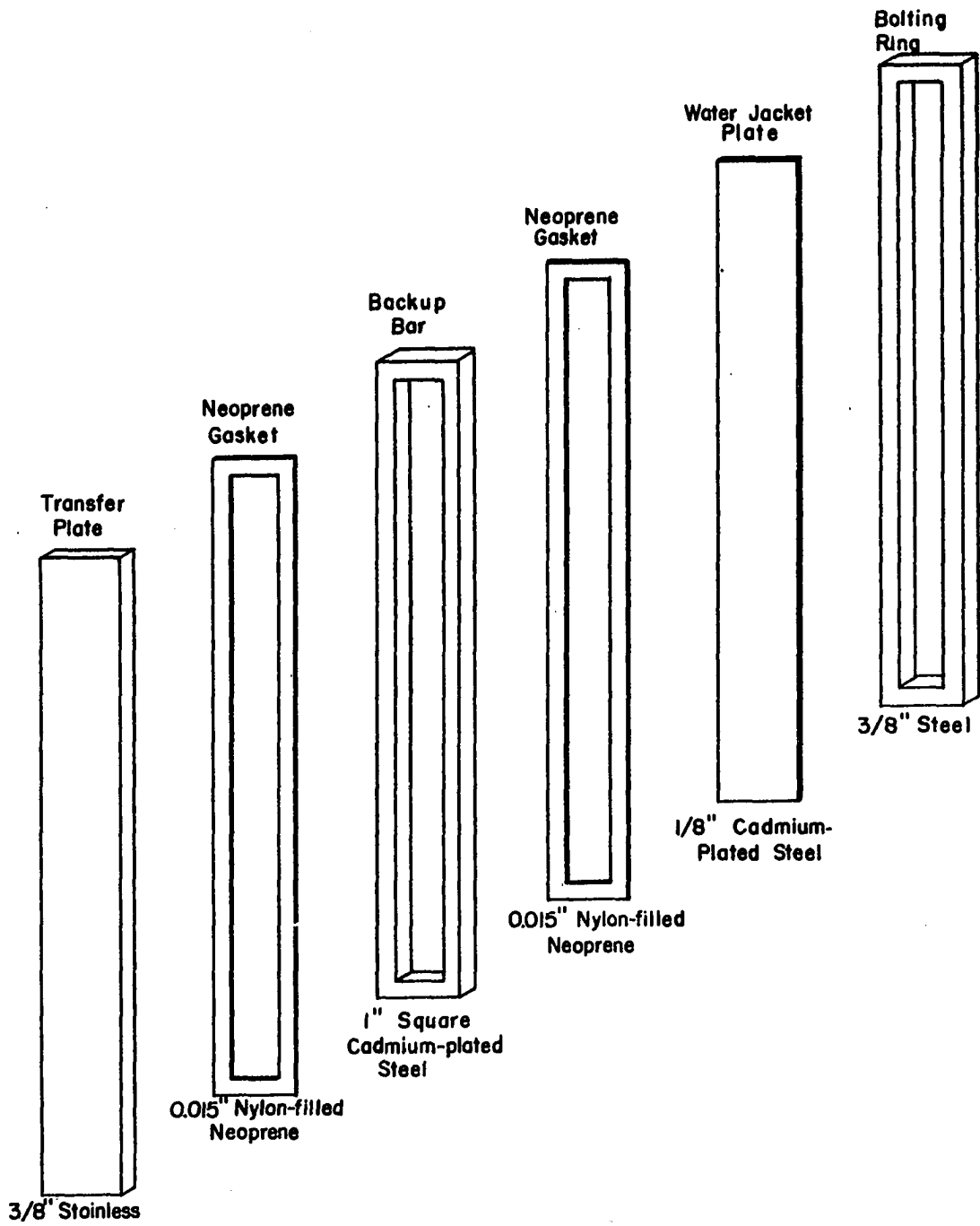
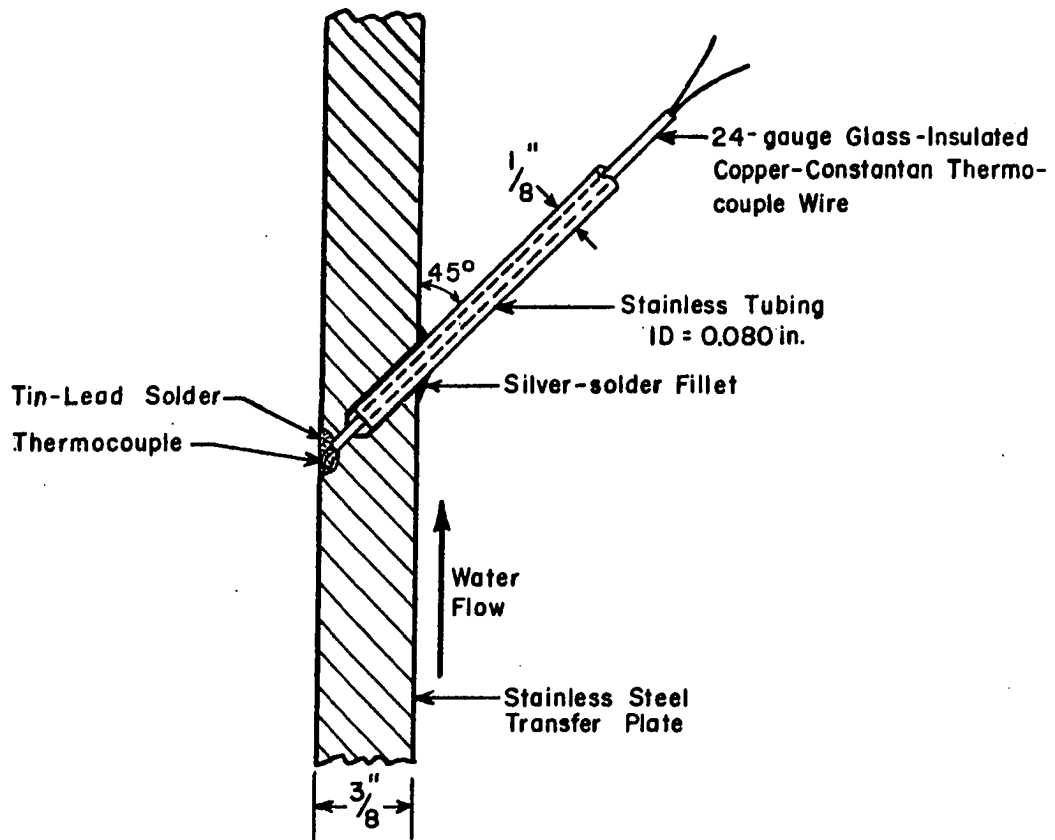


Figure 11

Detail of Thermocouple Installation in a Transfer Plate



Feeding the column was accomplished by gravity flow from a fifteen gallon aluminum feed barrel whose mean level was seven and one-half feet above the feed inlet. The feed level in the barrel was observed by means of a sight glass and its level was not allowed to vary more than one and one-half inches from the mean. The feed solution was degassed on leaving the feed barrel by passing it through a heater whose temperature was regulated with a Powerstat. In all cases the temperature of the feed solution leaving the heater was higher than the hot water temperature in the column. The gases released on heating the feed were vented through the sight glass which in turn was connected to a glass condenser cooled by tap water. (See Figure 12.) The feed solution was subsequently cooled before introduction into the column.

Feed entered the column through a feed port centered midway between the top and bottom of the cold plate. Feed was distributed laterally across the plate by means of a header and finally emerged through forty holes, one thirty-second of an inch in diameter, drilled equally-spaced in the inner three inches of the plate. (See Figure 13 for details of construction.) The overhead product drawoff port in the hot plate and bottom product drawoff port in the cold plate were constructed similarly.

Product samples were collected through the sample taps by gravity flow. The sample taps were basically twenty-six gauge 304

Figure 12

Gravity-Flow Feed System

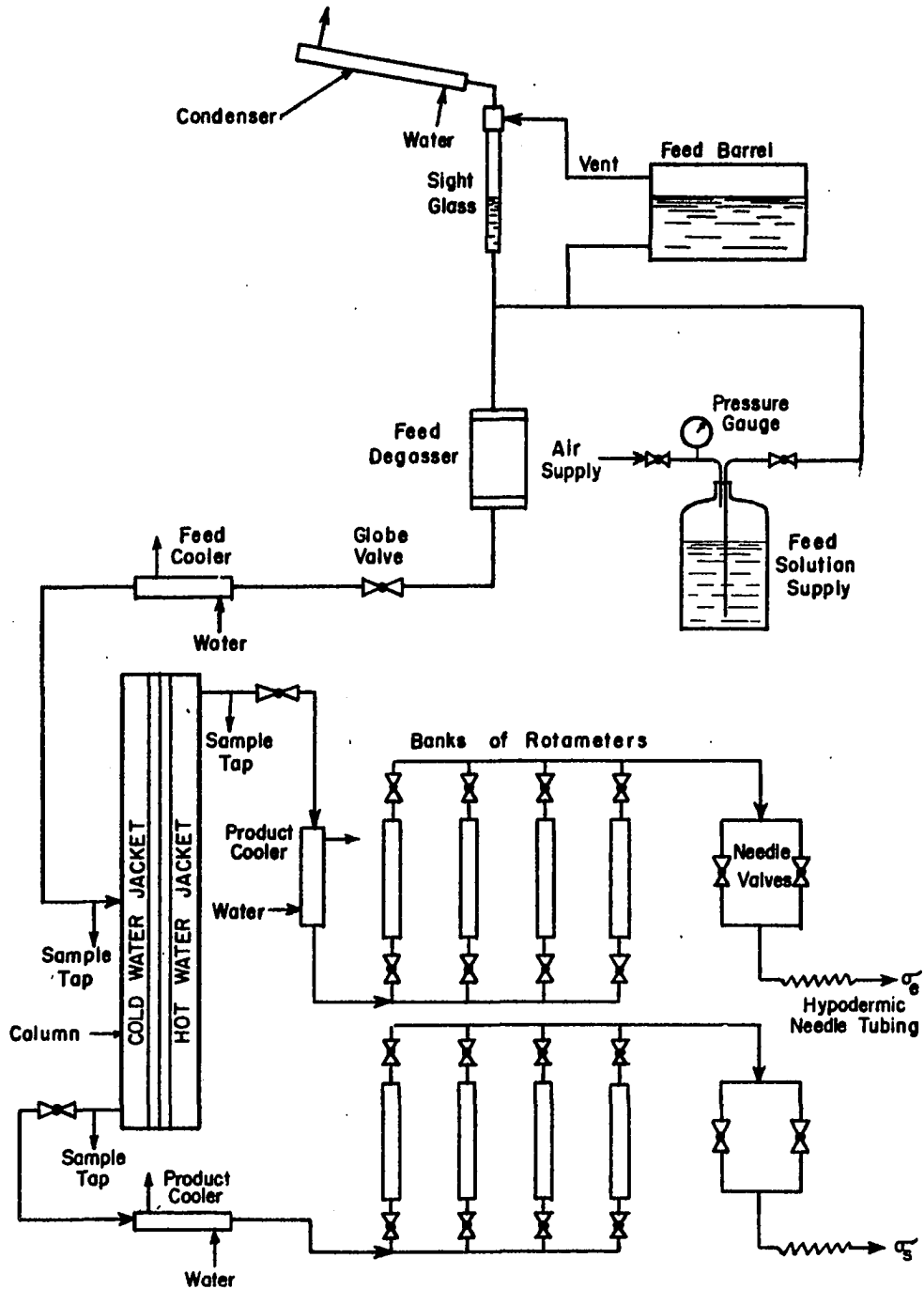
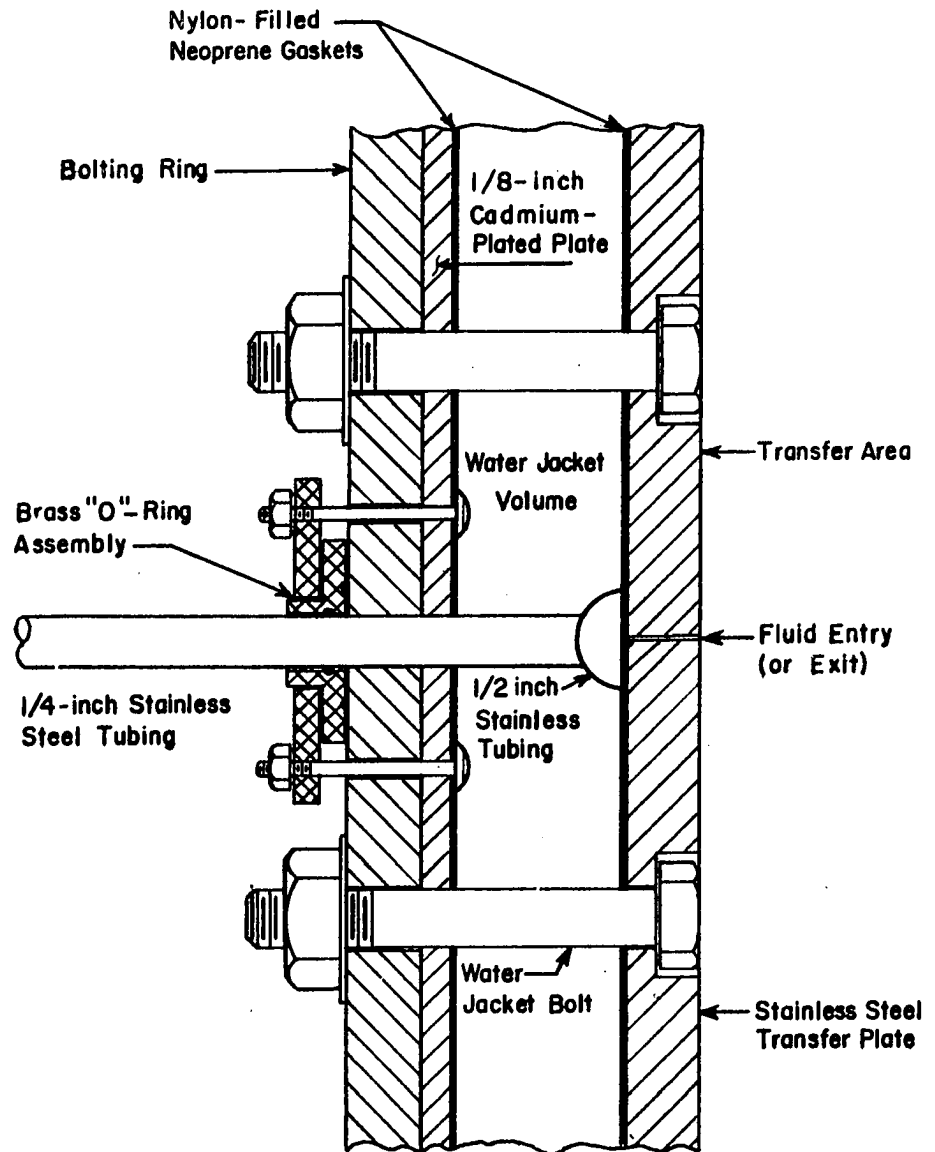


Figure 13

Feed and Product Port Construction



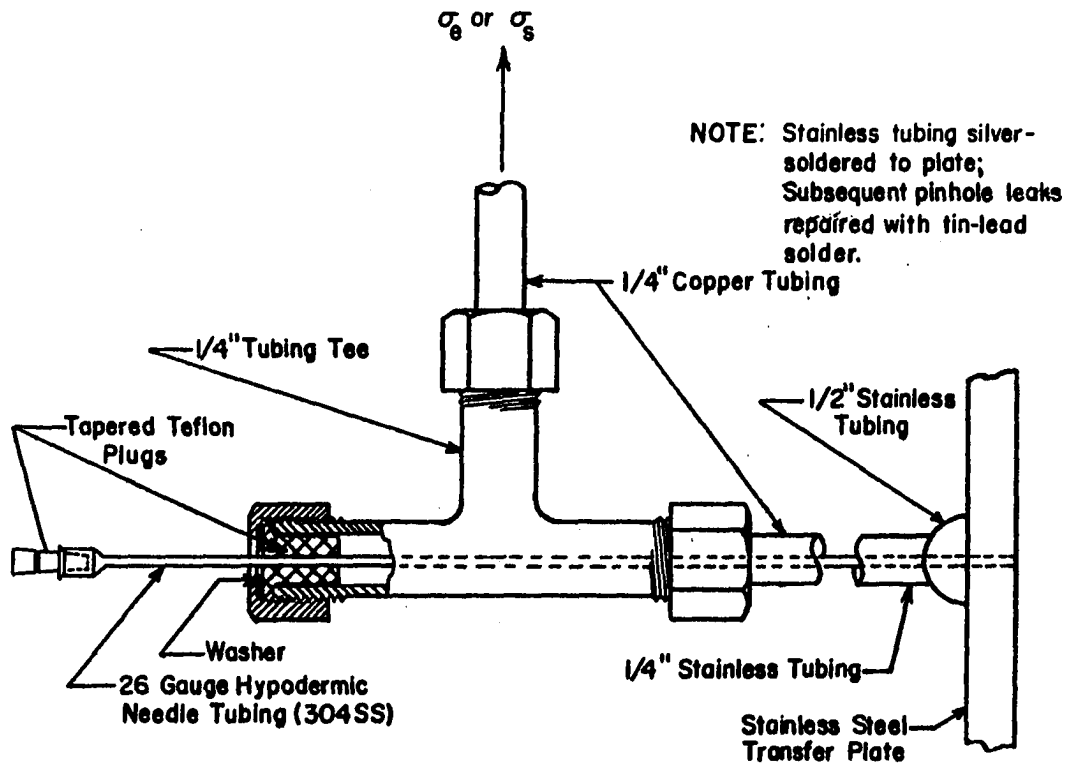
stainless hypodermic needle tubing; one end of the tubing was flush with the plate's surface and the other end adapted so that it would accept a hypodermic syringe for sample withdrawal. When no sample was being taken, the tap was plugged. (See Figure 14 for details.)

For flow runs, one-quarter inch copper lines were used to introduce fluid to and remove fluid from the column. The product lines were equipped with valves placed just downstream from the sample taps. These valves were closed during batch runs to prevent diffusion into the product lines. The liquid in the product lines was cooled in the same cooler as the degassed feed. The cooler had adequate heat transfer area to bring exit temperatures near room temperature.

Two banks of four rotameters in parallel were used to indicate flow rates. One bank was used for the overhead product and one bank for the bottom product; each indicated flow from 0.02 to 200 grams per minute. Product flow rate control was accomplished through use of stainless steel hypodermic needle tubing of various gauges and lengths. Two needle valves (AVECO Series 1050) in parallel were placed on each product line and were helpful in adjusting and equalizing flow rates at flows greater than approximately 0.20 grams per minute. (See Figure 15.)

Figure 14

Sample Tap Construction



NOTE: Hypodermic needle tubing end is flush with transfer plate overhead and bottom product ports; Tubing end extends only three inches into the tubing for the feed port since the concentration is the same throughout.



Figure 15

Control Panel

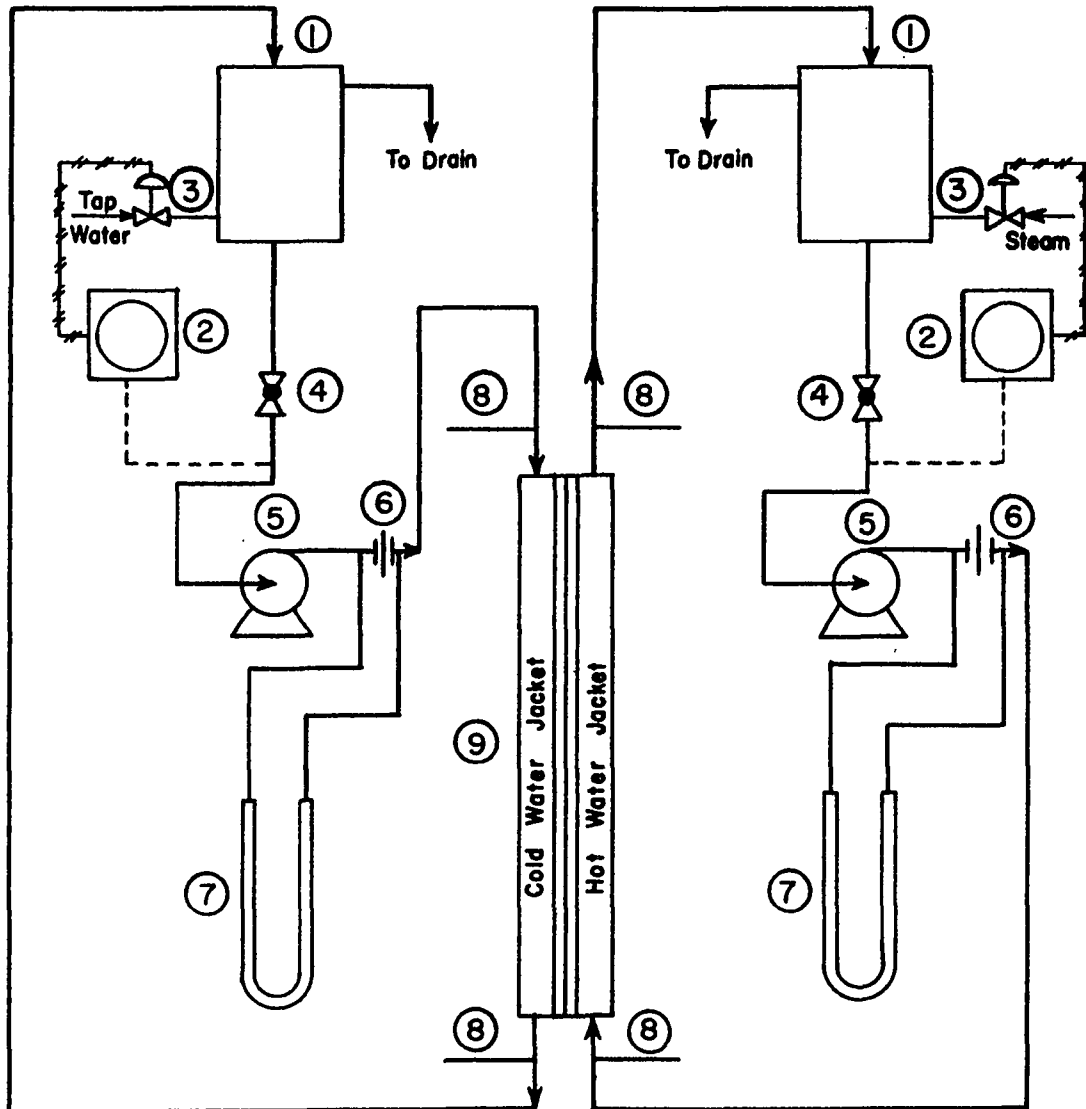
All material contacting the feed or product alcohol solutions was either copper, aluminum, stainless steel, teflon, glass, or neoprene.

The hot and cold water systems (See Figure 16.) were designed to limit the temperature drop or rise through the column to less than 0.6°C . Both the hot and cold water loops were closed systems; that is, the water was recirculated. The hot water was heated by open steam through a sparge near the bottom of an insulated fifty-five gallon barrel; the cold water was cooled by mixing with tap water in a similar, insulated barrel. Each barrel was equipped with an overflow line one foot from the top and with a sight glass so that the water level could be observed. The steam and tap water rates were regulated by Honeywell air-operated diaphragm motor valves which were controlled by Brown circular-chart Electronic Air-O-Line Controllers. Brown iron-constantan thermocouples served as sensing elements and were located in the pipelines just upstream from the pump inlets.

Two one-half horsepower Worthington centrifugal motor-pump combinations provided flow rates up to thirty gallons per minute in the closed loops. Square edged orifices were calibrated in place and were used in conjunction with mercury-under-water U-tube manometers to measure water flow rates. Standard one and one-half inch globe valves were used on the pump inlet lines to regulate flow

Figure 16

Cooling and Heating Water Systems



- | | |
|-------------------------------------|------------------------------|
| ① 55 - Gallon Barrels | ⑥ Orifices |
| ② Temperature Recorder- Controllers | ⑦ Mercury Manometers |
| ③ Air-Operated Diaphragm Valves | ⑧ Thermometers |
| ④ Globe Valves | ⑨ Thermogravitational Column |
| ⑤ Centrifugal Pumps | |

rates to twenty-five gallons per minute for all experimental runs. The hot water entered at the bottom of the water jacket on the hot plate and flowed counter-current to the colder water which entered at the top of the water jacket on the cold plate. Inlet and outlet hot and cold water temperatures were measured with standard mercury-in-glass thermometers with 0.1°C graduations. All water lines were standard one and one-half inch and were insulated with Air-O-Cell pipe insulation. Small lengths of rubber hose were used to connect the water lines to the column to minimize vibrations and to allow greater flexibility.

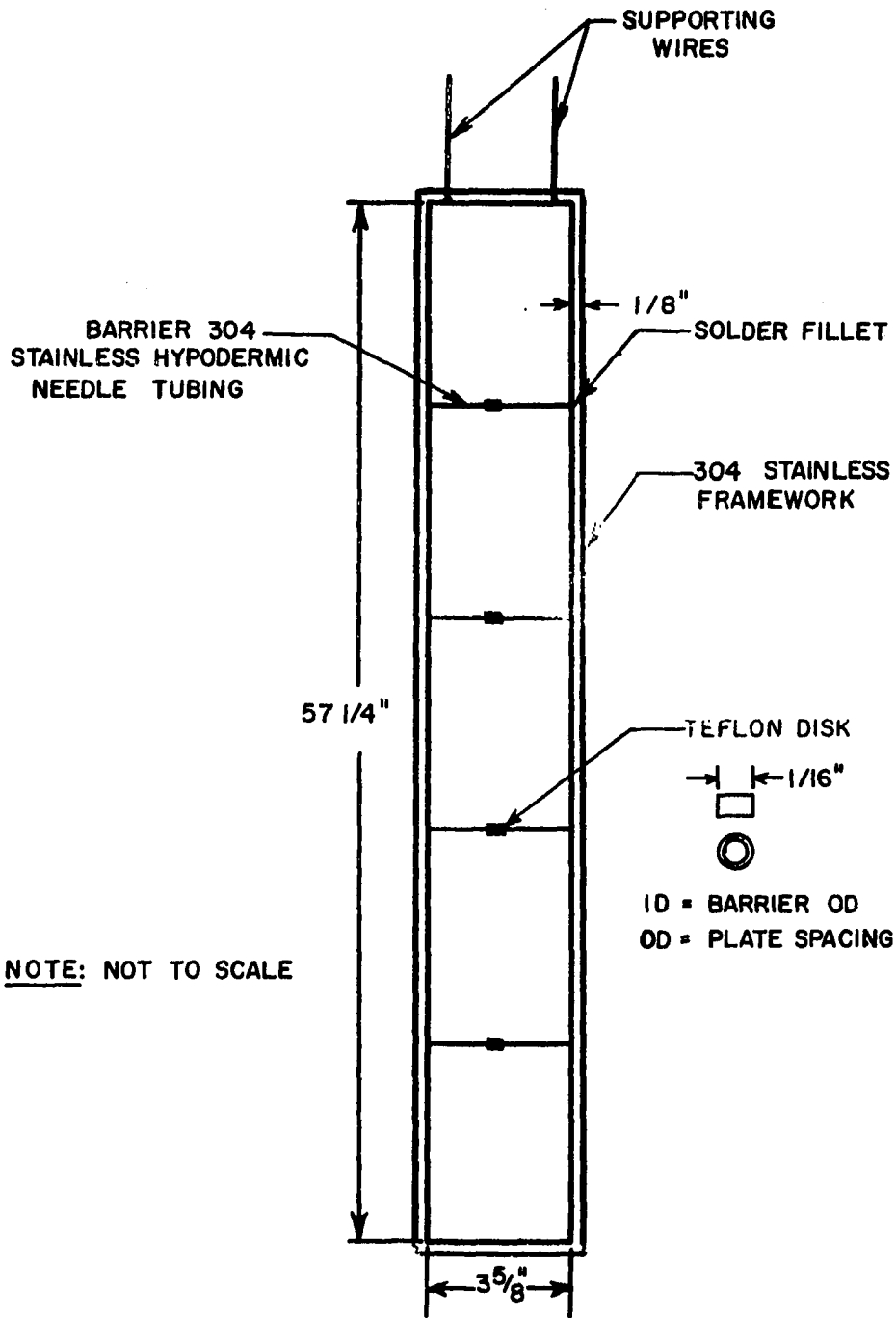
Horizontal Barrier Systems

A barrier framework (See Figures 17 and 18.) was fabricated from 304 stainless steel sheet; the framework was the same thickness as the desired distance between the plates and, in fact, fixed the plate spacing. The framework was utilized to hold the barriers and was sandwiched, with barriers and gasket, between the transfer plates which were bolted together. (See Figure 10.)

In order to prevent possible bowing of the plates when tightened on the framework, it was necessary to place three-quarter inch wide stainless steel strips along the bolt holes. These strips were necessary to counteract the cantilever effect which resulted because the barrier framework was entirely within the bolt circle. The strips, one on each edge of the plates, ran vertically the length

Figure 17

Barrier Framework with Four Barriers Showing
Teflon Spacer Detail



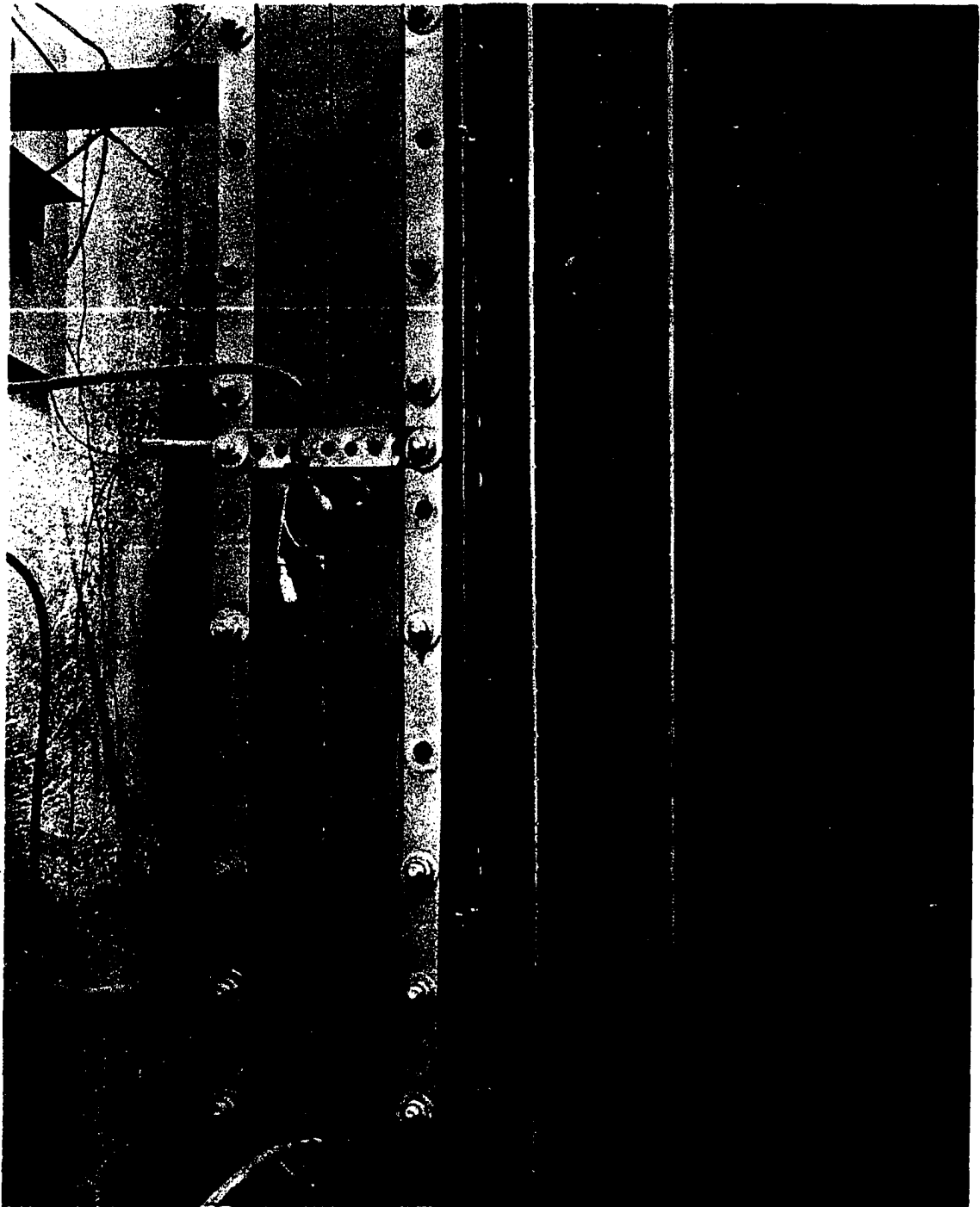


Figure 18

Barrier Framework with Fifty Barriers

of the column and were cut from material of the same thickness as the framework; thus, their thickness was also equal to the plate spacing.

Horizontal barriers were fabricated from 304 stainless steel hypodermic needle tubing. The barriers were soldered equally-spaced (with one exception) between the top and bottom of the barrier framework. The solder joints were scraped and sanded flush with the frame, and all joints were cleaned thoroughly with cotton and distilled water to remove traces of acid flux and bits of excess solder.

The barriers were centered in the framework so that when installed in the column they were positioned equidistant from both plates. A small teflon disc with outer diameter equal to the plate spacing and inner diameter the same as the barrier's outer diameter was positioned on each barrier to help prevent contact of the barrier with the plates as a result of the possible bowing of the barrier. (See Figures 17 and 18.)

The inner dimensions of the barrier framework defined the working volume and were held constant during all runs at a width of 9.21 cm, a length of 145 cm, and a thickness (plate spacing) of 0.0794 cm. (See Figure 17.) Sealing the working volume was accomplished by cutting a gasket from a sheet of one-eighth inch thick sponge neoprene; the inner dimensions of the gasket were cut approximately

two percent smaller than the outer dimensions of the framework in order to insure a good fit around the framework. When cut and ready for installation, the gasket was approximately one-eighth inch square in cross section. The framework was supported vertically in the column during installation by two fine wires soldered to the top of the frame. These two support wires were run through the center of the gasket with a needle, and no trouble was encountered with leakage in this area. The sponge neoprene gasketing material proved very satisfactory since no leaks were observed at any time and since it was inert in ethyl alcohol solutions. The material did have one characteristic which proved a disadvantage: it acquired a permanent set when compressed between the plates for a period of time. It was thus necessary to cut a new gasket each time the column was disassembled.

The above "framework" method of sealing the working volume and defining the plate spacing was utilized for all experimental runs with barriers, and for all of the no barrier runs that were used for comparison with the barrier data. These runs were included in experimental sets F through T.

A characteristic of gaskets that has hampered several previous experimental investigations with parallel-plate columns (B8) (P3) is "gasket creep," or plastic deformation. In these investigations, a gasket was compressed between the transfer plates and

served the dual purpose of sealing and defining the working volume. Since the degree of creep is largely dependent on the characteristics of a particular gasket, it was difficult in these previous investigations to reproduce the same working volume (in particular, the same plate spacing) each time a new gasket was installed. In addition, the creep is a function of time. Therefore, unless one waits a period of time for a gasket to "settle," the working volume will change somewhat during the course of a run. It should be noted that this same method of sealing the working volume and defining the plate spacing was utilized for experimental sets A through E in this work. The gasket was installed, the bolts inserted and torqued uniformly to 100 inch-lbs, and a period of one week allowed for the gasket to settle. Reproducibility of the plate spacing was not a problem here since all of the experimental runs in sets A through E were run with the same gasket. The equipment, other than the gasket, was the same for these runs as described above for the runs in experimental sets F through T.

Apparatus for Determination of Ratio of C-Factors

The C-factor has been discussed previously in connection with Equation (III-121) in Chapter III. A plastic model was constructed in order to determine experimentally the ratio of the C-factors at the two barrier diameter to plate spacing ratios considered in this work. The results of this experimental work are given in Chapter VII.

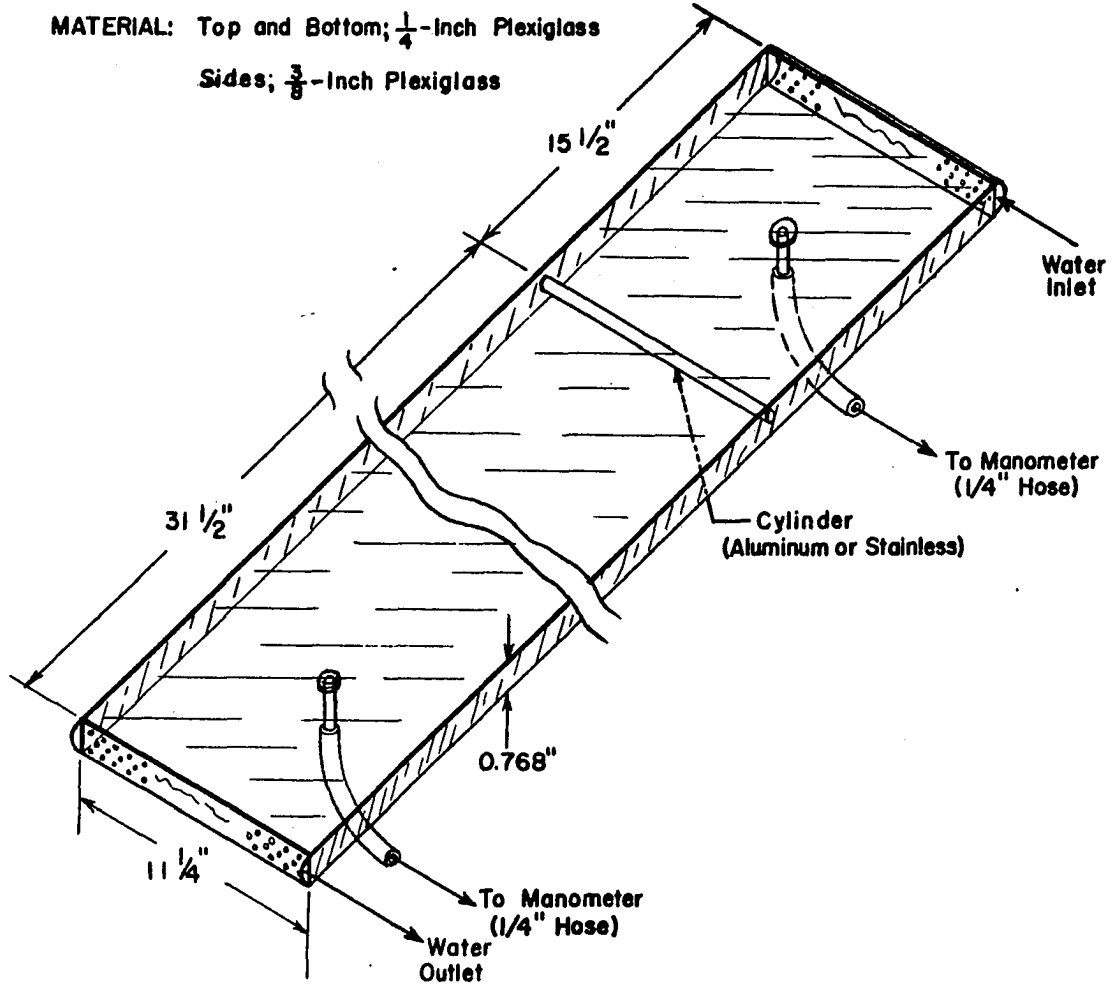
An experimental apparatus (See Figure 19.) was fabricated from Plexiglas, the two parallel plates from one-quarter inch sheet four feet long and one foot wide. The plates were approximately three-fourths of an inch apart (0.768 inch). A right circular cylinder was placed equally distant between the plates and two different diameters were used. A one-half inch cylinder gave a cylinder diameter to plate spacing ratio of 0.65 and a five-eighths inch diameter cylinder a ratio of 0.815. Both ratios are close to the barrier to plate spacing ratios used in the thermogravitational column.

Pressure taps were located two feet downstream and one foot upstream from the cylinder. The taps consisted of one-eighth inch holes in the bottom plate and were connected by one-quarter inch rubber hose to a manometer. Pressure measurement was by means of a differential manometer using benzaldehyde (specific gravity = 1.05) under water as a manometer fluid.

Flow rates were determined by collecting 1000 ml of water over a measured period of time. Inlet and outlet water temperatures were measured in order to obtain an average viscosity for the fluid.

Figure 19

Experimental Apparatus for the Determination of
the Ratio of Drag Factors



CHAPTER V

EXPERIMENTAL PROCEDURE

The thermogravitational column, barrier system, and auxiliary equipment have been described in some detail in Chapter IV. In this chapter, the procedure by which data were actually obtained is described. The measurement of the plate spacing is discussed at length as well as the method of obtaining transient batch data, and continuous flow data.

Ten sets of experimental data were obtained using horizontal barriers, and, in addition, several sets of data were taken with no barriers in the separation space so that the results from these no-barrier runs could be used for comparison with the barrier data. A "set" of steady-state continuous flow data consisted of a rate-separation curve with all system and column variables, other than the flow rate, held constant. Different rate-separation curves were obtained with the mean temperature difference between the plates, ΔT , barrier diameter, d , and number of barriers, N , as parameters. Changes in ΔT could be made easily by setting the temperature recorder-controllers. The barrier diameter and number

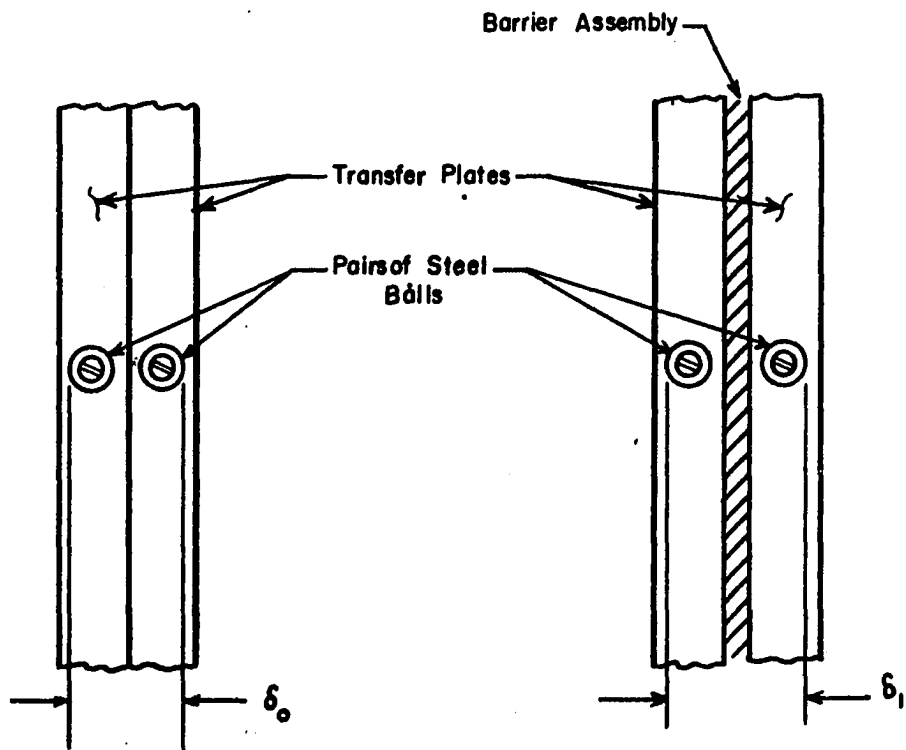
of barriers could be changed by preparing a barrier framework with the desired number of barriers of a given diameter. The average temperature level, \bar{T} , plate spacing, 2ω , plate width, B , and feed concentration, C_F , were held essentially constant for all experimental runs with barriers.

Procedure for Obtaining Plate Spacing

Since the plate spacing was the most important measurement so far as accuracy and precision were concerned, the manner of measuring the plate spacing for all of the experimental runs with barriers will be discussed in some detail. The plates were well cleaned with fine emery paper and finally with a clean cloth. The plates were positioned by means of alignment pins and the eighteen assembly bolts inserted. At this point there was no framework or gasket between the plates. All bolts were tightened to approximately thirty inch-lbs with a torque wrench and finally uniformly tightened to 100 inch-lbs. The hot and cold water flows were started, allowed to reach the preset temperature, and their flow rates adjusted to the operating flow rate of twenty-five gallons per minute. When it was felt that the plates had reached their equilibrium temperature, micrometer readings (designate δ_0 -- see Figure 20) were taken at each of the eight pairs of steel balls which were attached opposite

Figure 20

Plate Spacing Measurement



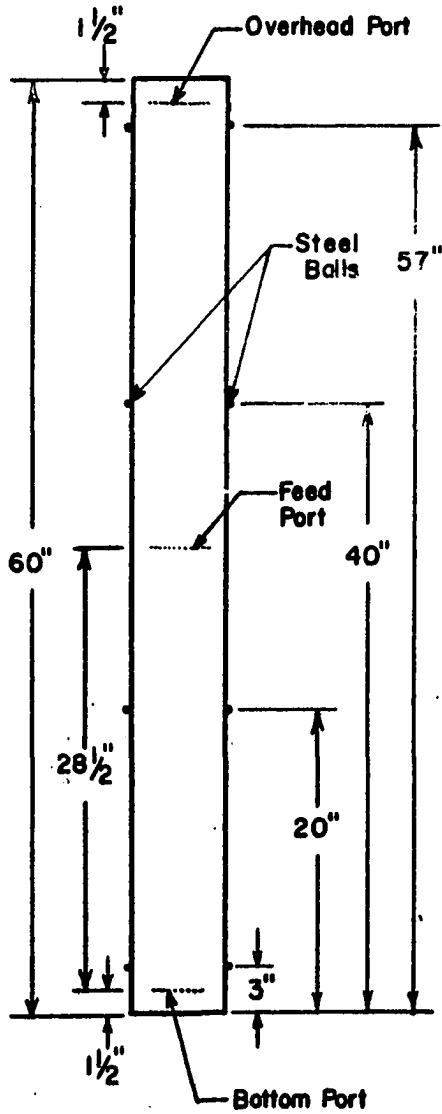
(a) Blank Measurement

(b) Plate Spacing Measurement
(Plate Spacing = $\delta_1 - \delta_0$)

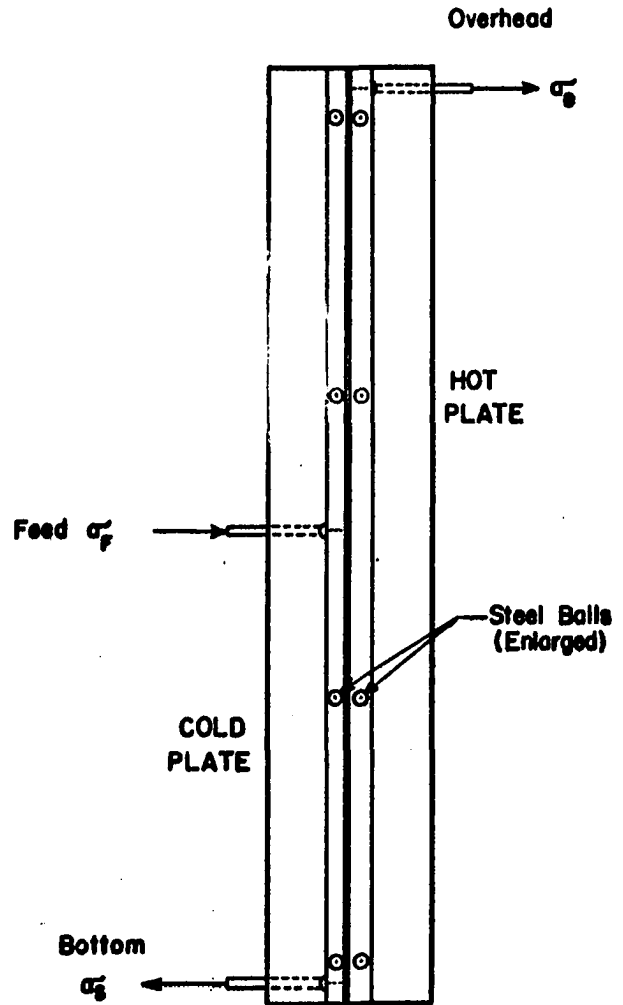
one another around the periphery of the hot and cold plates. (See Figure 21.) Three readings were taken at each location using a micrometer (modified Lufkin Model 1945V) capable of reading to 0.0001 inch. The column was then disassembled, the strips placed along the bolt holes, and the barrier framework with barriers and neoprene gasket positioned in the column. The framework assembly was suspended by two fine wires (which in no way affected column operation) and held in place laterally by thread where needed until the plates were aligned and brought together. After sufficiently tightening the bolts such that the framework was no longer free to move, the threads were carefully removed and the tightening completed, bolts being torqued to 100 inch-lbs. The alcohol feed was started, the working volume allowed to fill with feed solution, the overhead and bottom product flow rates adjusted, and the column observed for approximately thirty minutes to check for any obvious leaks. There being none, the hot and cold water flows were started as described above, and after steady-state temperatures had been reached, three (or more) micrometer readings (designate δ_i) were again taken at each of the eight pairs of steel balls. The three readings of δ_0 and δ_1 at each point were averaged and subtracted to obtain a plate spacing, 2ω , at each of the eight locations. The eight values of 2ω were then averaged for a final grand average. In general, readings of δ_1 were taken for every other point on a

Figure 21

Location of Steel Balls Utilized for Measuring Plate Spacing



(a) Front view of transfer plate
(Column Disassembled)



NOTE: Not to Scale

(b) Side view of column
(Assembled)

rate-separation curve. It was felt that this was sufficient since no plastic deformation or "creep" was observed with the method of gasketing used in the barrier runs. Evidence of the absence of creep is demonstrated in Table 1.

The variations of the plate spacings with time for a given experimental set (shown in Table 1) are felt to be due almost entirely to measurement error. There seems to be no definite trend in the readings to justify any other conclusion. It can be noticed, however, that successive experimental sets have somewhat lower average plate spacings. This is probably because the barrier framework and spacing strips were sanded clean each time the column was disassembled. This sanding evidently removed enough metal to change slightly the plate spacing over a period of a year.

The above procedure utilizing steel balls to measure the plate spacing was introduced by Boyer (B⁸) and was found quite successful for measuring the spacing. It should be pointed out, however, that it was not necessary to have measured the plate spacing in the manner described above. The plate spacing could have been obtained directly by measuring the thickness of the barrier framework and strips along the bolt holes, since these components fixed the plate spacing, and since no measurable creep was detected.

The initial thickness of the barrier framework and strips

TABLE 1
 PLATE SPACING MEASUREMENTS TAKEN FOR
 EXPERIMENTAL SETS I, M, Q AND R

Set I		Set M		Set Q		Set R	
Day	Spacing cm	Day	Spacing cm	Day	Spacing cm	Day	Spacing cm
0*	0.0792	0*	0.0790	0*	0.0790	0*	0.0792
1	0.0790	4	0.0790	3	0.0788	1	0.0792
2	0.0792	5	0.0790	8	0.0788	3	0.0792
3	0.0790	6	0.0792	9	0.0788	6	0.0795
3	0.0795	6	0.0792	17	0.0790	10	0.0792
4	0.0795	7	0.0790			28	0.0795
5	0.0792	14	0.0790			30	0.0792
7	0.0795					35	0.0792
						40	0.0791

* Initial plate spacing measurement was taken on the day
 column assembled.

was 0.0794 cm. It can be seen in Tables 1 and 5 that the plate spacings for the first runs with barriers (sets F, G, H, etc.) had average plate spacings close to this value. Successive experimental runs had somewhat lower average plate spacings, but this is because of the metal removed by sanding each time the framework and strips were cleaned.

It is felt by the author that direct measurement of the strips and framework is the easiest and most precise way to measure the plate spacing. The use of the steel balls provided a good check, but it is felt that more error is encountered with the balls than by direct measurement. It would be desirable, however, to find a method other than sanding to clean the framework and strips: a suitable solvent might be used. The use of a solvent would prevent the removal of metal by sanding, and thus assure reproducibility of the working volume.

It should be noted that the "framework" manner of gasketing was not used for experimental sets A, B, C, D, and E. (These sets of data are considered under "Additional Work" and are independent of the work with horizontal barriers.) In these sets, the gasket itself defined the working volume and a week was allowed for the gasket to "settle" before any data were taken. (See Chapter IV.) Plate spacing measurements were taken for every run in these experimental sets.

Procedure for Obtaining Batch-Transient Data

The above procedure for column start-up described in connection with the measurement of the plate spacing was followed in all experimental runs with horizontal barriers. However, when a batch transient run was to follow, the overhead and bottom flow rates were set at a very high flow rate of approximately one hundred grams per minute. It was felt that no detectable separation could occur with such a large flow rate since it was found experimentally that no appreciable separation occurred at flow rates greater than approximately three grams per minute. When the hot and cold water systems reached their preset temperatures (or after about five minutes of purging the column with the large product flow rates), the valves on the overhead and bottom product lines were closed as rapidly as possible, and time zero for the transient data was designated as the time when the valves were closed. It should be noted that transient data were obtained only for batch runs. In general, an attempt was made to take samples at time intervals such that values of Δ/Δ_{∞} of 0.2, 0.4, 0.6, 0.8, and 1.0 were realized. Three samples were then taken at time intervals large compared to the relaxation time in order to insure that steady-state conditions had been reached. In general, samples were taken about ten times during a transient run. The three readings taken at steady-state were averaged for the reported values in this work. Each time a sample was withdrawn, one or two

drops was allowed to escape before the sample was collected, in order to purge the tap of previous solution. The samples were collected in hypodermic syringes which filled by gravity flow. Approximately one-half milliliter of fluid was withdrawn from each sample tap each time a reading was taken. During the time between sampling, the inlet and outlet hot and cold water temperatures were recorded, and the temperature recorder-controller readings were noted. Eight thermocouples were read using a precision potentiometer; four thermocouples were located in the column (two in each plate), and others were located on the hot feed line out of the feed degasser, and on the cooled feed line and overhead and bottom product lines from the product cooler. Other miscellaneous information was recorded: the ice bath temperature for the potentiometer, the water temperature in the product cooler, the room temperature, the manometer readings for hot and cold water systems, the Powerstat setting, and the liquid levels in the feed barrel and hot and cold water barrels.

Procedure for Obtaining Continuous Flow Data

Continuous flow data were obtained in a manner similar to the batch data except that feed was introduced to the center of the column and overhead and bottom product continuously removed. Periodic samples were taken from the overhead, bottom, and feed sample taps until the column reached steady-state conditions. Three

readings were again taken at steady-state and averaged for the reported values.

Analytical Procedure

Product samples (overhead and bottom) and feed solutions were analyzed for weight fraction ethyl alcohol by refractive index with a Bausch and Lomb Precision Refractometer (No. 33-45-01). (See Figure 22.) The refractometer could be read to ± 0.005 scale units corresponding to approximately 0.0007 weight fraction alcohol. All analyses were made at 25°C and the refractometer was calibrated with ethyl alcohol-water solutions at this temperature. The refractometer prisms were maintained at the required temperature of 25°C by steady water flow from a constant temperature bath.

Product flow rates were determined by collecting samples in iced bottles (to hinder evaporation) over a measured time interval. The amount of solution collected was determined by weight difference, and all weighings were made on a Right-a-Weigh Balance which could be read to 0.0001 gram.

Thermocouple voltages were measured on a Leeds and Northrup Portable Potentiometer (No. 8662) and the voltages converted to temperatures through use of standard conversion tables (L1). The potentiometer could be read to ± 0.001 millivolt, which corresponds to approximately $\pm 0.4^\circ\text{F}$. The reference junction was maintained at a constant 32°F by use of crushed ice and water in a thermos bottle.

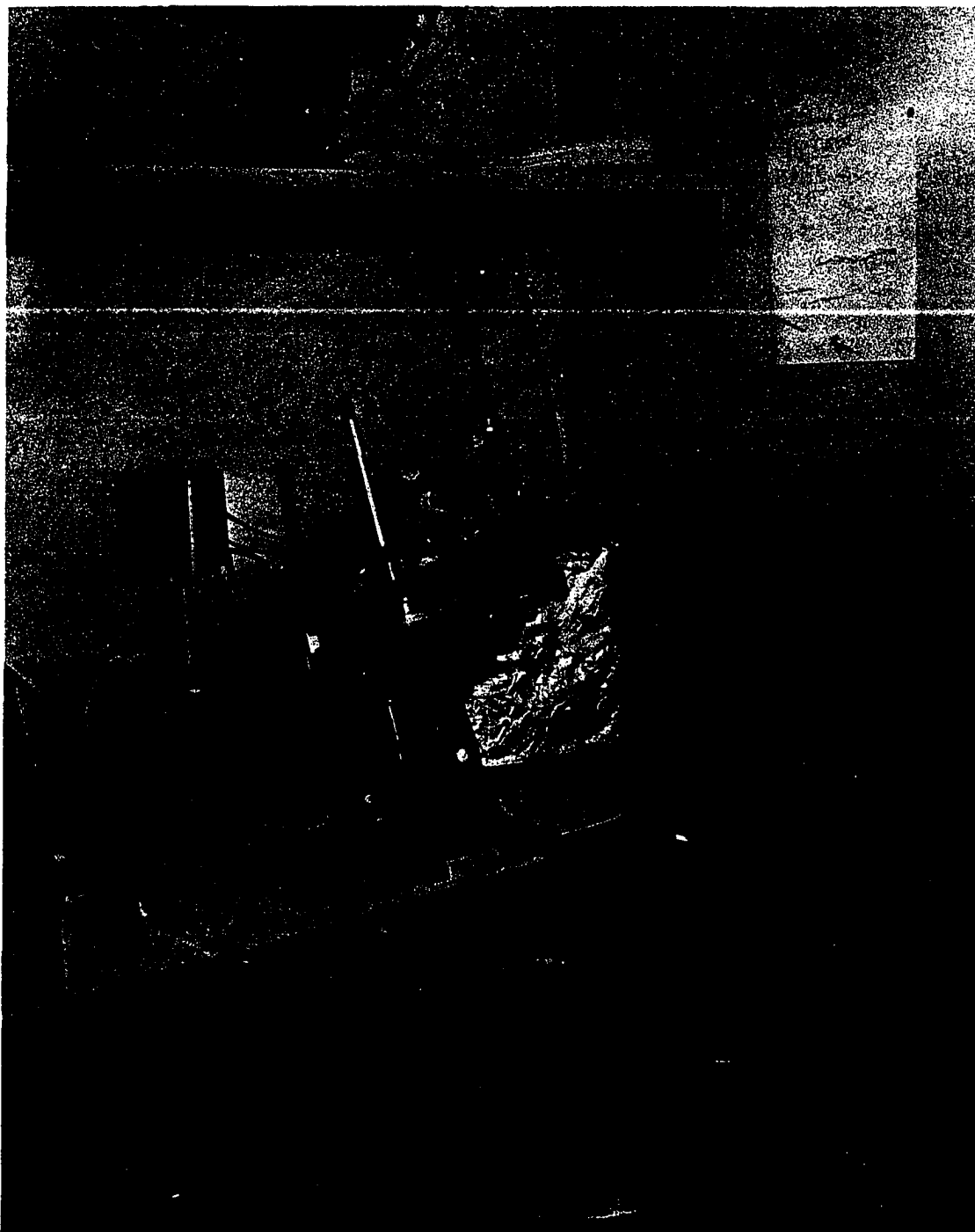


Figure 22

Analytical Instruments

CHAPTER VI

PRESENTATION AND INTERPRETATIONS OF EXPERIMENTAL RESULTS

In Chapter III the theoretical treatment for the open column originally developed by Furry, Jones and Onsager (F7) was reviewed. It was pointed out that, although conventional theory did not predict an increase in the steady-state batch separation when horizontal barriers were placed in the separation space, it was found experimentally that such an increase did occur. An ex post facto line of reasoning was then used to develop a modified theory to explain this increase in the batch separation, and subsequently the theory was expanded to include the transient case and the continuous flow case. Data obtained using the equipment described in Chapter IV provide a means of testing the modified theory, and the data and interpretation of the results are presented in this chapter.

The experimental results are presented in three groups: (1) steady-state batch, or no bulk flow, data, (2) transient batch data, and (3) steady-state continuous flow data. The effect of varying the parameters studied (N , ΔT , and d) is discussed in each of the three groups.

110
Batch Case

Effect of Number of Barriers

The more interesting case with horizontal barriers is the batch, or no bulk flow, case. Experimental batch runs were made with zero, two, four, eight, sixteen, and fifty horizontal barriers. The experimental data are shown plotted in Figure 23 and are presented in tabular form in Appendix B.

The steady-state batch separation with barriers can be obtained from Equation (III-53), and the ratio of the batch separation with barriers to the batch separation in the open column is given by Equation (III-54).

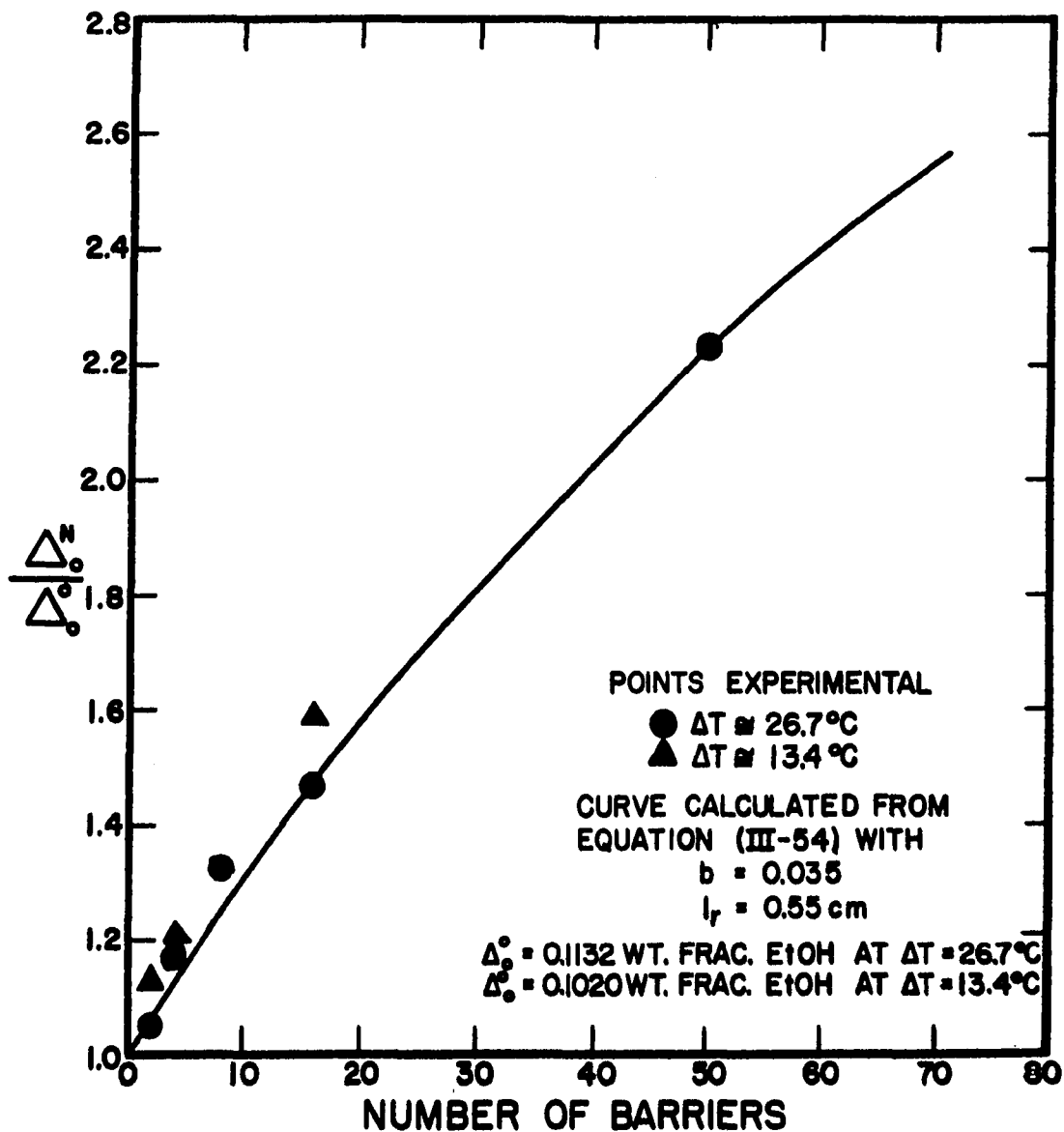
$$\frac{\Delta_o^N}{\Delta_o^0} = (1 + bN) \frac{(L - Nl_T)}{L} \quad \text{(III-54)}$$

The value of b in Equation (III-54) to give the experimental ratio of batch separations was determined for two and for four barriers at the temperature difference between the plates of 26.7°C (with $l_T = 0.55\text{cm}$. See Appendix D.). It should be noted that b is small ($b = 0.035$), so the contribution for an individual barrier is not great.

The average value of b of 0.035 was then used in conjunction with Equation (III-54) to predict the batch separations for any number of horizontal barriers. Figure 23 compares the experimentally obtained batch separations for two, four, eight, sixteen, and fifty barriers. Notice that, whereas the plotted curve shows reasonable agreement with the data at a temperature difference of 26.7°C

Figure 23

Comparison of Experimental Results with Equation (III-54)
for Steady-State Batch Case with N Horizontal Barriers



(the solid circles), data at the lower temperature difference of 13.4° C (the solid triangles) are higher than the curve values. There are two possible explanations for this inconsistency: (1) the value of b may be a function of the temperature difference between the plates, or (2) the value for Δ_o^0 at the lower temperature difference may be in error. (Values on the ordinate in Figure 23 are obtained by dividing the batch separation with N barriers, Δ_o^N , by the batch separation in the open column, Δ_o^0 . Therefore a change in Δ_o^0 at a given temperature difference will affect all of the points plotted at that temperature difference.) Two batch runs for the open column were taken at the lower temperature difference: $\Delta_o^0 = 0.0890$ for run 52H and $\Delta_o^0 = 0.1150$ for run 83L. The two points were averaged for the reported value of 0.1020 weight fraction ethyl alcohol since there was no apparent reason to prefer one run over the other. Notice, however, that if a value of Δ_o^0 of 0.1100 were used, then the points at the lower temperature difference would also fall on the curve. Thus, it is difficult to say for certain why the experimental points at the lower temperature difference are higher than the curve values. It should be pointed out that such a large discrepancy in the batch separation is unusual, but the author has no reasonable explanation for the different values.

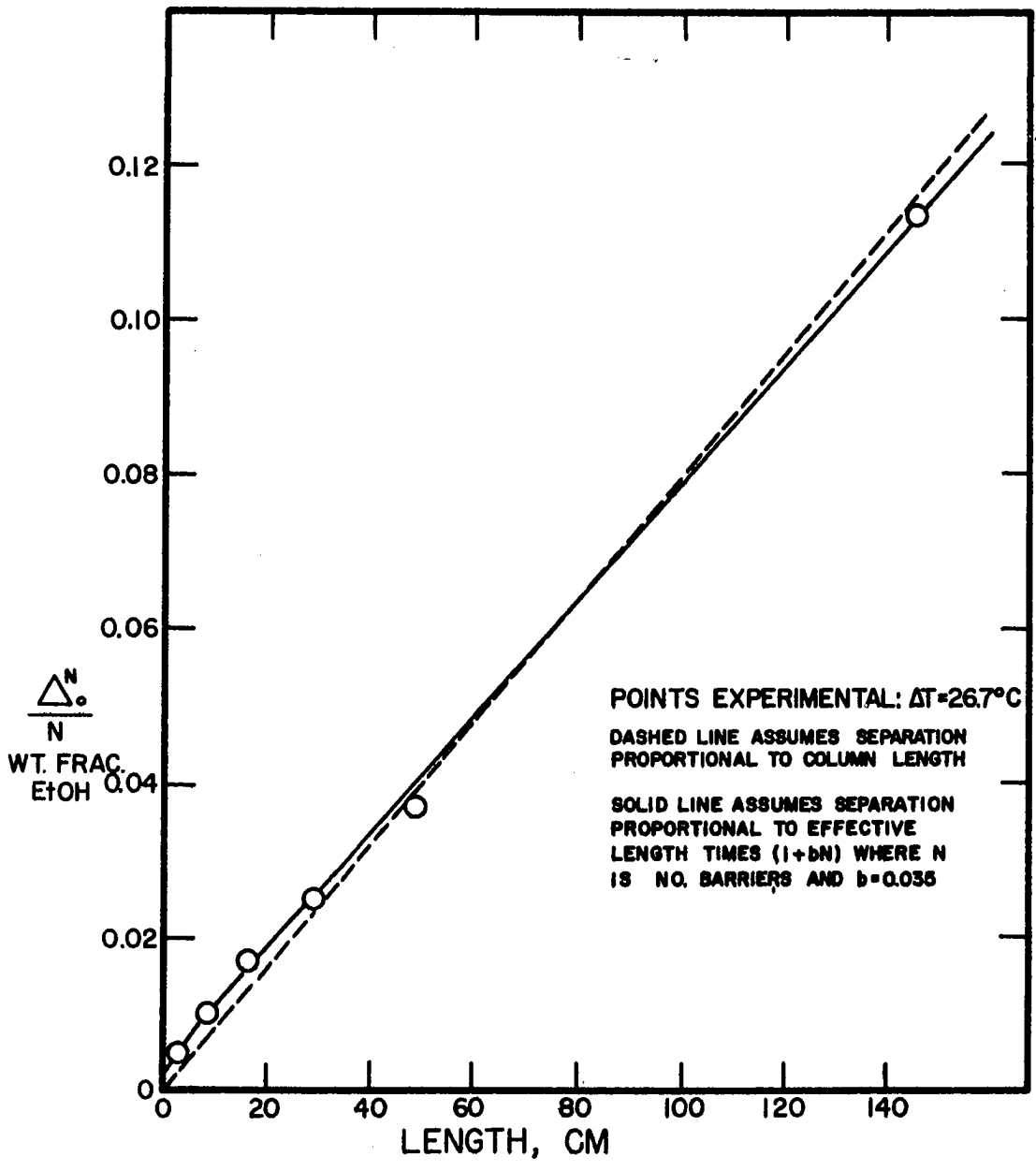
The work of Treacy and Rich with horizontal barriers in gases is included in Appendix F. Their batch data with N as a parameter can also be correlated by use of Equation (III-54).

It should be noted that varying the number of horizontal barriers in a column of fixed length is closely akin to varying the length of each of the (N+1) small columns formed by the N barriers. This is because each of the (N+1) small columns, each one $\frac{1}{N+1}$ as long as the open column, performs as if it were independent of the other small columns. Since the number of barriers used in this work ranged from two to fifty, the open column (L = 145 cm) was divided into as many as fifty-one small columns ($L = \frac{145}{51} = 2.84$ cm). Other investigators (C13) (D4) (H5) (P3) have considered column length as a parameter, but no investigator has considered a large enough range of column lengths to test the theory adequately. An excellent paper concerning the column length as a parameter was presented by Crowover (C13). However, Crowover's data also suffered from lack of a sufficiently large range of column lengths.

It is predicted by theory that the separation should be proportional to column length. However, this is true only if the value of b introduced in this work is equal to zero, and such is not the case, for it was found experimentally that $b = 0.035$. The straight dashed line through the data (obtained at a temperature difference of 26.7 ° C) in Figure 24 is the best line based on the assumption that the separation is proportional to the length. Notice that for the smallest length, the separation is off by a factor of two. Consequently, it was assumed that the separation was proportional to the

Figure 24

Separation as a Function of Column Length



effective length ($L-Nl_r$), multiplied by the factor $(1+bN)$:

$$\text{Separation} \propto \text{Effective Length} (1+bN) \quad (\text{VI-1})$$

Since the separation is known for $N = 0$ ($\Delta_0^0 = 0.1132$ at $\Delta T = 26.7^\circ \text{C}$)

$$\text{Separation} = 7.8 \times 10^{-4} (L-Nl_r) (\text{cm}) (1+bN) \quad (\text{VI-2})$$

Equation (VI-2) was then plotted as the continuous line in Figure 24 with b equal to 0.035. It can be seen that, with the exception of one point, this line represents the data very well. Thus based on this data, it can be said that the conventional theory is not quantitatively correct for the effect of length on the batch separation. However, the effect of length is small as can be seen by the value of b of 0.035.

Effect of Temperature Difference Between the Plates

The conventional as well as the modified theory shows that the steady-state batch separation should be independent of the temperature difference between the plates (assuming that $K_d \ll K_c$). However, it was found experimentally that the temperature difference does influence the batch separation for both an open column and a column with barriers. Two temperature differences between the plates were considered experimentally: an average temperature difference of approximately 26.7°C and an average temperature difference of about 13.4°C . Experimental data are presented in tabular form in Appendix B. In general, the separation dependence on temperature difference can be represented by

$$\frac{\text{Separation at Higher Temperature Difference}}{\text{Separation at Lower Temperature Difference}} = \left(\frac{\Delta T_H}{\Delta T_L} \right)^{0.088} \quad (\text{VI-3})$$

Other investigators (B8) (H1) (P4) have found a similar dependence of the batch separation on the temperature difference, although not necessarily of the same order of magnitude.

Theory does predict that the temperature difference will affect the transient behavior of a column, and this effect will be discussed in the section on the "Transient Batch Case."

Effect of Barrier Diameter

Only two barrier diameter to plate spacing ratios were considered experimentally in this work, and only two sets of data were obtained at the larger barrier diameter. Therefore, it is difficult to draw any conclusion as to the effect of barrier diameter on column performance based solely on this data. It is felt, however, that the value of b in Equations (III-52) through (III-54) should be essentially independent of the barrier diameter to plate spacing ratio. As mentioned previously in Chapter III, b arises because of the momentum loss as the circulating fluid in each of the small columns reverses its direction in the vicinity of the barrier. This momentum loss should not be a strong function of the barrier diameter to plate spacing ratio, and, for a first approximation, one would not expect an appreciable change in the steady-state batch separation as the barrier diameter is increased relative to the plate spacing (as long as the

barrier diameter is not equal to the plate spacing).

The limited experimental results are compared in Table 2. Data are presented for the steady-state batch separation for four barriers with a barrier diameter to plate spacing ratio of 0.643 and for four barriers with a barrier diameter to plate spacing ratio of 0.803. It can be seen in the Table that the separation with the large diameter barriers is somewhat lower than the separation given by the smaller diameter barriers at both the temperature differences considered experimentally. The difference in the separation is small, however, and can be attributed to experimental error.

Effect of Plate Spacing

No experimental work was done with the plate spacing as a parameter, but its effect is readily discernible from examination of Equations (III-51) and (III-52). That is, assuming that the value of b does not change as the plate spacing is varied, the batch separation is inversely proportional to the fourth power of the plate spacing for both an open column and a column with barriers.

Transient Batch Case

Effect of Number of Barriers

Horizontal barriers increase the batch separation ability of a given column, but the time required to reach any fraction of the

TABLE 2

COMPARISON OF BATCH SEPARATIONS WITH FOUR
HORIZONTAL BARRIERS:
BARRIER DIAMETER A PARAMETER

Column and System Values:

L = 145 cm B = 9.21 cm
T = 322°K C_F = 0.40 wt. frac. EtOH
2ω = 0.0791 cm

A. ΔT = 26.7° C

Exp. No. and Set	Barrier Diameter	Barrier Diameter to Plate Spacing Ratio	Experimen- tal Sepn.
	cm		Weight Frac. EtOH
90M	0.0508	0.643	.1330
1040	0.0635	0.803	.1286

B. ΔT = 13.6° C

Exp. No. and Set	Barrier Diameter	Barrier Diameter to Plate Spacing Ratio	Experimen- tal Sepn.
	cm		Weight Frac. EtOH
102N	0.0508	0.643	.1233
117P	0.0635	0.803	.1226

steady-state separation is appreciably longer than for a similar open column. Thus, increased separation ability is obtained through the use of barriers, but with increased relaxation times.

It was found in Chapter III that the transient behavior of a column with N equally-spaced barriers could be predicted by the simultaneous solution of a system of Laplace equations: one equation of the type given by Equation (III-76)

$$C_{n+1}(s) = \frac{R}{s+R} \left[C_n(s) + \frac{\Delta_{\infty}^N (s+2R)}{2Rs(N+1)} \right] + \frac{C_F}{s+R} \quad (\text{III-76})$$

$\frac{(N-2)}{2}$ equations of the type given by Equation (III-75)

$$C_n(s) = \frac{R}{s+2R} \left[C_{n+1}(s) + C_{n-1}(s) + \frac{\Delta_{\infty}^N}{2R(N+1)} \right] + \frac{C_F}{s+2R} \quad (\text{III-75})$$

and one equation of the type given by Equation (III-77)

$$C_1(s) = \frac{C_F}{s} + \frac{\Delta_{\infty}^N}{2s(N+1)} \quad (\text{III-77})$$

The final solution of the system of equations yields a series of negative exponential terms of the type e^{-cRt} (See Appendices G and H.) where c is a constant, and R is equal to $\sigma_c / \rho V$. The flow past the barriers, σ_c , is dependent on the relative ratio of the diameter of the barriers to the distance between the plates, as shown by Equation (III-116), and also it is proportional to the magnitude of the

convective circulation given by Equation (III-121). Therefore, if a value for σ_c is obtained for a number of barriers, N , of a given barrier diameter to plate spacing ratio, then a new σ_c can be calculated for any other number of barriers of the same diameter to plate spacing ratio. This follows since σ_c is proportional to the convective circulation, and the circulation is inversely proportional to $(1 + bN)$ as given by Equation (III-121).

Consequently, a value for σ_c was obtained experimentally from the transient data for four equally-spaced barriers (See Appendix B for transient data.), and this value of σ_c was then used to calculate a new σ_c for each transient curve with N barriers using the relation

$$\sigma_{cN} = \sigma_{cN=4} \frac{(1+4b)}{1+bN} \quad (\text{VI-4})$$

where b is the same constant as first introduced in Equation (III-44). The experimental value of σ_c for four barriers was obtained in the following manner. The system of equations for $N = 4$ was solved (See Appendix H.), and the resulting equation was

$$\frac{\Delta}{\Delta_{\infty}^{N=4}} = 0.20 + 0.80 (1 - 0.947e^{-.382Rt} - 0.053e^{-2.618Rt}) \quad (\text{H-10})$$

Now since $R = \sigma_c / \rho V$ and since ρ and V are known, curves of $\Delta / \Delta_{\infty}^{N=4}$ as a function of t can be calculated for different values of R (or σ_c).

The value of R that gave the best fit of the experimental transient data shown in Figure 25 for four barriers at a temperature difference of 26.7°C gave a value of σ_c of 0.070 gram/min. [The curve in Figure 25 for the open column was calculated from Equation (III-65)] With this value of $\sigma_{c_{N=4}}$, Equation (VI-4) can be written

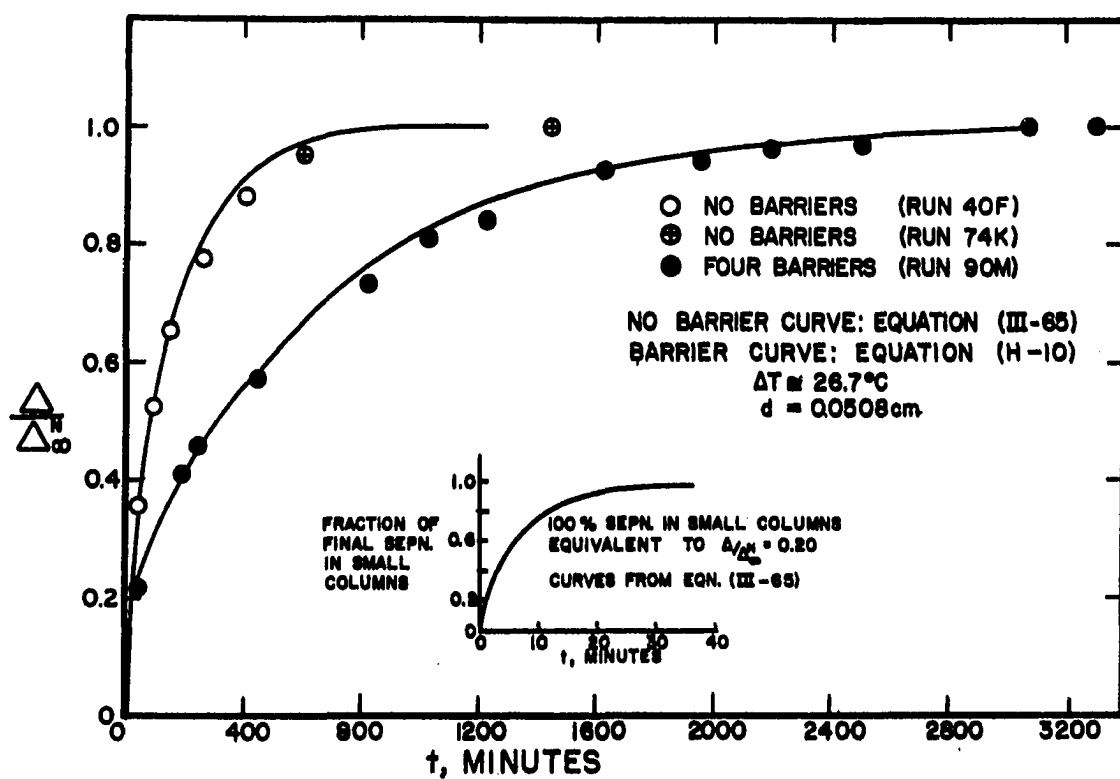
$$\sigma_{cN} = 0.070 \frac{(1+4b)}{1+bN} \frac{\text{gram}}{\text{min}} \quad (\text{VI-5})$$

It should be noted that an empirical value of σ_c could have been obtained from any of the other transient curves with barriers. The only reason for selecting the four barrier transient data was that this was one of the runs used to find the empirical value of b in Equation (III-54).

The effect of sampling on the transient behavior of a column was discussed in Chapter III. A dimensionless flow term, P, was found to be the quantity of interest, and it was concluded by this author that P-values greater than approximately 0.1 introduced a sampling error larger than a typical experimental error. (See Figure 3.) The values of P for the transient runs obtained in this work range from 0.001 for sixteen barriers to 0.035 for two barriers. It is concluded, therefore, that for this range of P-values, the effect of sampling can be satisfactorily neglected. [It should be noted (See Figure 3.) that any corrections would, in general, make the agreement between theory and experiment better.]

Figure 25

Comparison with Theory of the Transient Behavior of Columns
with Zero and Four Horizontal Barriers



The insert in Figure 25 shows the magnitude of the error introduced by assuming instantaneous equilibrium in the $(N + 1)$ small columns. In other words, rather than reaching equilibrium instantaneously, the small columns in the column with four barriers required about twenty minutes to reach ninety-five percent of the steady-state separation at the temperature difference of 26.7°C . (The value of ninety-five percent was chosen arbitrarily.) This twenty minutes is about one percent of the approximately 1900 minutes needed to reach ninety-five percent of the equilibrium separation in the column with four barriers, and hence could be satisfactorily neglected. However, it is a simple matter to correct for the error by adding a correction (the time to reach ninety-five percent of the equilibrium separation) to all of the time values at which the transient data points were taken. This is equivalent to saying that time zero is not the time when the purging flows were stopped, but the time when the small columns reached ninety-five percent of their steady-state separation. It should be noted that when the $(N + 1)$ small columns reach steady-state conditions (one hundred percent of the separation at infinite time), the separation in the column with the N equally-spaced barriers is but $\Delta_\infty^N / (N + 1)$. The term Δ_∞^N is the steady-state separation at infinite time in a column with N horizontal barriers, and should not be confused with Δ^N (or Δ) which is the separation at any time t .

Additional inserts showing the magnitude of the error introduced by the assumption of instantaneous equilibrium are found in Figures 31, 34, and 35 and are discussed in connection with these figures.

Equation (VI-5) was used in conjunction with Equations (III-75) through (III-77) to calculate transient curves for the other runs with barriers.

Figure 26 compares the transient behavior of columns with zero (open column) and two horizontal barriers, both at a temperature difference of 26.7° C. The open column curve was calculated from Equations (III-65) and the two barrier curve from Equations (III-76) and (III-77).

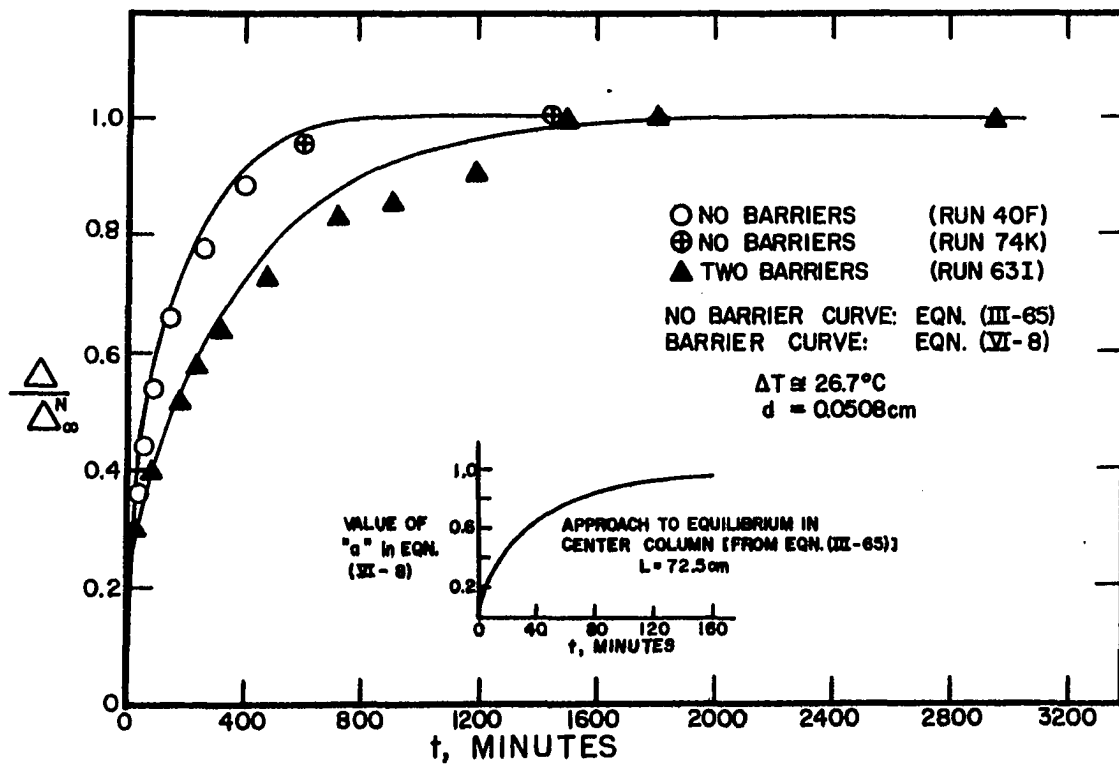
In general, the barriers were equally-spaced in the column. However, for the two-barrier runs, one barrier was midway between the center of the column and the overhead product drawoff, and the other barrier was midway between the center of the column and the bottom product drawoff. This meant that the column above the point of symmetry (the x-axis) was the same length as the top column, and thus the system of equations is

$$C_2(s) = \frac{R}{s+R} \left\{ C_1(s) + \frac{\Delta_{\infty}^{N=2}(s+2R)}{8Rs} \right\} + \frac{C_F}{s+R} \quad (\text{VI-6})$$

$$C_1(s) = \frac{C_F}{s} + \frac{a \Delta_{\infty}^{N=2}}{4s} \quad (\text{VI-7})$$

Figure 26

Comparison with Theory of the Transient Behavior of
Columns with Zero and Two Horizontal Barriers



where \underline{a} is a factor that has been introduced to compensate for the fact that the center column does not reach equilibrium instantaneously. The value of \underline{a} as a function of time is shown plotted in the inserts in Figures 26 and 30, and was calculated from Equation (III-65) [with $L = 72.5$ cm, $\mu = 0.665$, and $K = 0.0102 (\Delta T)^2$].

Notice that the correction introduced in connection with Figure 25 (because of the assumption of instantaneous equilibrium) will not suffice for this special case with two barriers. This is because the center column between the barriers is twice as long as the top or bottom column and requires four times as long to reach equilibrium; thus, the factor \underline{a} is necessary for this special case.

It should be pointed out that a factor \underline{a} is needed only because the center column was so long, not because of the unequal spacing of the barriers. Had the center column been short enough such that the assumption of instantaneous equilibrium introduced little error, then the value of the factor \underline{a} would have been one and would have had no effect.

Solving Equations (VI-6) and (VI-7) and taking the inverse yields

$$\frac{\Delta}{\Delta_{\infty}^{N=2}} = \frac{(1+a)}{2} - \frac{(1+2a)}{4} e^{-Rt} \quad (VI-8)$$

At $t = 0$, $\Delta/\Delta_{\infty}^{N=2} = 0.25$ which results from the fact that instantaneous equilibrium still has been assumed for the top and bottom columns..

The correction discussed previously in connection with Figure 25 accounts for this error, and it was calculated that about thirty-five minutes was required to reach ninety-five percent of equilibrium in the top and bottom columns.

Figures 27 and 28 compare predicted and experimental results for eight and sixteen barriers. The equations used to calculate the predicted curves for these cases were obtained in the same manner as for four barriers, and the equations are presented in summary form in Appendix G. As pointed out earlier in Chapter III, solving for the final equation describing the transient behavior of a column with N barriers involves finding the roots of a $(N/2)$ th order polynomial. The roots of the resulting fourth and eighth degree polynomials for $N = 8$ and $N = 16$ were found by trial and error in this work. In general, only the smallest root contributed materially to the form of the transient curve [recall the form $(1 - e^{-cRt})$ where c is a root], and for $N = 8$ and $N = 16$ only the two smallest roots were used to calculate the transient curves. (Even the second smallest root did not contribute enough to be detected on a plot of a transient curve.)

The insert found in Figure 25 showing the magnitude of the error introduced by the assumption of instantaneous equilibrium in the small columns has been omitted in Figures 27 and 28. In both cases, the error was less than one percent and was simply neglected.

Figure 27

Comparison with Theory of the Transient Behavior of
Columns with Zero and Eight Horizontal Barriers

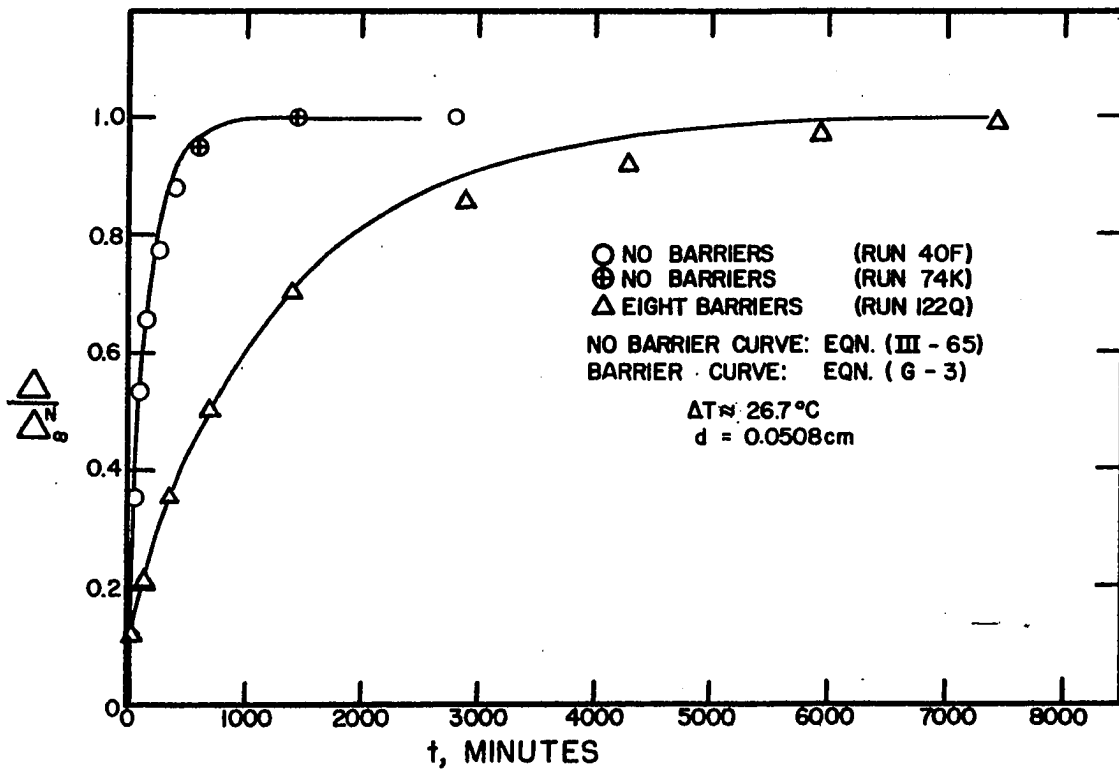


Figure 28

Comparison with Theory of the Transient Behavior of Columns with Zero and Sixteen Horizontal Barriers

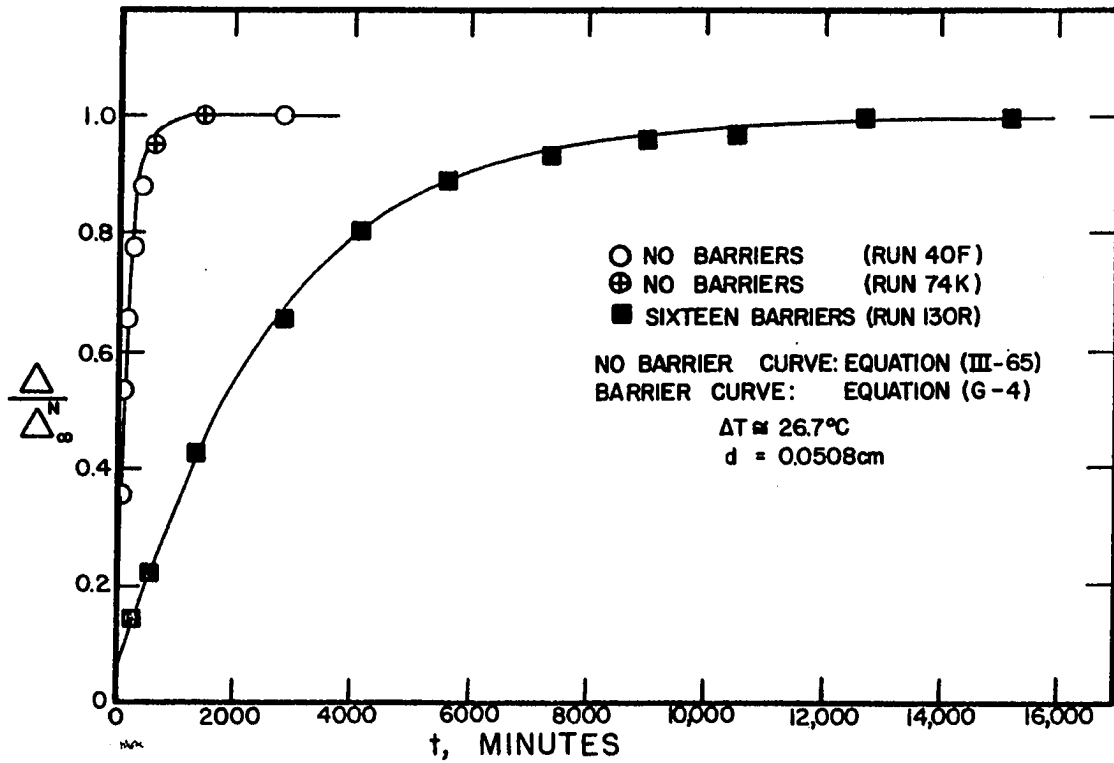


Figure 29 summarizes Figures 25 - 28 and shows the magnitude of the effect on the transient behavior of a column brought about by the introduction of various numbers of horizontal barriers at the temperature difference of 26.7°C. The agreement between the predicted curves and the experimental data is satisfactory in all cases.

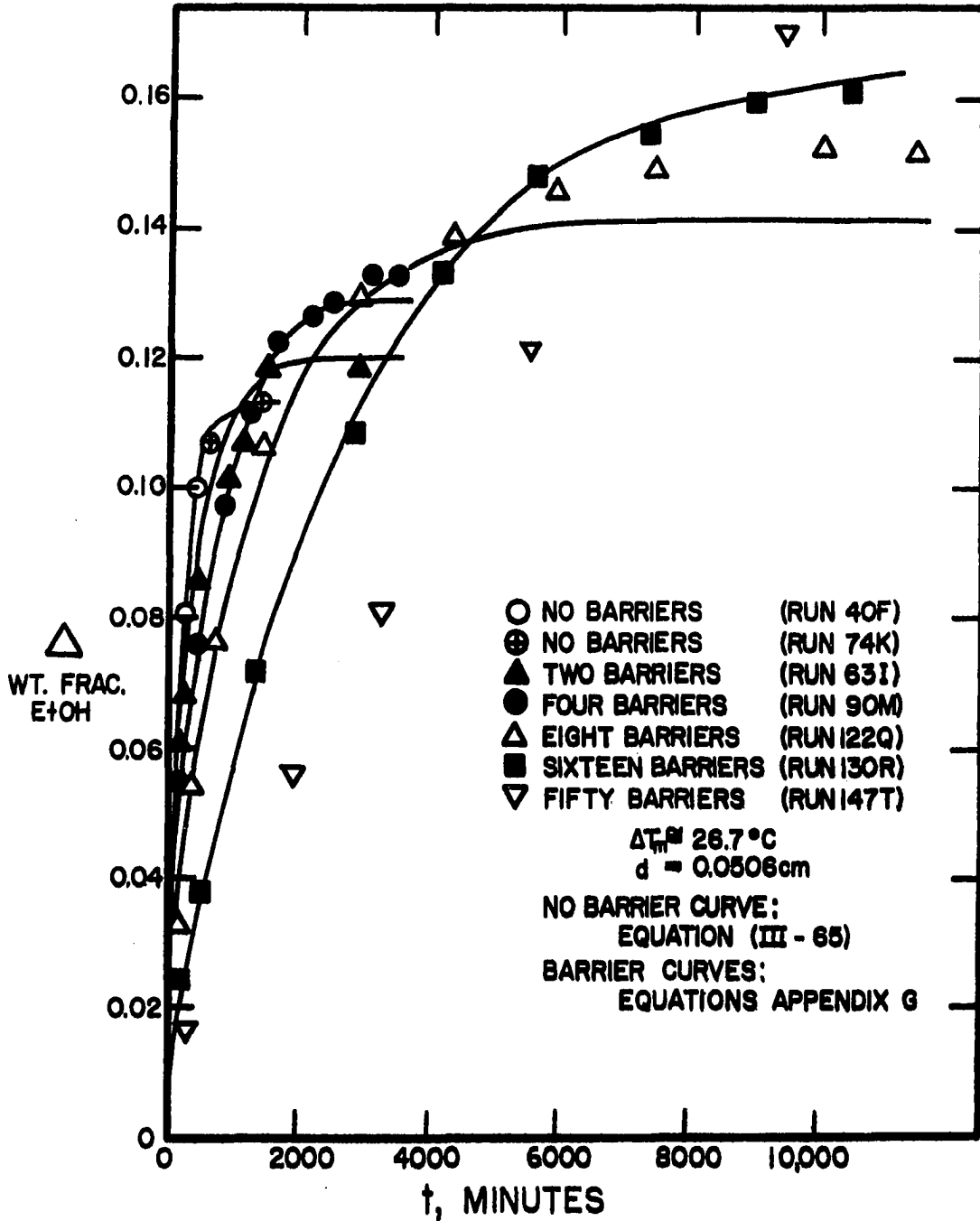
It should be mentioned that an attempt to obtain transient data for the batch run with fifty barriers was terminated by a malfunction in the hot water temperature recorder-controller before steady-state conditions had been reached. The transient data obtained for fifty barriers are presented in Figure 29 and in Appendix B. No theoretical curve was calculated for fifty barriers because of the incomplete transient data, and because a computer solution would have been necessary to obtain the final equation.

Effect of Temperature Difference between the Plates

As mentioned previously, theory predicts that the temperature difference between the plates should influence the approach to equilibrium in a given column. However, the effect of temperature difference on the transient behavior of a column with barriers is different than the effect on an open column. Inspection of Equation (III-65) shows that the relaxation time in an open column is inversely proportional to K , and hence to the square of the temperature difference as seen from Equation (III-35). A two-fold increase in temperature

Figure 29

Comparison with Theory of the Transient Behavior of Columns
with Zero, Two, Four, Eight, and Sixteen Horizontal
Barriers: Higher Temperature Difference



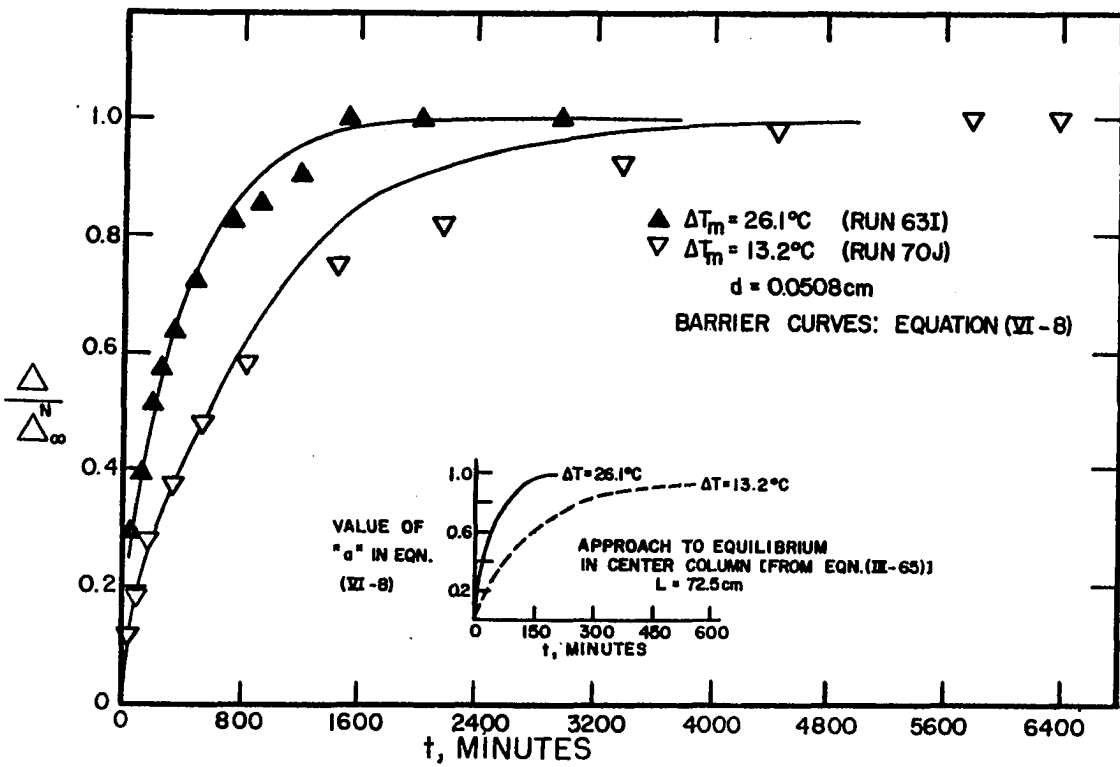
difference should, then, reduce the relaxation time in an open column by a factor of four, and the data obtained in this work (See Appendix B for transient data.) as well as the data of numerous prior investigators (B8) (H1) (H2) (L3) (P3) substantiate this temperature difference dependence.

For a column with barriers, R is the quantity of interest as can be seen from Equations (III-75) and (III-76) or from Appendix H. Since $R = \sigma_c / \rho V$, R is proportional to σ_c alone for changes in the temperature difference. Now σ_c is proportional to the magnitude of the convective circulation which in turn is proportional to the first power of the temperature difference as shown by Equation (III-121). Therefore, a two-fold increase in temperature difference should but halve the relaxation time in a column with barriers whereas a similar temperature difference increase in an open column reduces the relaxation time by a factor of four.

Comparison of the transient data (shown in Figures 30 - 32) obtained at the two temperature differences considered experimentally in this work (approximately 26.7°C and 13.4°C) shows that, indeed, the relaxation time is reduced by a factor of two rather than four when the temperature difference is halved. Figure 30 compares the predicted and experimental results for a column with two barriers. The predicted curve at the lower temperature difference was calculated in the same manner as discussed previously for Figure 26

Figure 30

Effect of the Temperature Difference between the Plates
on the Transient Behavior of a Column with Two
Horizontal Barriers



except that σ_c was approximately one-half as large (smaller by the ratio of the temperature differences: $13.2^\circ/26.1^\circ = 0.507$). Notice that, although the agreement between experiment and theory is satisfactory for two barriers at the higher temperature difference, the agreement is poor at the lower temperature difference. Although there is no way to be certain, there is a possible explanation for the discrepancy between theory and experiment at the lower temperature difference. The batch transient run at the lower temperature difference was the next-to-last run taken in experimental set J. During the last run in set J and the first two runs in set K (runs 72K and 73K, subsequently thrown out), erratic column behavior was noted in that the concentration of alcohol in the overhead product sample would increase and then decrease at times. Normal behavior is for a continuous increase in the alcohol concentration in the overhead product until steady-state conditions are reached. Subsequent investigation revealed a pin-hole leak in the overhead product port, and the column was torn down for repairs. This leak allowed exchange between the alcohol solution in the working volume in the column and the water heating the transfer plate. Thus, it is possible that this pin-hole leak, which was discovered later, might have been responsible for the poor agreement between theory and transient data for two barriers at the lower temperature difference.

The insert in Figure 30 again shows the magnitude of the factor \underline{a} as a function of time with temperature difference as a parameter. The additional error because of the assumption of instantaneous equilibrium in the top and bottom columns was calculated to be thirty-five minutes for the higher temperature difference, and 120 minutes for the lower temperature difference. Compensation for these errors was made by adding correction times as discussed in connection with Figure 25.

Figure 31 shows the effect of temperature difference on a column with four equally-spaced horizontal barriers. The manner of obtaining the curve at the higher temperature difference has been discussed previously in connection with Figure 25. The curve for the lower temperature difference was obtained using the same equation as for the higher temperature difference, Equation (H-10), but with σ_c reduced by the ratio of the temperature differences. That is,

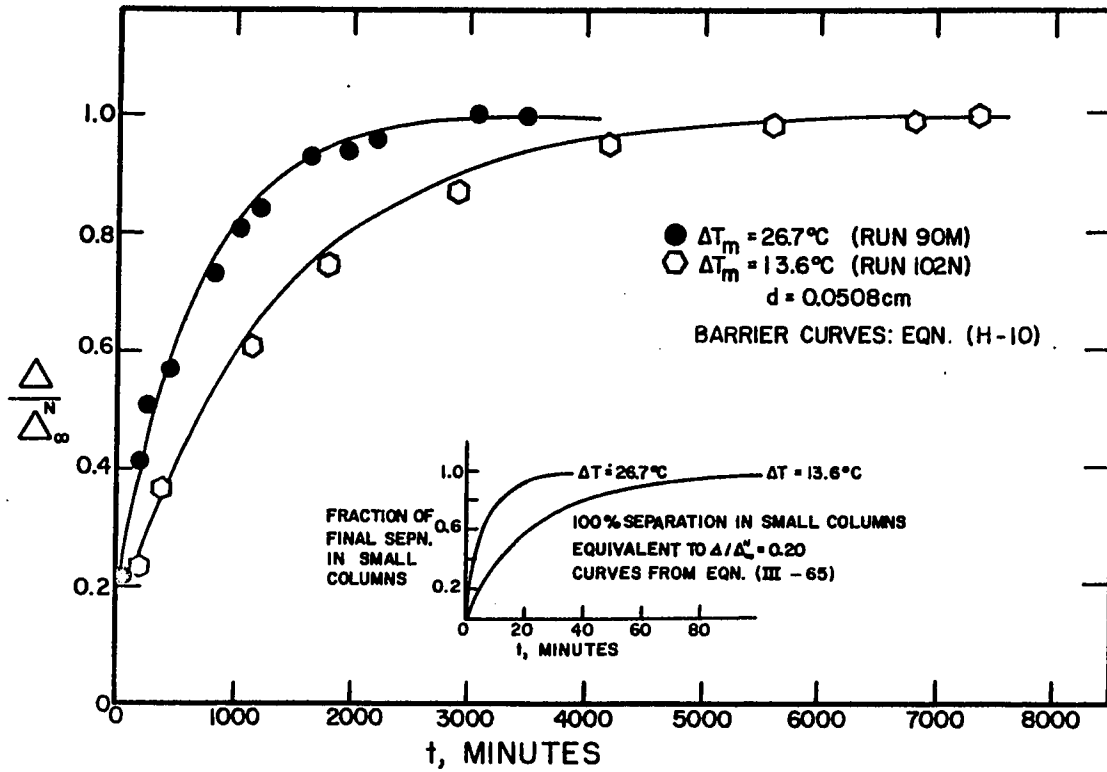
$$\begin{aligned}\sigma_c(\text{Lower } \Delta T) &= \sigma_c(\text{Higher } \Delta T) \times \frac{13.6^\circ\text{C}}{26.7^\circ\text{C}} \\ &= (0.070)(0.509) = 0.0356 \frac{\text{gram}}{\text{min}}\end{aligned}\tag{VI-8}$$

The agreement between theory and experiment is good.

The insert in Figure 31 again shows the magnitude of the error introduced by the assumption of instantaneous equilibrium. The error at the higher temperature difference is 0.8

Figure 31

Effect of the Temperature Difference between the Plates on the Transient Behavior of a Column with Four Horizontal Barriers



percent and the error at the lower temperature difference 2.2 percent of the time to reach ninety-five percent of the equilibrium separation. Once again compensation was made for the above errors in the same manner as described previously.

Figure 32 compares the effect of temperature difference on a column with sixteen equally-spaced barriers. The value of σ_c for the lower temperature difference was obtained from σ_c at the higher temperature difference multiplied by the ratio of temperature differences:

$$\sigma_{cN=16} = 0.070 \left[\frac{1 + 4(.035)}{1 + 16(.035)} \right] \times \frac{13.5^\circ\text{C}}{26.6^\circ\text{C}} \quad (\text{VI-9})$$

$$\sigma_{cN=16} = 0.0259 \frac{\text{gram}}{\text{min}}$$

Again the agreement between the predicted curves and the experimental results is excellent.

Figure 33 re-emphasizes the fact that the relaxation time in a column with barriers is proportional to ΔT and not to $(\Delta T)^2$. Empirical values of σ_c were obtained from each set of transient data in the same manner as described for the four barrier case. The empirical values of σ_c were then plotted as a function of N in Figure 33. The value of C in Equation (III-117), used in conjunction with Equation (III-121), was obtained which best represented the data at the higher temperature difference

Figure 32

Effect of the Temperature Difference between the Plates on
the Transient Behavior of a Column with Sixteen
Horizontal Barriers

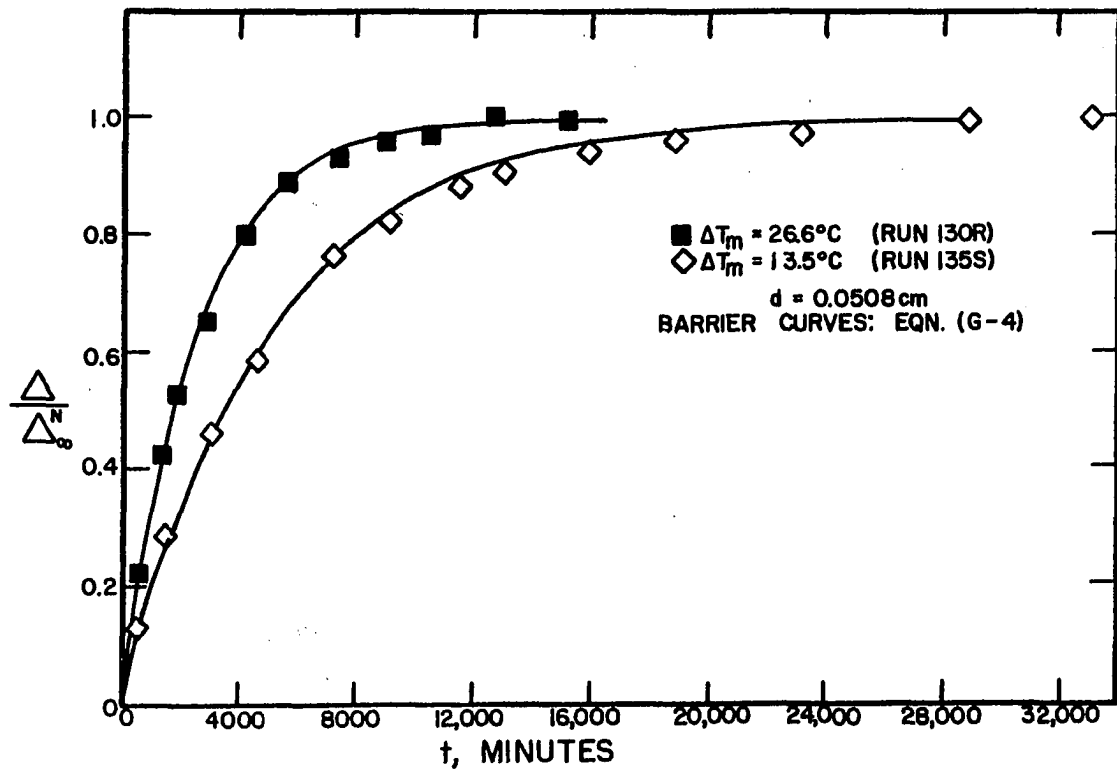
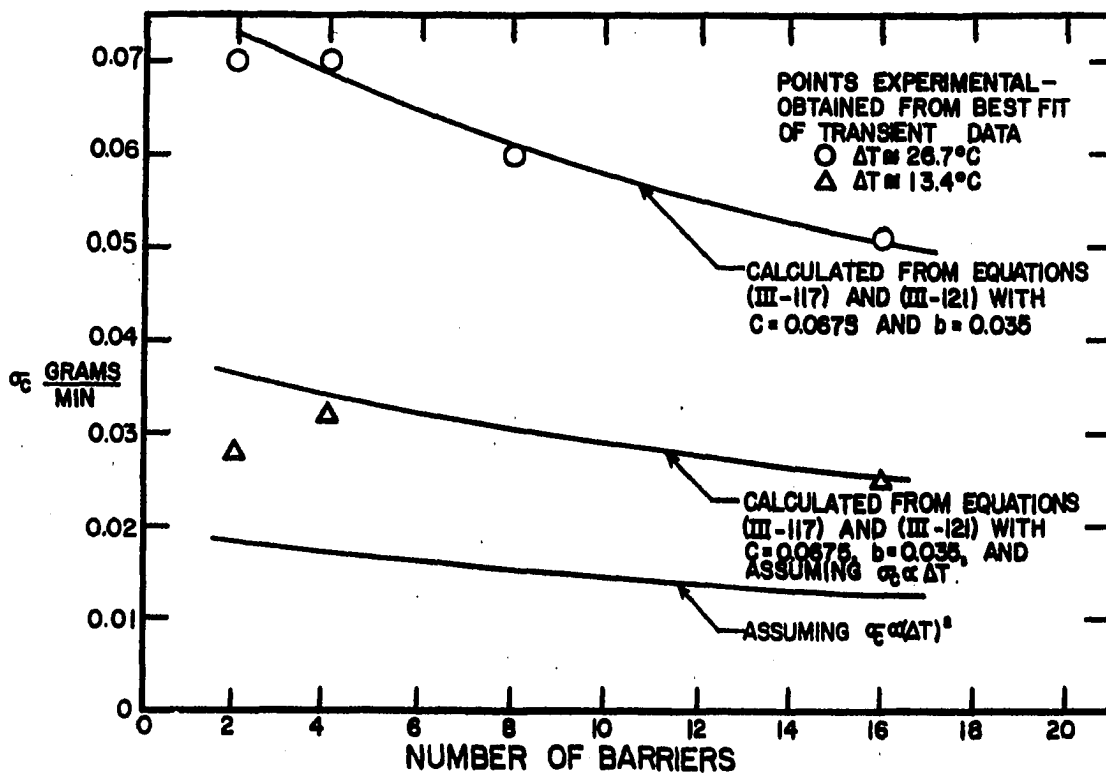


Figure 33

Effect of the Temperature Difference between the Plates on σ_c , the Flow Past the Barriers: Transient Data



($\Delta T = 26.7^\circ\text{C}$):

$$\sigma_c = C \cdot (\text{Convective Circulation}) \quad (\text{III-117})$$

$$\text{Circulation} = \frac{5\beta_T \rho g (2\omega)^3 B \Delta T}{32 \eta (1 + bN)} \quad (\text{III-121})$$

$$= \frac{5(7.8 \times 10^{-4})(0.912)(980)(0.0792)^3 9.21(\Delta T)}{32(1.15 \times 10^{-2})(1 + bN)} \quad (\text{VI-10})$$

$$\text{Circulation} = 0.0435 \frac{\Delta T}{(1 + bN)} \frac{\text{gram}}{\text{min}} \quad (\text{VI-11})$$

and finally

$$\sigma_c = \frac{0.0435(\Delta T)C}{(1 + bN)} \frac{\text{gram}}{\text{min}} \quad (\text{VI-12})$$

It was found that $C = 0.0675$ gave a curve which was a good representation of the data at the higher temperature difference in Figure 33. (The value of C is not a function of the temperature difference between the plates.) Curves were then calculated and plotted in Figure 33 assuming that σ_c was proportional to (ΔT) and to $(\Delta T)^2$. The data definitely indicate a first power dependence of σ_c on the temperature difference. The point that is off is for two barriers at the lower temperature difference, and this run was discussed earlier in connection with Figure 30.

Effect of Barrier Diameter

Equation (III-117) can be used to predict the effect realized by changing the barrier diameter to plate spacing ratio.

$$\sigma_c = C \cdot (\text{Convective Circulation}) \quad (\text{III-117})$$

As pointed out in Chapter III, the value of C in Equation (III-117) is thought to be dependent primarily on the barrier diameter to plate spacing ratio. The value of C at a ratio of 0.643 was determined above, and it was found to equal 0.0675. (A value of C of 0.0675 means that 6.75 percent of the circulating fluid flows past the barrier, and 93.25 percent of the fluid is "turned-around.") The problem then becomes one of obtaining a value of C at the large barrier diameter to plate spacing ratio of 0.803. The ratio of the C-values at the two barrier diameter to plate spacing ratios was determined experimentally in a plastic flow apparatus, and the experimentally determined ratio of the two C-values was 1.49. (See Chapter on Additional Work.) In other words, the amount of circulating fluid that flowed past the barriers was 1.49 times as great for the smaller ratio as for the larger ratio. Thus, the value of C for the larger barrier diameter to plate spacing ratio is $0.0675/1.49$ or 0.0453, and

$$\sigma_{cN} (\text{Larger diameter barriers}) = \frac{.0435(.0453)\Delta T}{(1 + bN)} \quad (\text{VI-12})$$

For four barriers of the larger diameter at a temperature difference of 26.7°C

$$\sigma_{cN=4} = \frac{0.0526}{1 + (.035)4} \quad (\text{VI-13})$$

$$= 0.0462 \frac{\text{gram}}{\text{min}}$$

Using the above value of σ_c , the system of simultaneous equations given by Equations (III-75) through (III-77) was solved to give the transient curves for four barriers of the larger diameter at the two temperature differences considered experimentally in this work. The system of equations is the same as for four barriers of the smaller diameter, and hence the final equation is the same. Thus, Equation (H-10) is used in conjunction with the value of σ_c above ($\sigma_c = 0.046 \text{ gram/min}$) to calculate the predicted transient curve. The value of σ_c at the lower temperature difference of 13.4°C (actually 13.7°C for this case) was obtained from the value of σ_c at the higher temperature difference by using the fact that σ_c is proportional to ΔT :

$$\begin{aligned} \sigma_c(\text{Lower } \Delta T) &= \sigma_c(\text{Higher } \Delta T) \times \frac{13.7^\circ\text{C}}{26.7^\circ\text{C}} \\ &= (0.0462)(0.513) = 0.0237 \frac{\text{gram}}{\text{min}} \end{aligned} \tag{VI-14}$$

Figures 34 and 35 compare the experimental results with the predicted curves for four barriers of both barrier diameters and at the two temperature differences. The agreement between the experimental results and the predicted curves is very good.

Figure 34

Effect of the Barrier Diameter on the Transient Behavior
of a Column with Four Horizontal Barriers: Higher
Temperature Difference

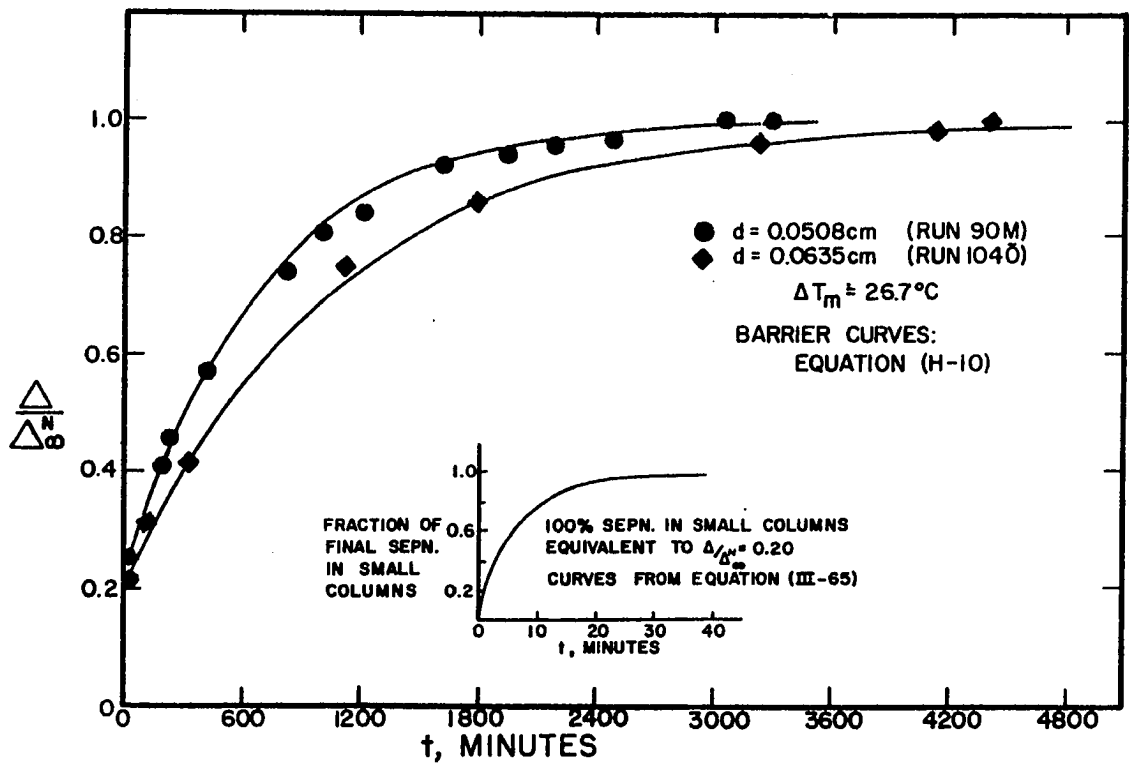
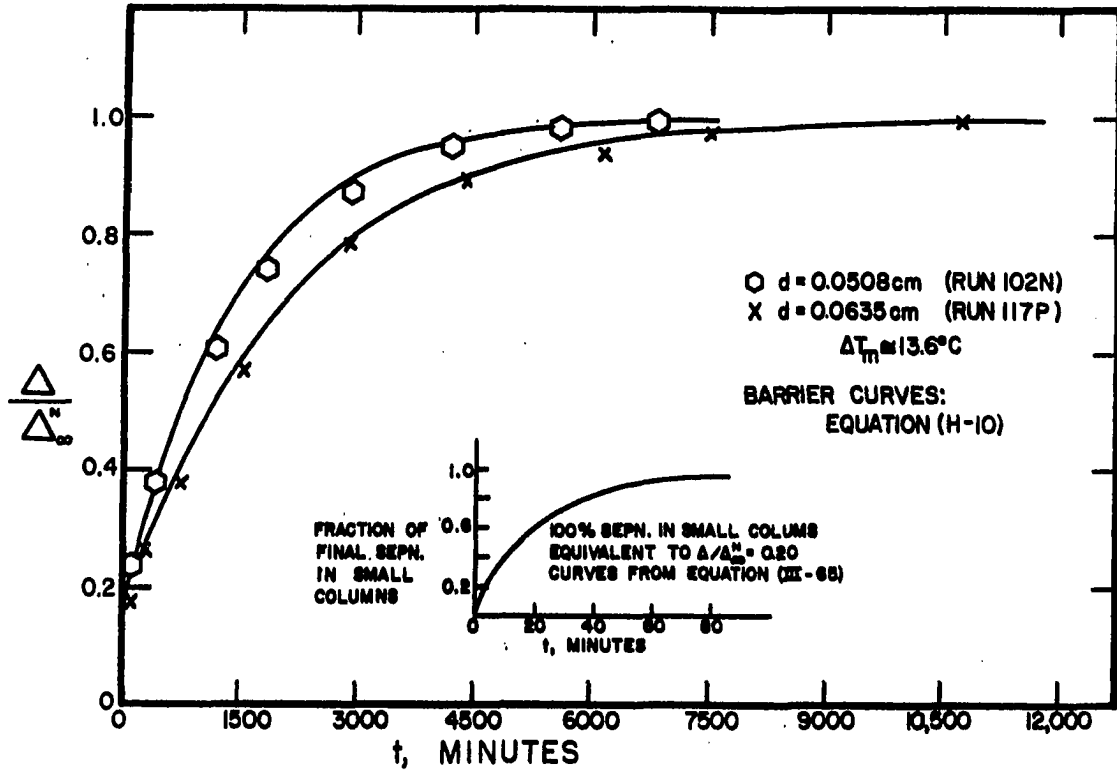


Figure 35

Effect of the Barrier Diameter on the Transient Behavior
of a Column with Four Horizontal Barriers: Lower
Temperature Difference



The inserts in Figures 34 and 35 have been discussed previously in connection with Figures 25 and 31.

Continuous Flow Case

Effect of Number of Barriers

Rate-separation curves were obtained for zero, two, four, eight, sixteen, and fifty barriers. (See Appendix B for continuous flow data.) The equation describing the rate-separation curve for N equally-spaced horizontal barriers is Equation (III-111):

$$\Delta^N = 2 \left[\Delta_L + \Delta_B \sum_{n=1}^N \zeta^n \right] \quad \text{(III-111)}$$

where

$$\zeta = \frac{\sigma_c}{\sigma_c + \sigma} \quad \text{(III-112)}$$

and

$$\Delta_B = \frac{H^N}{4\sigma} \left[1 - e^{-\frac{\sigma L}{K^N(N+1)}} \right] \quad \text{(III-113)}$$

$$\Delta_L = \frac{H^N}{4\sigma} \left[1 - e^{-\frac{\sigma L}{2K^N(N+1)}} \right] \quad \text{(III-114)}$$

In deriving Equation (III-111), it was assumed that the overhead and bottom product rates were equal ($\sigma = \sigma_e = \sigma_s$), that H_e^N and

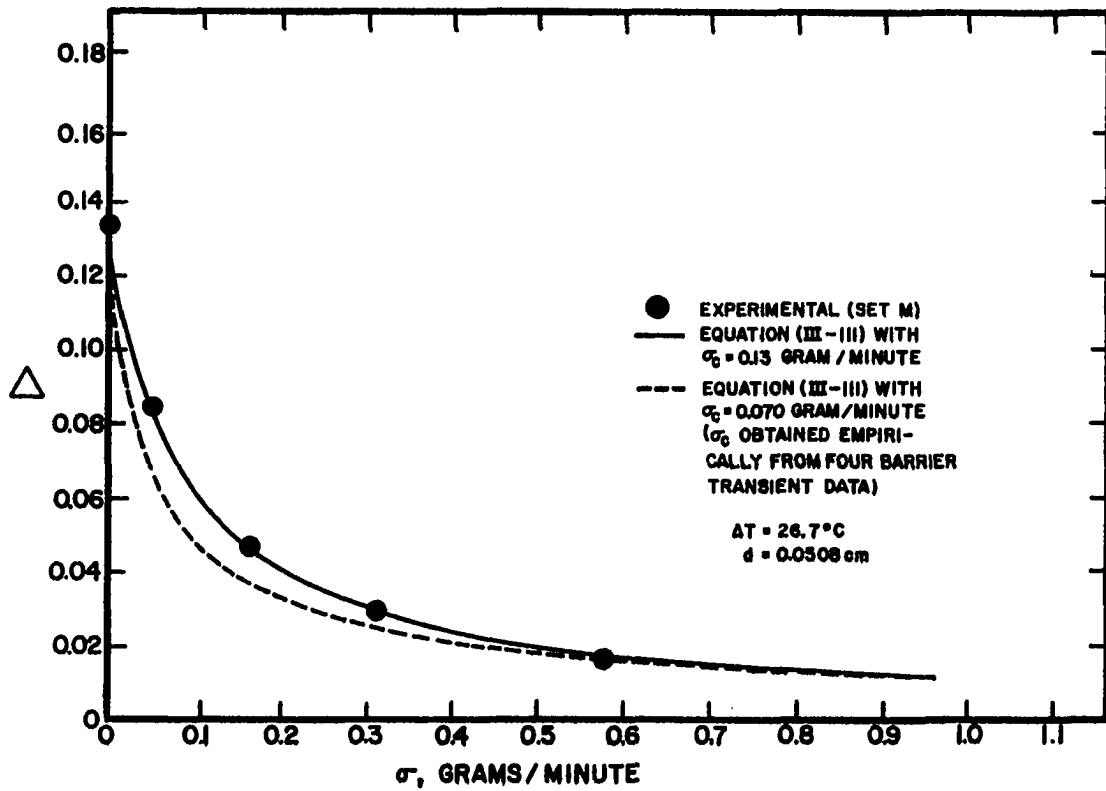
K_e^N for the enriching section of the column were equal to H_s^N and K_s^N for the stripping section of the column, and that the N barriers were equally-spaced in the column.

As mentioned in the previous section, an empirical value of σ_c for four barriers was obtained from the best fit of the transient data for four equally-spaced barriers at the temperature difference of 26.7°C . It was felt that the empirical value of σ_c might also correlate the four barrier flow data at the same temperature difference since it was assumed that the flow past the barriers should be independent of the bulk flow rate. However, it was found that the rate-separation curve calculated using the value of σ_c obtained from the four barrier transient data did not quantitatively represent the experimental flow data. (See the dashed line in Figure 36.) The point that is disturbing here is that any "correction" made for the bulk flow opposing the flow past the barriers is in the wrong direction. That is, the supposed correction makes the discrepancy between theory and experiment worse, since the values of σ_c for the flow case are larger, rather than smaller, than the values of σ_c for the transient case.

A possible explanation of the larger value of σ_c for the flow data might be a changed hydrodynamic flow pattern, conceivably even turbulence, near the barriers because of the increased flow. However, regardless of the reason for the

Figure 36

Comparison of Rate-Separation Curves for Four
Horizontal Barriers with Different Values
of σ_c , the Flow Past the Barriers



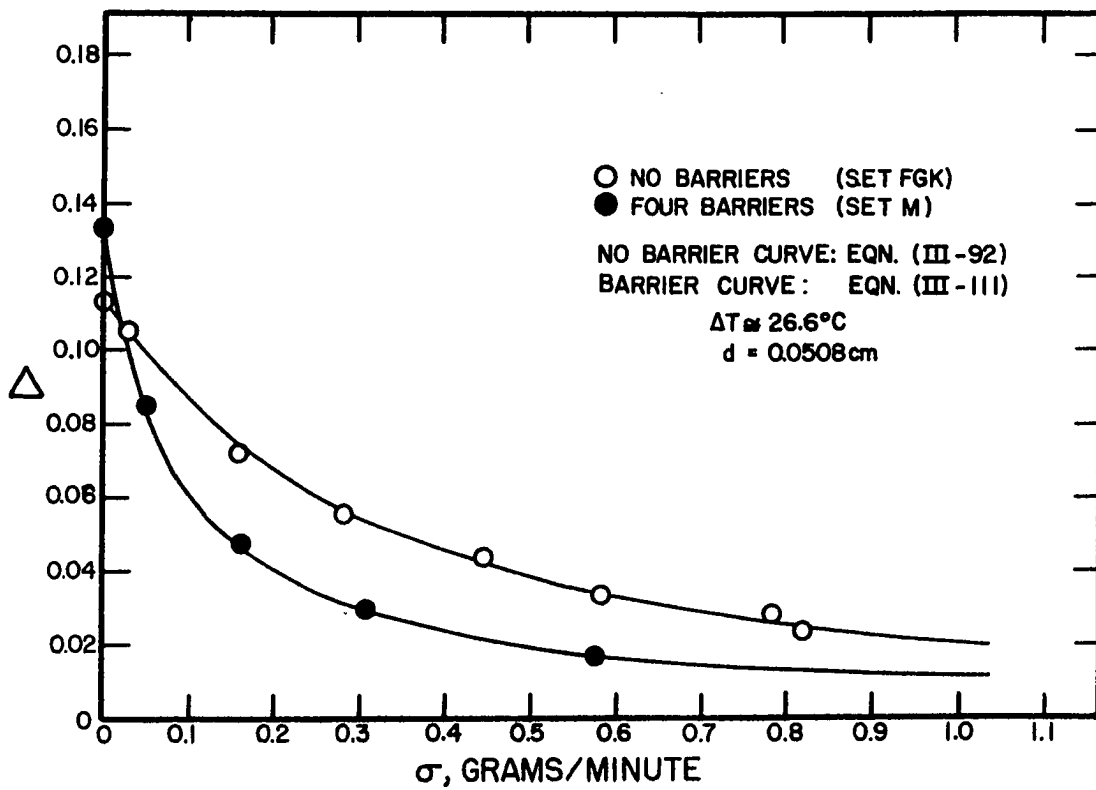
discrepancy, a value of σ_c for a rate-separation curve with a given number of barriers must be obtained in one of two ways: (1) empirically from a rate-separation curve with N barriers, or (2) by finding a relationship between σ_c from transient data and σ_c from flow data. Consequently, an empirical value of σ_c was obtained from the four barrier flow data at a temperature difference of 26.7°C (shown in Figure 36) in the following manner.

Values of Δ_B and Δ_L were calculated as a function of the bulk flow rate from Equations (III-113) and (III-114). [The values of $H^{N=4}$ and $K^{N=4}$ were calculated from Equations (III-45) through (III-48).] By assuming a value for σ_c , ξ can be obtained as a function of the bulk flow rate, σ , from Equation (III-112), and consequently a rate-separation curve can be calculated using Equation (III-111) with $N = 4$. Curves were calculated for different values of σ_c until the best fit of the four barrier flow data was obtained: a value of σ_c of 0.13 gram/min gave the best fit of the continuous flow data as shown by the solid line in Figure 36.

The rate-separation curve for a column with four barriers is compared with the rate-separation curve for the open column in Figure 37. Notice that the separation in the column with barriers is lower than the separation in the open column at all bulk flow rates greater than approximately 0.02 gram/min. Thus,

Figure 37

Comparison of Rate-Separation Curves for Columns
with Zero and Four Horizontal Barriers



the use of barriers in this case would apparently allow greater separations than the open column only for very low flow rates, rates less than 0.02 gram/min. (No experimental points were taken in this range.)

[It should be pointed out that the rate-separation curve for the open column was calculated from Equations (III-34), (III-35), and (III-92). The experimental points plotted for the open column were the average of points taken in experimental sets F, G, and K at the higher temperature difference of 26.7°C, and experimental sets H and L at the lower temperature difference of 13.4°C. These sets are noted on the graphs as simply set FGK and set HL.]

The empirical value of σ_c for four barriers was used in conjunction with Equation (VI-4) to predict values of σ_c at the higher temperature difference as a function of the number of barriers:

$$\sigma_{cN} = \sigma_{cN=4} \left(\frac{1 + 4b}{1 + bN} \right) \quad (\text{VI-4})$$

$$\sigma_{cN} = 0.13 \left(\frac{1 + 4b}{1 + bN} \right) \frac{\text{gram}}{\text{min}} \quad (\text{VI-15})$$

Rate-separation curves were then calculated for two, eight, sixteen, and fifty barriers and the curves compared with the experimental results in Figures 38 through 41. It should be

Figure 38

Comparison of Rate-Separation Curves for Columns
with Zero and Two Horizontal Barriers

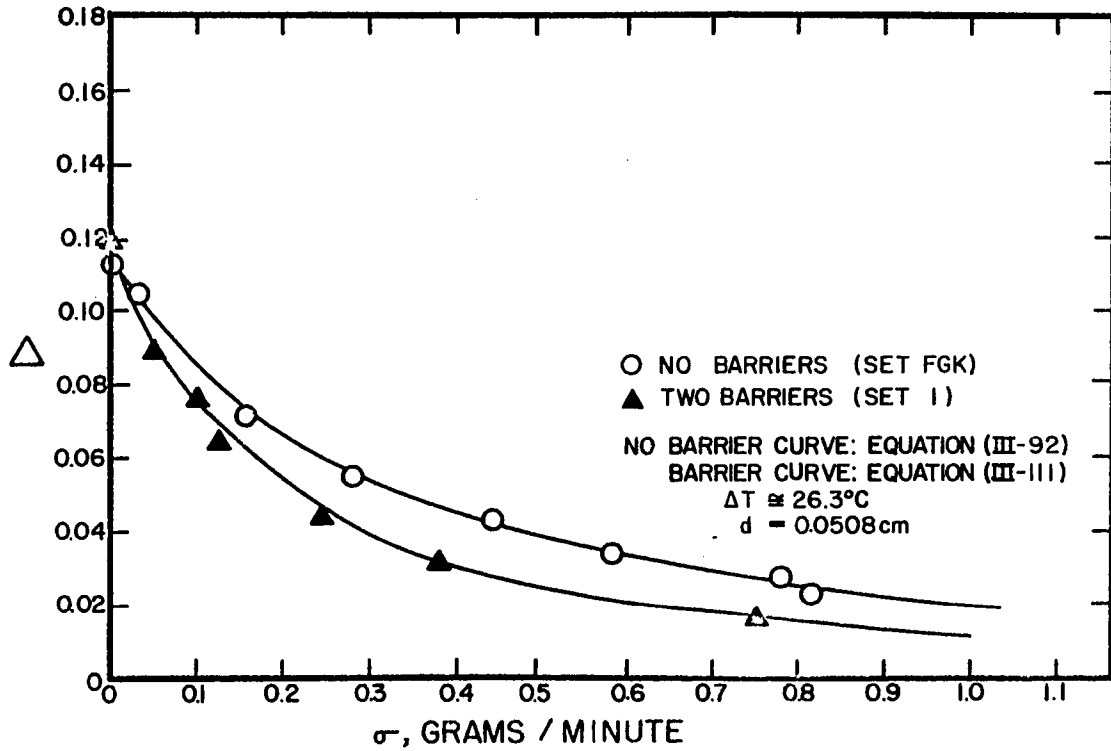


Figure 39

Comparison of Rate-Separation Curves for Columns
with Zero and Eight Horizontal Barriers

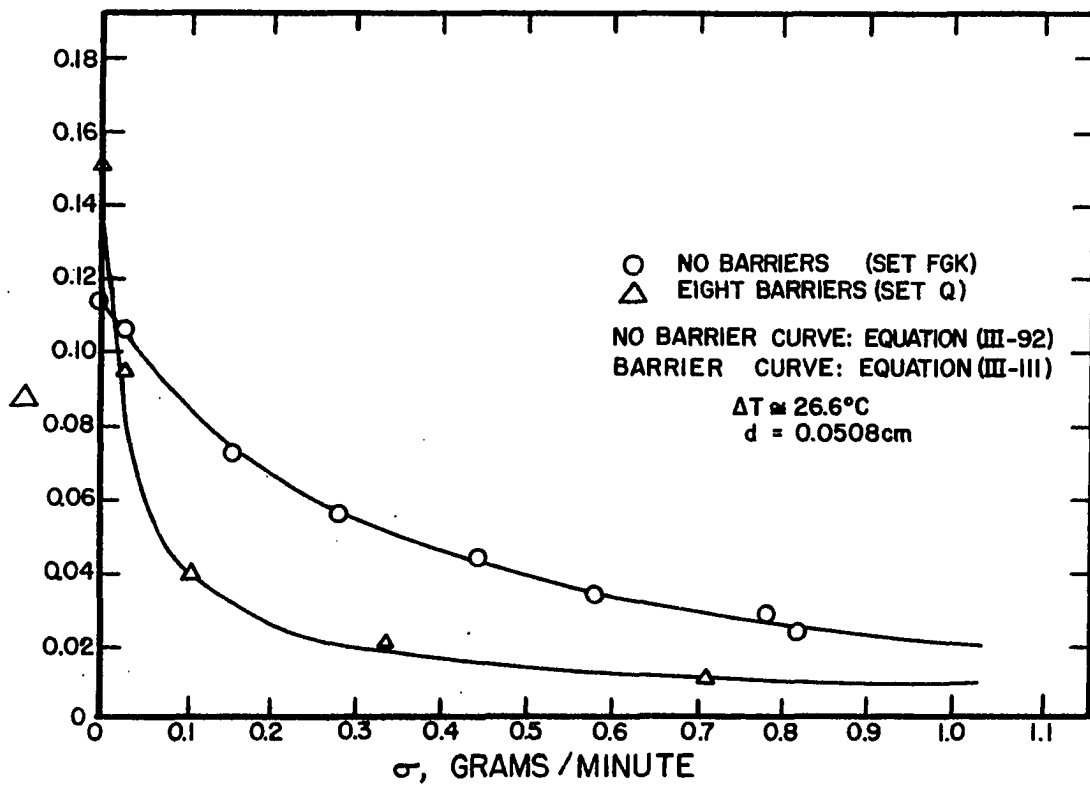


Figure 40

Comparison of Rate-Separation Curves for Columns
with Zero and Sixteen Horizontal Barriers

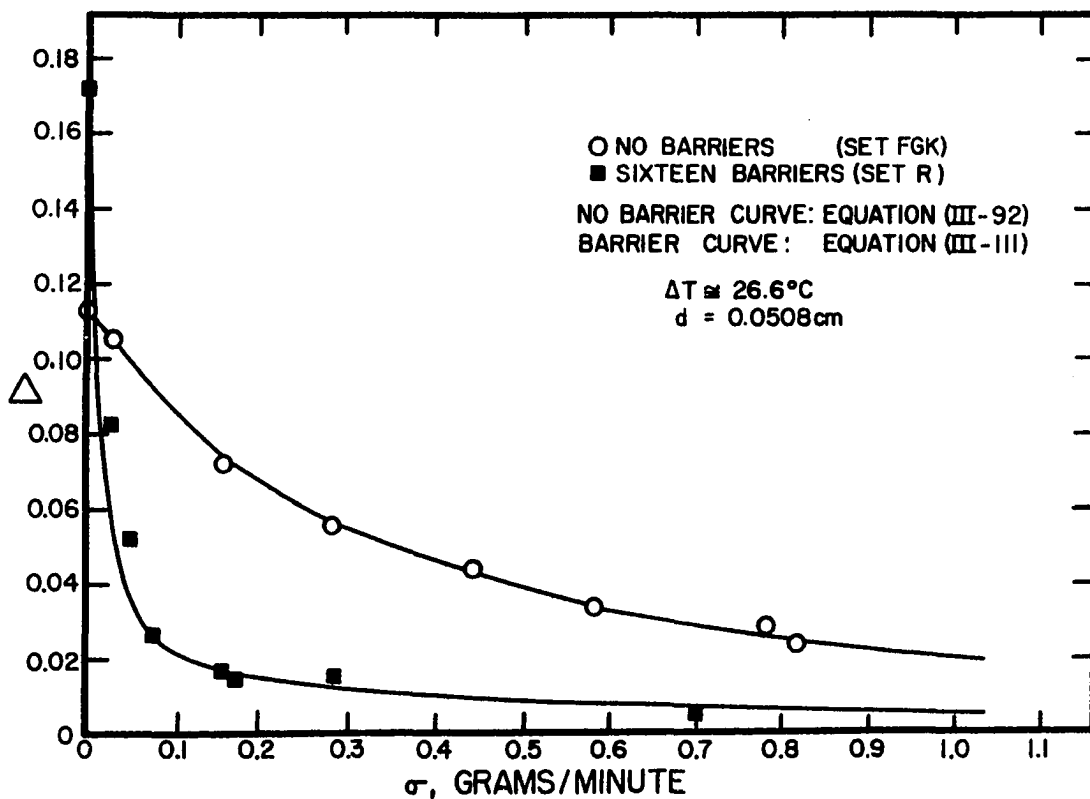
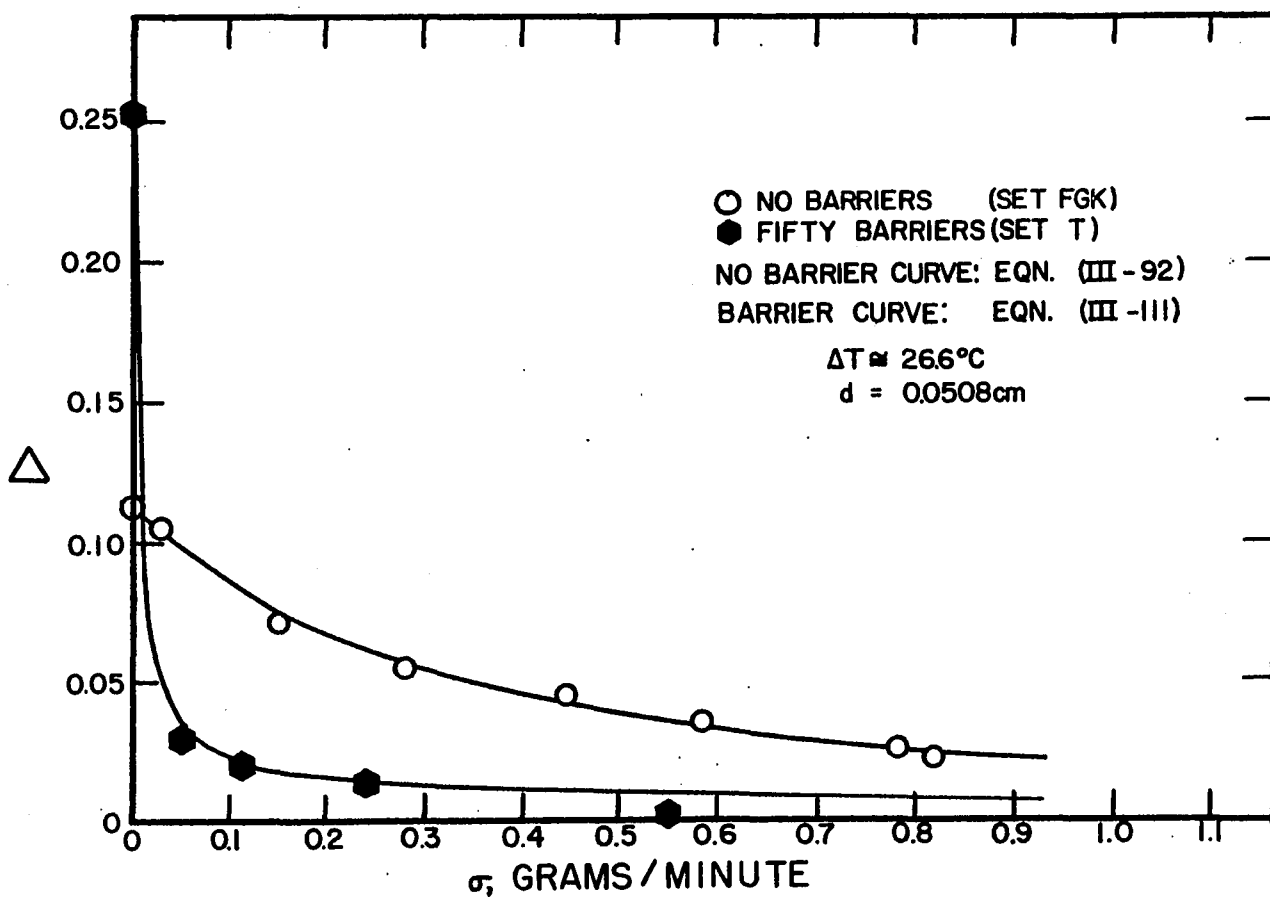


Figure 41

Comparison of Rate-Separation Curves for Columns
with Zero and Fifty Horizontal Barriers



noted that in calculating the rate-separation curves from Equation (III-111) for different values of N , the values of Δ_B and Δ_L change as well as the value of ζ . The value of ζ changes because of new values of σ_c calculated from Equation (VI-15). The values of Δ_B and Δ_L , given by Equations (III-113) and (III-114), change for two reasons: (1) the expressions for H^N and K^N include the terms $(1 + bN)$ and $(1+bN)^2$ respectively, and hence are a function of the number of barriers, and (2) the exponential term in Equations (III-113) and (III-114) is a function of the number of barriers (independent of K^N). Therefore, it is necessary to calculate ζ , Δ_B , and Δ_L as a function of the bulk flow rate for each value of N .

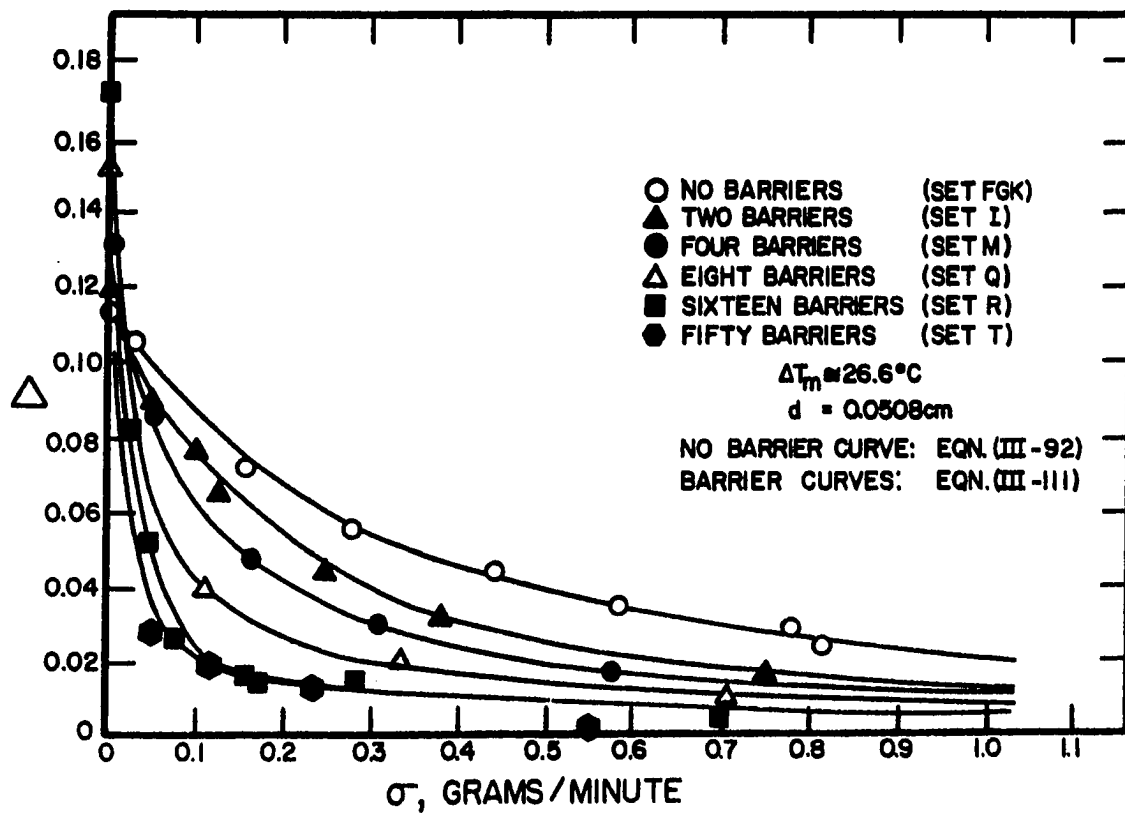
Figure 42 summarizes all of the continuous flow data and the predicted curves at the higher average temperature difference of 26.6°C . The agreement between the predicted curves and the experimental results is good in all cases.

Effect of Temperature Difference between the Plates

The effect of temperature difference on continuous flow column performance in the open column is well-known: increasing the temperature difference between the plates increases the separation at a given flow rate. Numerous investigators (B8) (H1) (L3) (P3) have shown the theory to be qualitatively correct for this effect.

Figure 42

Comparison of Rate-Separation Curves for Columns
with Zero, Two, Four, Eight, Sixteen, and
Fifty Horizontal Barriers: Higher
Temperature Difference



The temperature difference between the plates alters both H^N and K^N as shown by Equations (III-45) and (III-46). The dependence of σ_c on the temperature difference is illustrated in Figure 43. Empirical values of σ_c were obtained from the best fit of the rate-separation data for each value of N in the same manner as described previously in connection with Figure 36. The empirical values of σ_c were then plotted as a function of the number of barriers in Figure 43. The value of C in Equation (III-117) that best represented the values of σ_c at the higher temperature difference of 26.7°C was then obtained ($C = 0.1275$), and additional curves were calculated assuming that σ_c was a function of ΔT , and of $(\Delta T)^2$. The data clearly indicate a first power dependence of σ_c on the temperature difference between the plates.

Figure 44 shows the effect of temperature difference on continuous flow column performance of a column with two horizontal barriers. Once again, it can be seen that an increase in temperature difference gives a greater separation at a given flow rate. The value of σ_c for the higher temperature difference was obtained from Equation (VI-15). The value of σ_c for the lower temperature difference was then obtained by utilizing the fact that σ_c is proportional to ΔT :

$$\sigma_c(\text{Lower } \Delta T) = \sigma_c(\text{Higher } \Delta T) \times \frac{13.2^\circ\text{C}}{26.1^\circ\text{C}}$$

(VI-16)

Figure 43

Effect of the Temperature Difference between the Plates on the Flow Past the Barriers, σ_c : Continuous Flow Data

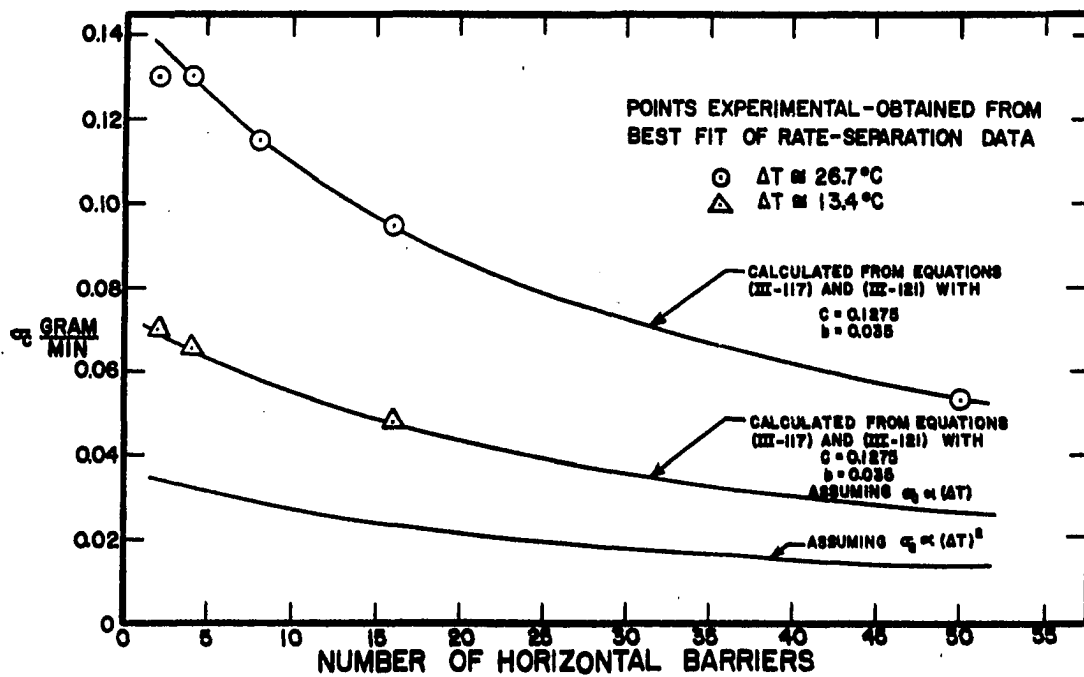
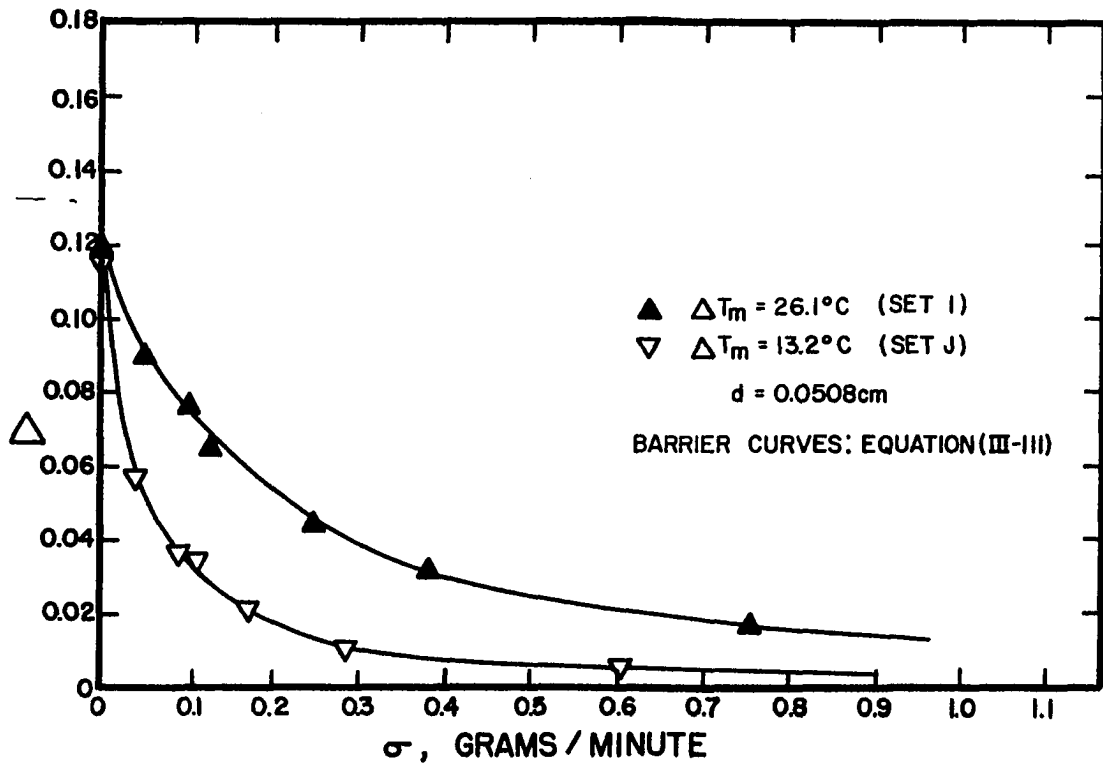


Figure 44

Effect of the Temperature Difference between the Plates on
the Rate-Separation Curve of a Column with Two
Horizontal Barriers



$$= (0.138)(0.506)$$

$$= 0.070 \frac{\text{gram}}{\text{min}}$$

Figures 45 and 46 illustrate the effect of temperature difference on columns with four and sixteen barriers. The agreement between experiment and theory is excellent in all cases.

Effect of Barrier Diameter

As mentioned previously, two barrier diameters were studied in this work (barrier diameter to plate spacing ratios of 0.643 and 0.803). Again it is known that as the barrier diameter is increased relative to the plate spacing, the value of C in Equation (III-117) decreases and hence the flow past the barriers, σ_c , should be decreased. This in turn effectively reduces ζ , as shown by Equation (III-112), and, since H^N and K^N are thought to be independent of the barrier diameter, increasing the barrier diameter should reduce the separation at a given flow rate (and, of course, decreasing the barrier diameter should increase the separation).

As pointed out in the previous section on transient behavior, Equation (III-117) can be used to predict the effect realized by changing the barrier diameter to plate spacing ratio. The value of C at the small diameter to plate spacing ratio was determined above and was found to equal 0.1275. (See also Figure 43.) Recalling that the ratio of C -values at

Figure 45

Effect of the Temperature Difference between the Plates on
the Rate-Separation Curve of a Column with Four
Horizontal Barriers

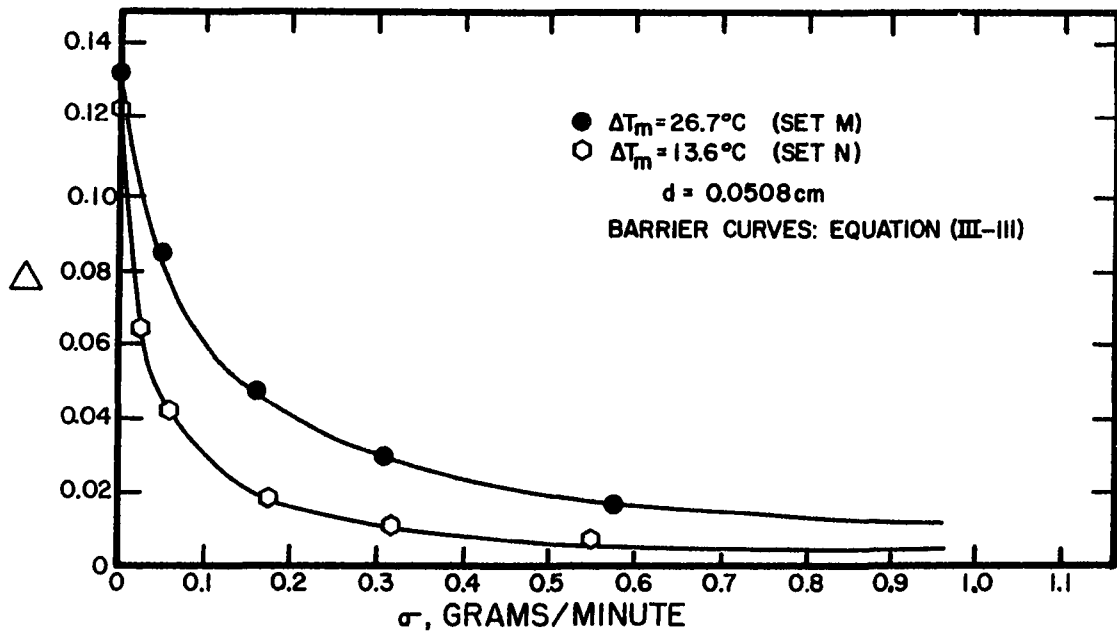
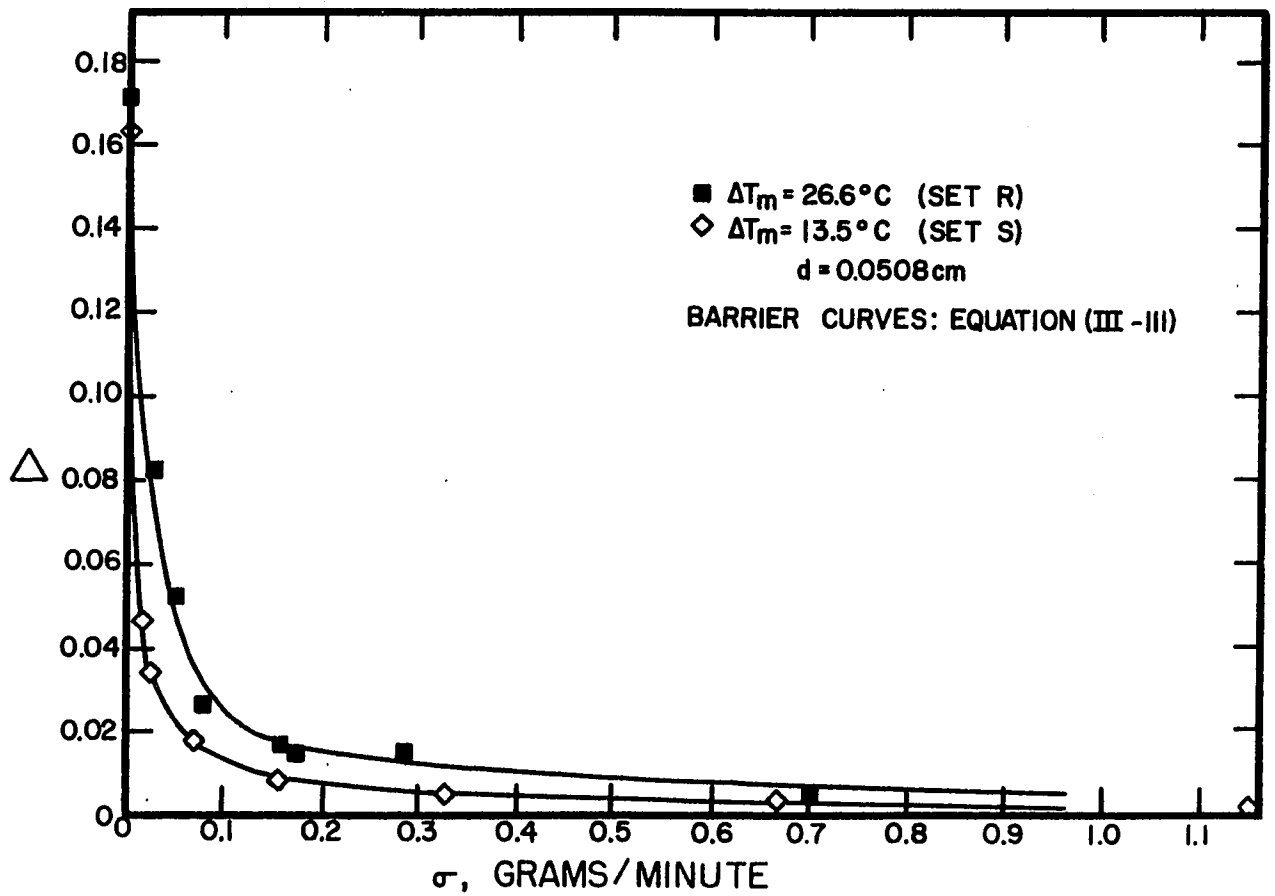


Figure 46

Effect of the Temperature Difference between the Plates on
the Rate-Separation Curve of a Column with Sixteen
Horizontal Barriers



the two barrier diameter to plate spacing ratios was found experimentally to be 1.49 (See Chapter VII.), the C-value at the larger diameter to plate spacing ratio can be calculated: the C-value at the large ratio is equal to $0.1275/1.49$ or 0.0857 . A value of σ_c at the temperature difference of 26.7°C can then be calculated from Equation (VI-12):

$$\sigma_{cN} \text{ (Larger diameter barriers)} = 0.0435 \frac{(0.0857)\Delta T}{(1 + bN)} \quad (\text{VI-12})$$

For four barriers of the larger diameter at $\Delta T = 26.7^\circ\text{C}$

$$\begin{aligned} \sigma_{cN=4} &= \frac{0.0993}{1 + (.035)4} \\ &= 0.087 \frac{\text{gram}}{\text{min}} \end{aligned} \quad (\text{VI-17})$$

This value of σ_c of 0.087 gram/min for the larger barrier diameter was then used in conjunction with Equations (III-111) through (III-114) to calculate the rate-separation curves at the two temperature differences considered. The effect of temperature difference was introduced by using the fact that σ_c is proportional to the first power of ΔT . Therefore, for the lower temperature difference

$$\begin{aligned} \sigma_c &= 0.087 \times \frac{13.6^\circ\text{C}}{26.7^\circ\text{C}} \frac{\text{gram}}{\text{min}} \\ &= 0.0443 \frac{\text{gram}}{\text{min}} \end{aligned} \quad (\text{VI-18})$$

Figures 47 and 48 compare the predicted and experimental results at the two temperature differences considered. The agreement is very satisfactory.

Summary

In this chapter, experimental results have been presented and compared with the modified theory developed in Chapter III. Experimental data with horizontal barriers in the separation space were obtained with two, four, eight, sixteen, and fifty barriers. In addition, two temperature differences were investigated experimentally and several runs were made with the barrier diameter as a parameter. Data were also obtained with no barriers in the separation space in order to compare the barrier data with open column data. Three types of data were obtained with horizontal barriers: (1) steady-state batch, or no bulk flow, data, (2) transient data on a column operated under batch conditions, and (3) steady-state continuous flow data where feed was added to the center of the column, and overhead and bottom products were removed continuously from the ends of the column.

The batch data show agreement with the ex post facto theory, and increased batch separations resulted from the addition of barriers. The increase per barrier was approximately 3.5 percent for this work, ($b = 0.035$), with the percent increase falling off for greater number of barriers because of an effective length correction ($L - Nl_T$). Although the theory does not predict

Figure 47

Effect of the Barrier Diameter on the Rate-Separation Curve
of a Column with Four Horizontal Barriers: Higher
Temperature Difference

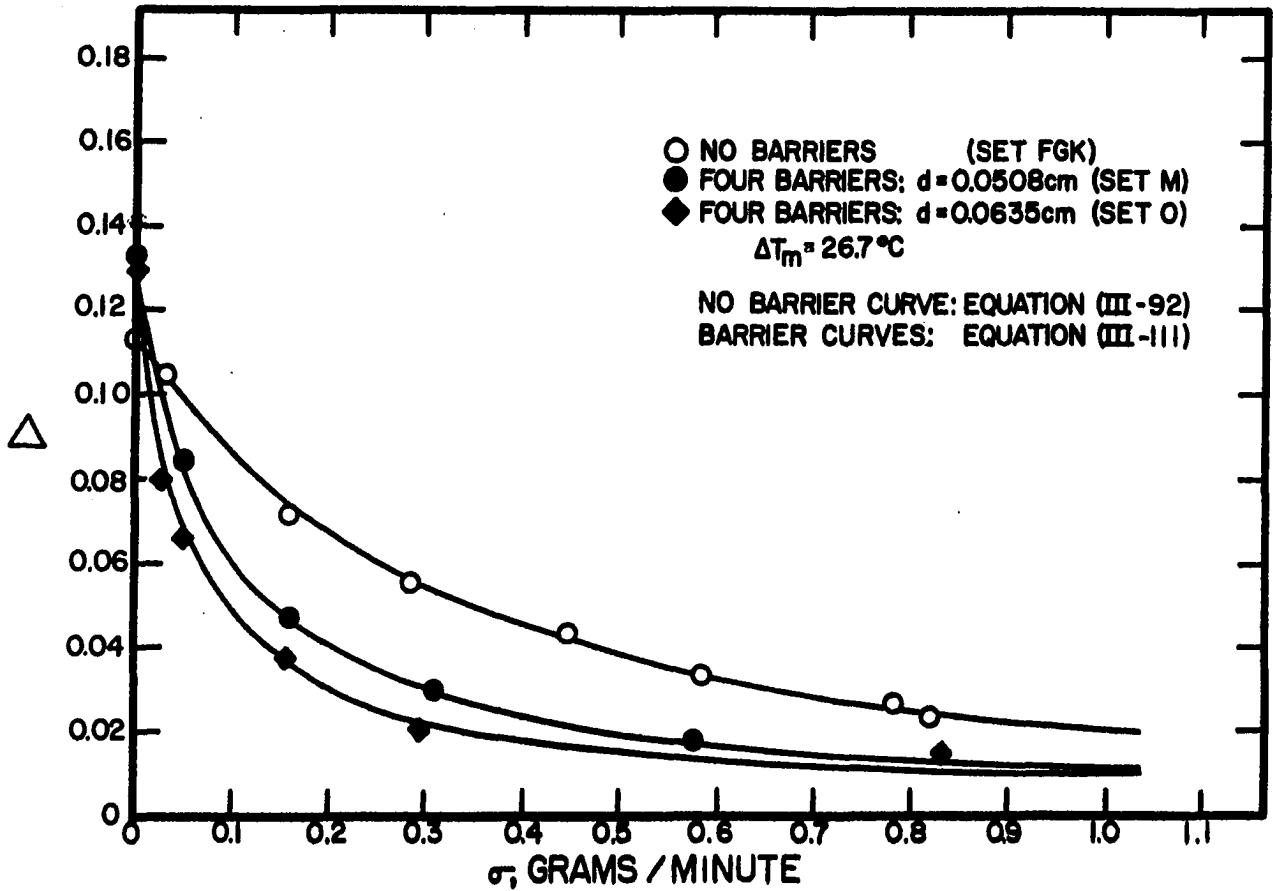
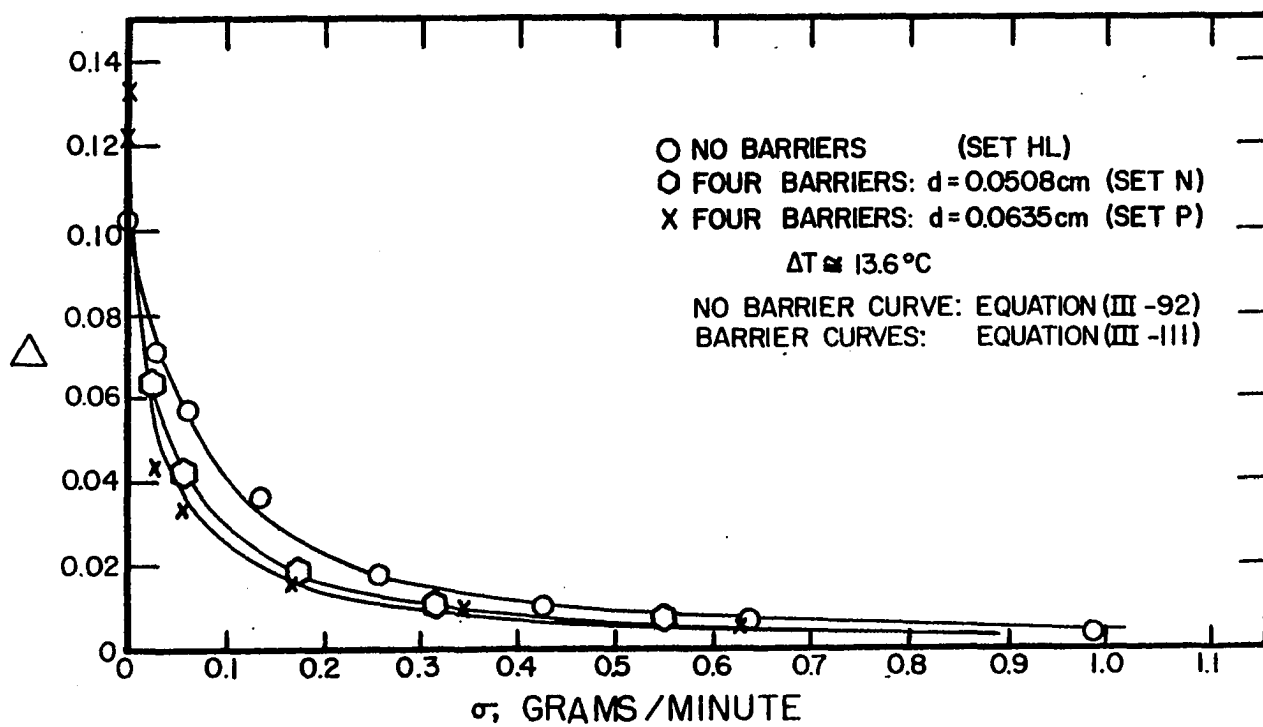


Figure 48

Effect of the Barrier Diameter on the Rate-Separation Curve
of a Column with Four Horizontal Barriers: Lower
Temperature Difference



an effect of the temperature difference on the batch separation, it was found experimentally that the steady-state batch separation is slightly decreased as the temperature difference between the plates is decreased. Other experimental investigators have found a similar dependence on the temperature difference. The lack of observed effect of the barrier diameter to plate spacing ratio on the batch separation supports the theory.

Transient data were obtained for zero, two, four, eight, and sixteen barriers, and amazing agreement between the experimental results and predicted curves is noted. Particularly striking is the fact that the relaxation time in a column with barriers is proportional to the first power of the temperature difference rather than the square of the temperature difference, as is true in the open column. The effect of the number of barriers and of the barrier diameter to plate spacing ratio on the transient behavior of a column with barriers is correctly predicted by the theory: increasing the number of barriers or increasing the barrier diameter relative to the plate spacing increases the time required to reach steady-state conditions. An experimentally determined ratio of C-factors was used to predict the effect of the barrier diameter to plate spacing ratio on the time to reach equilibrium. Corrections were made for the error incurred in assuming instantaneous equilibrium in the small columns formed by the barriers. An additional correction was necessary for the special case with two barriers. In general, good agreement is noted between the predicted curves and the experimental results.

The separation as a function of the bulk flow rate through the column constitutes the continuous flow data. Rate-separation

curves were obtained for zero, two, four, eight, sixteen, and fifty barriers. The effect of the number of barriers on a rate-separation curve is correctly predicted by the modified theory: the separation at a given flow rate drops as the number of barriers is increased. It is pointed out that apparently only for very low flow rates does a column with barriers offer an advantage over the open column. The effects of the temperature difference between the plates and of the barrier diameter to plate spacing ratio are also correctly accounted for by the theory. Lowering the temperature difference and increasing the barrier diameter relative to the plate spacing both decrease the separation at a given flow rate. In all cases, the agreement between the experimental data and predicted curves is excellent.

CHAPTER VII

ADDITIONAL WORK

Work is presented in this chapter which is not directly related to the experimental work with barriers presented in Chapter VI. The evaluation of the thermal diffusion coefficient, α , column operation with unequal product flow rates, and the determination of the C-coefficients at the two barrier diameter to plate spacing ratios are discussed.

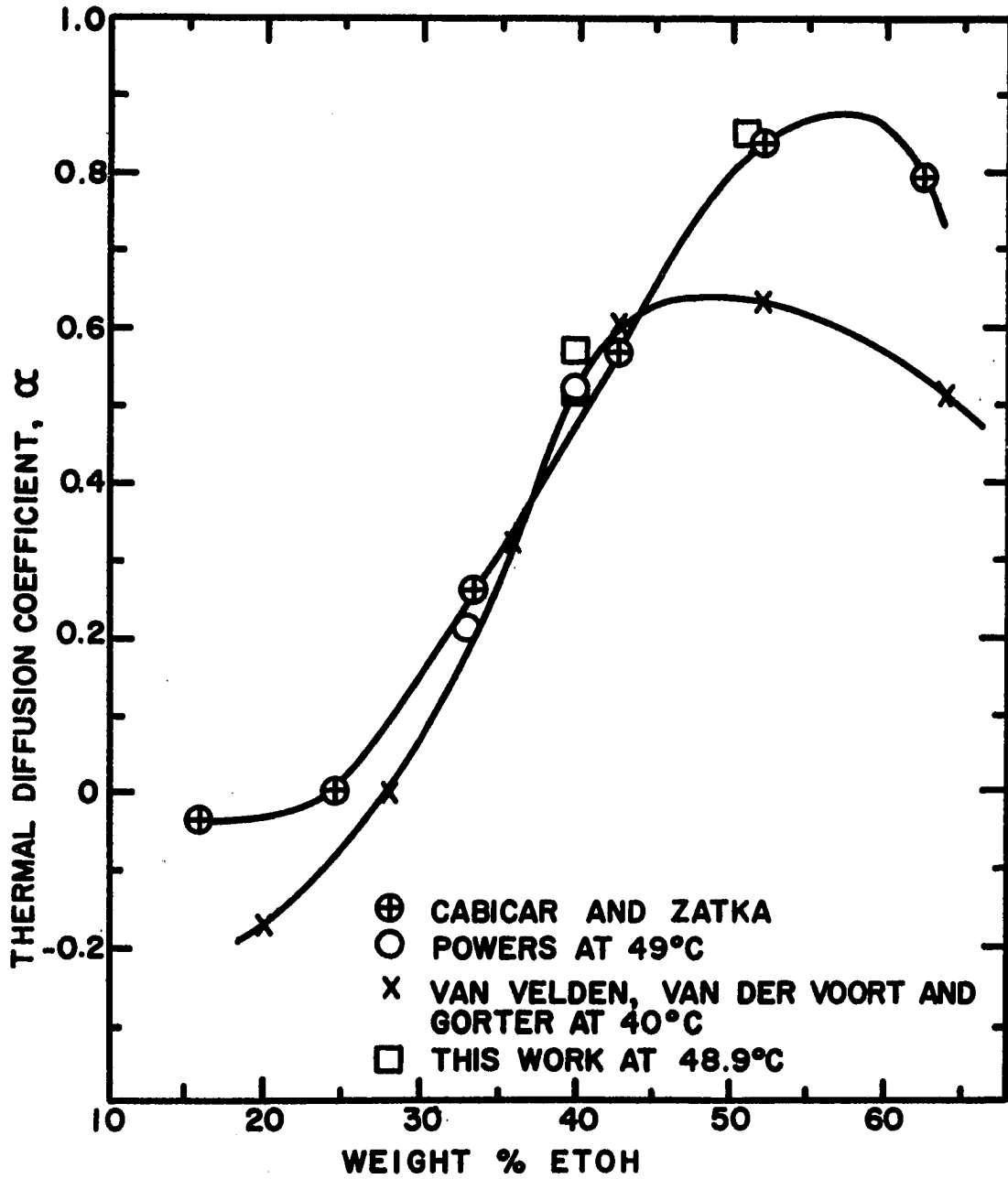
Evaluation of the Thermal Diffusion Coefficient

Data were obtained (see Experimental Set A.) such that the thermal diffusion coefficient, α , could be calculated for a fifty-one weight percent alcohol feed. The calculated value (See Appendix H.) of α was found to support the work of Cabicar and Zatka (C1) (See Figure 49.) in preference to the data presented by Van Velden, Van der Voort, and Gorter (V1).

This value of α will be discussed in more detail in the next section of column operation with unequal product flow rates.

Figure 49

Thermal Diffusion Coefficient, α , for the System Ethyl Alcohol-Water As a Function of the Concentration



Column Theory and Operation with Unequal
Product Flow Rates ($\sigma_e \neq \sigma_s$)

Numerous experimental investigations have confirmed the theory of Furry, Jones, and Onsager (F7) for center-feed continuous-flow thermogravitational columns with equal product flow rates. In the case of unequal product flow rates, ($\sigma_e \neq \sigma_s$), Equation (III-91) applies from conventional theory

$$\Delta = \frac{H_e}{4\sigma_e} \left(1 - e^{-\frac{\sigma_e L_e}{K_e}}\right) + \frac{H_s}{4\sigma_s} \left(1 - e^{-\frac{\sigma_s L_s}{K_s}}\right) \quad (\text{III-91})$$

Powers (P3) (P7) has shown that for low flow rates, assuming the column always adjusts to yield its maximum separation, the following expression can be derived for unequal product flow rates

$$\Delta = \frac{H \sigma}{2\sigma_e \sigma_s} \left(1 - e^{-\frac{\sigma_e \sigma_s L}{2\sigma K}}\right) \quad (\text{VII-1})$$

where $H = H_e = H_s$, $K = K_e = K_s$, and $\frac{L}{2} = L_e = L_s$.

Powers' data taken with unequal product flow rates were admittedly inconclusive, and the work done here is an effort to clarify the applicability of Equation (VII-1).

In order to facilitate plotting and calculation, Equations (III-91) and (VII-1) are first put in dimensionless form. In dimensionless form, Equation (III-91) becomes

$$\frac{\Delta}{\Delta_0} = \frac{1+X}{4Z} \left[\frac{1}{X} \left(1 - e^{-\frac{2XZ}{1+X}} \right) + \left(1 - e^{-\frac{2Z}{1+X}} \right) \right] \quad (\text{VII-2})$$

and Equation (VII-1) becomes

$$\frac{\Delta}{\Delta_0} = \frac{(1+X)^2}{4XZ} \left[1 - e^{-\frac{4XZ}{(1+X)^2}} \right] \quad (\text{VII-3})$$

where Δ/Δ_0 is the fraction of the steady-state separation for no bulk flow, and

$$X = \frac{\sigma_e}{\sigma_s} \quad (\text{VII-4})$$

$$Z = \frac{\bar{\sigma}L}{2K} \quad (\text{VII-5})$$

$$L = L_e + L_s \quad (\text{VII-6})$$

$$\sigma = \frac{\sigma_e + \sigma_s}{2} \quad (\text{VII-7})$$

Equations (VII-2) and (VII-3) again assume that $H_e = H_s$, $K_e = K_s$, and $L_e = L_s = \frac{1}{2}$ total column length.

For $Z = 0$ (no bulk flow), both equations reduce to $\Delta/\Delta_0 = 1.0$ while for $X = 0$, Equation (VII-2) reduces to

$$\frac{\Delta}{\Delta_0} = 0.50 + \frac{1}{4Z} (1 - e^{-2Z}) \quad (\text{VII-8})$$

and Equation (VII-3) reduces to simply

$$\frac{\Delta}{\Delta_0} = 1.0 \quad (\text{VII-9})$$

At $X = 1$ (equal product flow rates) both equations necessarily reduce to the same expression (See Appendix H.)

$$\frac{\Delta}{\Delta_0} = \frac{1}{Z} (1 - e^{-Z}) \quad (\text{H-19})$$

Earlier studies (B8) (P3) (P7) indicate that, for unequal product flow rates in the range $0.5 < X < 2.0$, use of either of the above expressions gives essentially the same result. Therefore, experimental work was concentrated mainly near the extremes of X , that is, near $X = 0$ and $X = \infty$.

It was decided to use a fifty weight percent alcohol feed solution for these runs in order to avoid skewing of the theoretical curves because of changes in the thermal diffusion coefficient, α . By examining Figure 49, it can be seen that the curve presented by Van Velden, Van der Voort, and Gorter (VI) is more nearly flat in this region than in any other.

However, when α was determined from rate-separation data (See Appendix H.), it was found that the indicated value was more than thirty percent higher than the value read from the curve for fifty-one weight percent alcohol ($\alpha = 0.83$ vs $\alpha = 0.63$). Therefore, the curve presented by Cabicar and Zatka (C1) was used since

the experimentally determined value of α was close to the curve value.

It should be pointed out that the data reported by Van Velden, Van der Voort, and Gorter, and Cabicar and Zatka have been corrected at high concentrations by the method suggested by Prigogine and Buess (P8). The corrected values were obtained from tables presented by Von Halle (V3), and the corrected values are plotted in Figure 49.

Experimental curves were taken for several different values of Z (where again $Z = \bar{O}L / 2K$ and \bar{O} is the average flow rate for a given experimental curve). Each experimental point taken for a curve usually had a σ a little different from the average, $\bar{\sigma}$, but no correction was made for this deviation. The maximum deviation from the average was six percent.

Theoretical curves were calculated from Equations (VII-2) and (VII-3) over the entire range of X (zero to infinity) with Z as a parameter; however, Z remains constant for a given curve. If the thermal diffusion coefficient, α , were constant over the concentration range considered, the theoretical curves would be symmetrical about the line $X = 1$ (equal product flows). However, as can clearly be seen by referring to Figure 49, α varies rapidly over almost the entire concentration range, and hence the theoretical curves are skewed accordingly. The theoretical and experimental results for two Z -values are compared in Figures 50 and 51.

Figure 50

Separation As a Function of the Ratio of Product

Flow Rates: $Z = 0.887$

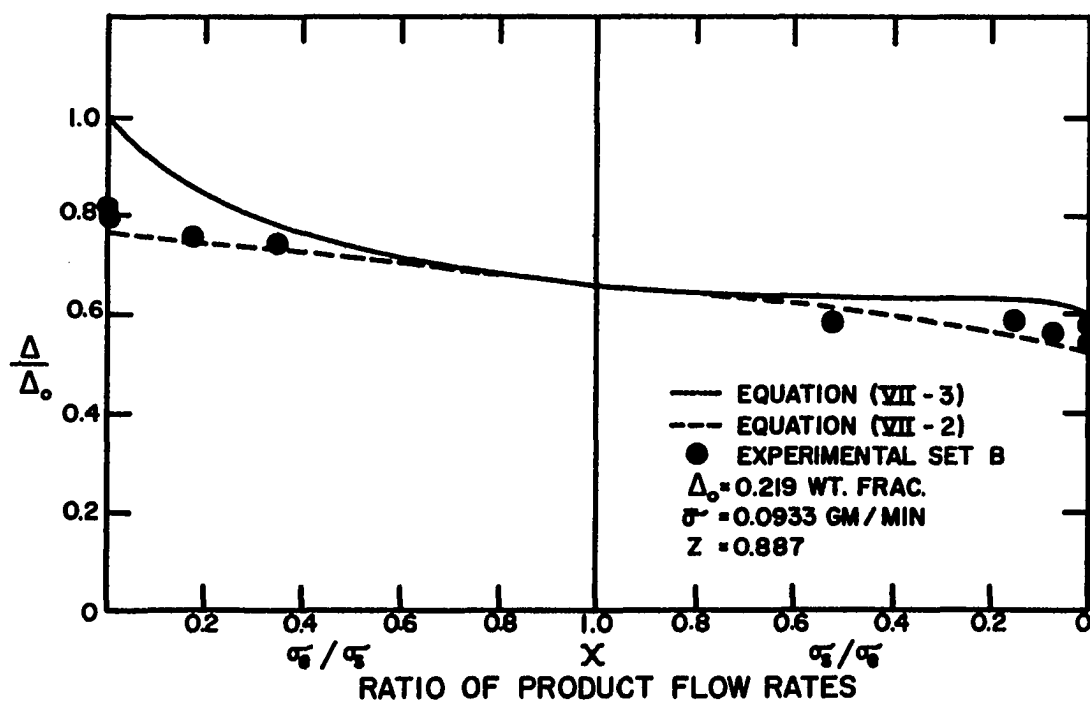
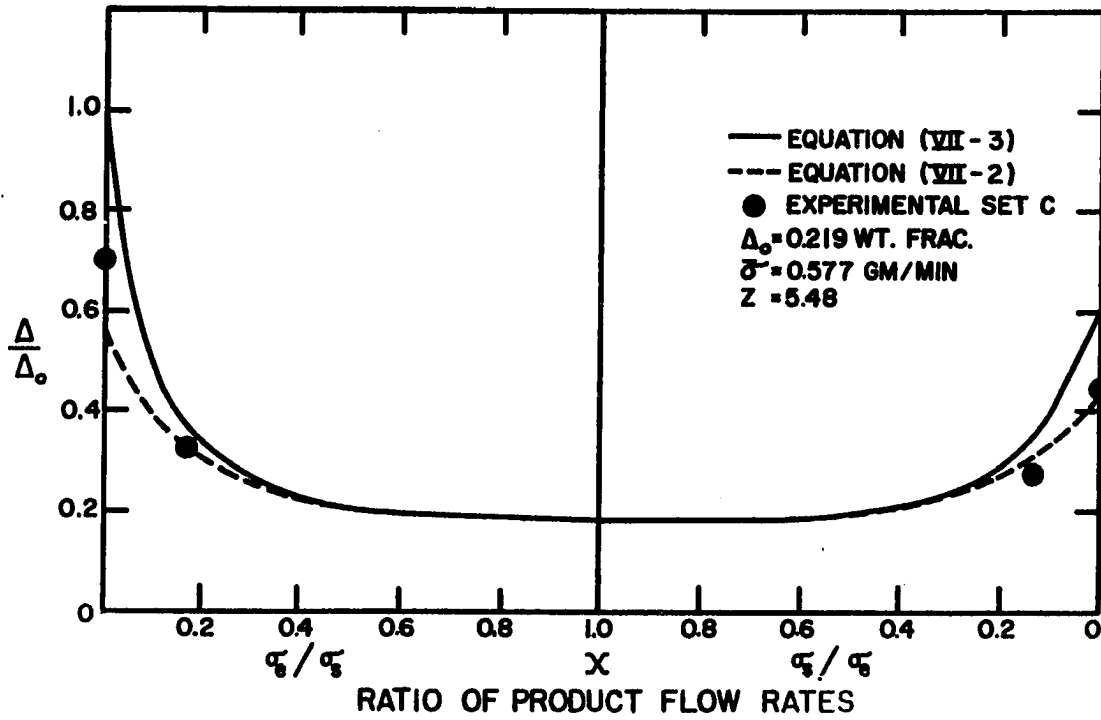


Figure 51

Separation As a Function of the Ratio of Product
Flow Rates: $Z = 5.48$



Although it may be argued that the data are inconclusive, the author feels that a preference is shown for Equation (VII-2). Since Powers indicated that Equation (VII-1) [or Equation (VII-3)] should apply only at low flow rates, two additional points were taken, one at $X = 0$ ($\sigma_e/\sigma_s = 0$) and one at $X = \infty$ ($\sigma_s/\sigma_e = 0$), both points at a Z-value of 0.493 which corresponds to an average flow rate of only 0.0519 grams/min. These two experimental points are compared with the theoretical curves in Figure 52. Here the results are inconclusive since the points fall nearly midway between the two theoretical curves. However, it becomes obvious that as one goes to lower and lower flow rates, the difference between Equations (VII-2) and (VII-3) must become ever smaller since the two equations give the same curve for $Z = 0$ (no bulk flow through the column).

Regardless of which of the two equations is more nearly correct at the extreme values of X and for large Z-values, two things are apparent: (1) either Equation (VII-2) or Equation (VII-3) is applicable in the range $0.5 < X < 2.0$, and (2) separation is always greater for unequal than for equal product flow rates (assuming that the thermal diffusion coefficient does not vary sufficiently with variations in concentration so that the separation is effectively reduced).

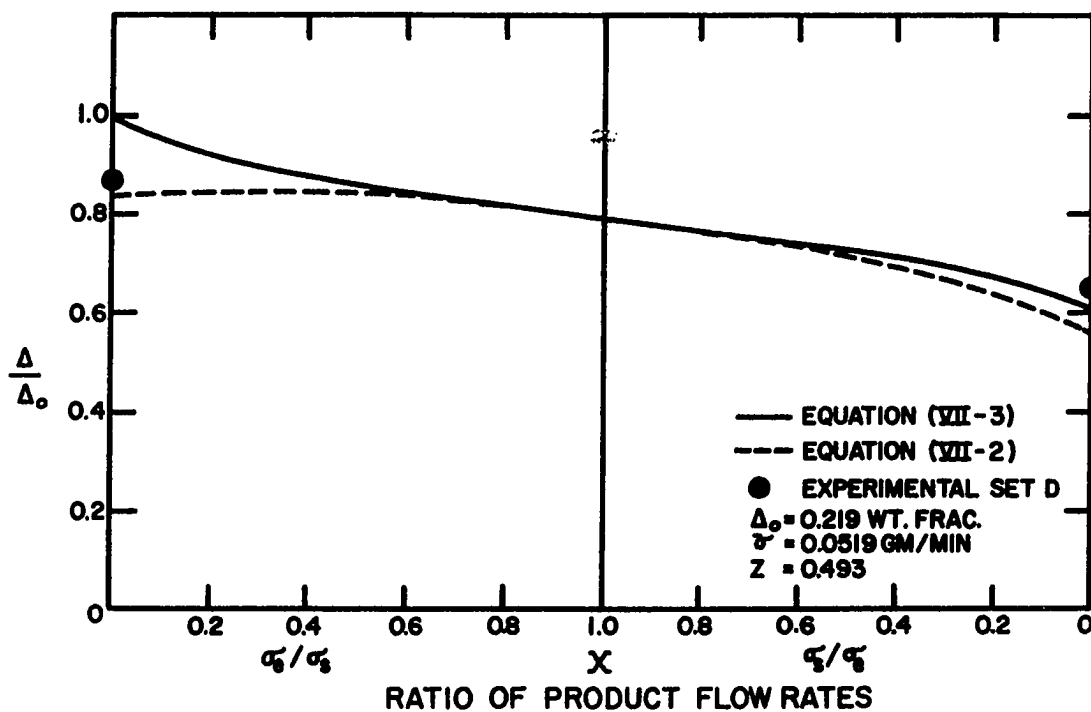
Results of Experimental Work with Plastic Flow Model

As mentioned previously, only the ratio of the C - coefficients at the two cylinder (barrier) diameter to plate spacing ratios was

Figure 52

Separation As a Function of the Ratio of Product

Flow Rates: $Z = 0.493$

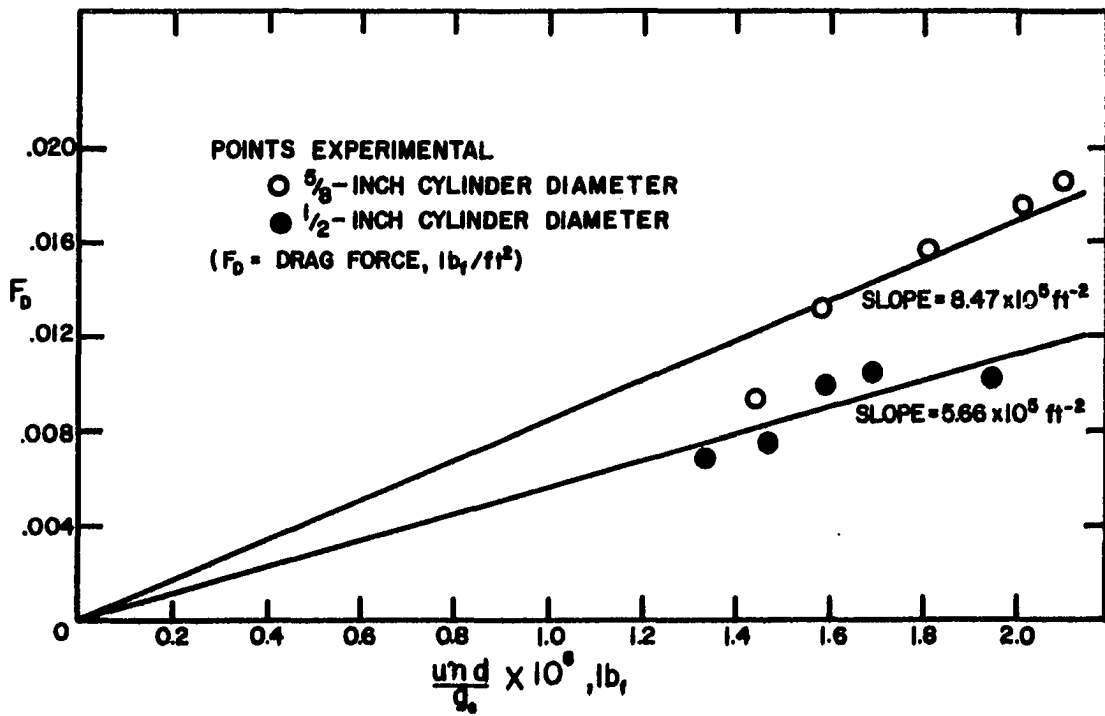


desired, not the absolute values. One inadequacy of the plastic model was mentioned in Chapter III; that is, the velocity distribution between the plates in the model was not the same as the velocity distribution between the plates in the thermogravitational column. In addition to this, there was another possible source of error that was investigated experimentally since it was felt that the error might influence not only the absolute values of the C-coefficients, but the ratio as well. The potential error was the possible effect that the disturbance, created by the cylinder, might have on the pressure measurement at the downstream pressure tap. Since the larger cylinder diameter should create a larger disturbance than the smaller cylinder diameter, it was felt that these different disturbances could alter the magnitude of the error at the downstream pressure tap. The pressure taps were located one and two feet from the cylinder, so it was a simple matter to investigate the magnitude of the error by merely reversing the flow; that is, the downstream tap became the upstream tap and vice-versa. No measurable difference in the pressure drop could be found when the flow was reversed, so the disturbance effect was assumed negligible.

Therefore, the experimental data are assumed satisfactory without corrections and were used to calculate the ratio of drag factors at the two cylinder diameter to plate spacing ratios experimentally considered. Figure 53 presents the experimental results.

Figure 53

Determination of the Ratio of Drag Factors: Graphical
Presentation of Experimental Data



For the one-half inch cylinder, the slope of the line through the data is found to be $5.66 \times 10^5 \text{ ft}^{-2}$, and for the five-eighths inch cylinder the slope is $8.47 \times 10^5 \text{ ft}^{-2}$. The ratio of the drag factors then is $8.47/5.66$ or 1.49. In other words, the drag imparted on the flowing fluid by the larger cylinder is 1.49 times as great as the drag imparted by the smaller cylinder.

CHAPTER VIII

CONCLUSIONS

The following conclusions may be drawn from the results of this investigation of the effect of horizontal barriers on the performance of a thermogravitational thermal diffusion column:

1. The use of horizontal barriers in a parallel-plate thermogravitational thermal diffusion column will increase the steady-state batch separation, and the batch separation with barriers can be predicted by Equation (III-53). The value of b in the Equation must be determined experimentally.
2. An "effective length" correction factor must be used in Equation (III-53), particularly when large numbers of barriers are used. This correction factor arises from the disturbance created by the barriers in the column. Although the length of the disturbance is small for a single barrier (in the range of a few plate spacings), the effect is appreciable when many barriers are used.
3. The steady-state batch separation is decreased slightly when the temperature difference between the plates is decreased, although the theory predicts no effect. The theory also predicts no change in the batch separation when the barrier diameter is changed

relative to the plate spacing, and the limited experimental results are in agreement with the theory for the effect of this parameter.

4. Although horizontal barriers increase the steady-state batch separation, the relaxation time is also increased when barriers are added. The transient behavior of a column with barriers can be predicted by solution of a system of equations given by Equations (III-75) through (III-77) for an even number of equally-spaced barriers, and Equations (III-75) and (III-76) for an odd number of equally-spaced barriers.

5. The relaxation time in a column with barriers is proportional to the first power of the temperature difference between the plates rather than the square of the temperature difference, as is true for the open column. This is predicted by the theory, and it is well verified by the experimental data.

6. Introduction of a C-factor enables the calculation of the effect of the barrier diameter to plate spacing ratio on the transient behavior of a column with barriers. Values of the C-factor can be determined experimentally from a plastic flow model if a value of C is obtained empirically from column data at any given barrier diameter to plate spacing ratio.

7. The addition of bulk flow to a column with barriers rapidly cancels the advantage gained by barriers in the batch case. Therefore, barriers offer an advantage under conditions of continuous

flow only for very low product flow rates. Rate-separation curves for columns with barriers can be predicted satisfactorily from Equation (III-111) in conjunction with Equations (III-112) through (III-114). The theory correctly predicts the effect of the number of barriers, of the temperature difference between the plates, and of the barrier diameter to plate spacing ratio on the continuous flow performance of a column with barriers.

8. When unequal product flow rates are considered, for values of X ($X = \sigma_e / \sigma_g$) in the range $0.5 < X < 2.0$, either the modification proposed by Powers (P3) (P7), Equation (VII-3); or the equations from conventional theory, Equation (VII-2) or the average flow-rate equation, Equation (H-19) [or Equation (III-92)], can be used. However, outside the aforementioned range, Equation (VII-2) is preferred to Equations (VII-3) or (H-19). In addition, the separation in a column operated with unequal product flow rates is greater than for equal product flow rates.

BIBLIOGRAPHY

Several excellent bibliographies have been published in recent years, and no effort has been made here to include all references in the field of thermal diffusion.

Von Halle (V3) published a thorough annotated bibliography compiled in conjunction with his thesis issued in 1959; the period through 1957 is covered. Powers' (P3) thesis in conjunction with "L'Effet Soret" by deGroot (G5); "Thermal Diffusion: A Bibliography" prepared by the Atomic Energy Research Establishment at Harwell, England; and "Thermal Diffusion in Gases" by Grew and Ibbs together give a complete bibliography through the year 1953. A recent thesis by Boyer (B8) covers the years 1954 through 1958, and Boyer's thesis with the above sources provide complete coverage of published material in the field of thermal diffusion up to 1959.

The following bibliography, therefore, lists only references not found in the above sources.

1959

- Fisher, G. T., and Prados, J. W. U. S. At. Energy Comm. AECU-4125 (1959).
- Gardner, R. A., et al., J. Chem. and Eng. Data 4, No. 2, 155-59 (1959).
- Heymann, D. Proc. U. N. Intern. Conf. Peaceful Uses At. Energy, 2nd, Geneva, 1958, 18, 200-9 (1959).
- Heymann, D., and Kistemaker, J. Physica 25, 556-68 (1959).
- Lorenz, M. G., and Emery, A. H. Chem. Eng. Sci. 11, 16-23 (1959).
- Mizushima, T., et al. Kagaku Kogaku 23, 446-9 (1959).
- Nadi, M. El, and Farag, N. J. chim. phys. 56, 631 (1959).
- Nathan, W. S., and Whitehead, D. M. Compt. rend. congr. intern. chim. ind., 31^e, Liege, 1958 (Pub. as Ind. Chim. belge, suppl) 1, 523-34 (1959).
- Papayannopoulos, A. G. Colorado School of Mines Dissertation (M. S.), 1959.
- 1960
- Brown, G. R., and Jones, A. L. Pet. Ref. 39, No. 6, 1956-62 (1960).
- Chanu, J. Compt. rend. 250, 2158-60 (1960).
- Henke, A. M., and Stauffer, H. C. U. S. Patent 2,936,887. May 17, 1960.
- Hoffman, D. T. "Thermal Diffusion in Liquids," Purdue University Thesis (Ph. D.), 1960.
- Lorenz, M. G. "Thermal Diffusion in Packed Columns," Purdue University Thesis (Ph. D.), 1960.
- Lykova, A. V. Inzhener-Fiz. Zhur., Akad. Nauk Belorus. S. S. R. 3, No. 3, 143-7 (1960).

- Makita, T. Rev. Phys. Chem. Japan 29, 47-54 (1960).
- Saxena, S. C., and Watson, W. W. Physics of Fluids 3, No. 1, 105 (1960).
- Thompson, C. J., et al. Ind. Eng. Chem. 52, No. 2, 53A (1960).
- Vries, A. E. de, and Laranjeira, M. F. J. Chem. Phys. 32, 1714-16 (1960).
- Weissman, S., Saxena, S. C., and Mason, E. A. Physics of Fluids 3, 510-18 (1960).
- White, J. R., and Fellows, A. T. Ind. Eng. Chem. 52, 389-90 (1960).
- YU, Y. C., and Sung, C. in, Jan Liao Hsueh Pao 5, 16-20 (1960).

1961

- Boyer, L. D. "An Experimental and Theoretical Investigation of Vertical Barriers in Liquid Thermal Diffusion Columns," University of Oklahoma Dissertation (Ph. D.), 1961.
- Vichare, G. G. University of Oklahoma Thesis (M. ChE.), 1961.

APPENDIX A

Column and System Parameters for Sets of Experimental Data

TABLE 3

COLUMN AND SYSTEM PARAMETERS FOR
SETS OF EXPERIMENTAL DATA

Exp. Set	Included Runs	2ω	ΔT	B	\bar{C}_F	N	d
		Mean Plate Spacing	Mean Temp. Diff.	Plate Width	Mean Feed Comp.	No. Barr.	Barrier Diam.
		cm	$^{\circ}\text{C}$	cm	Weight Frac. EtOH		cm
A	1-9	.0792	27.9	10.16	.5095	0	-
B	10-18	.0795	27.7	10.16	.5070	0	-
C	19-23	.0792	27.8	10.16	.5087	0	-
D	24-25	.0795	27.9	10.16	.5092	0	-
E	26-35	.0795	27.0	10.16	.3973	0	-
FG	36-45	.0792	26.5	9.21	.4012	0	-
H	46-54	.0798	13.3	9.21	.4021	0	-
I	55-63	.0792	26.1	9.21	.4019	2	.0508
J	64-71	.0795	13.2	9.21	.4013	2	.0508
K	72-81	.0792	26.8	9.21	.3986	0	-
L	82-88	.0792	13.6	9.21	.3986	0	-
M	89-96	.0790	26.7	9.21	.3966	4	.0508
N	97-102	.0792	13.6	9.21	.3994	4	.0508
O	103-111	.0790	26.7	9.21	.3997	4	.0635
P	112-117	.0790	13.7	9.21	.3989	4	.0635
Q	118-123	.0790	26.7	9.21	.3984	8	.0508
R	124-134	.0792	26.6	9.21	.3981	16	.0508
S	135-142	.0792	13.5	9.21	.3993	16	.0508
T	143-147	.0790	26.7	9.21	.3997	50	.0508

Note: The column length, L was held constant at 145 cm, and the average temperature level, \bar{T} , was fixed at 322°K for all experimental runs.

APPENDIX B

Table of Experimental Data

TABLE 4

EXPERIMENTAL BATCH-TRANSIENT DATA

Exp. No. and Set	t Time	C _e Top Product Comp.	C _s Bottom Product Comp.	Δ C _e -C _s
	minutes	Weight Frac. EtOH	Weight Frac. EtOH	Weight Frac. EtOH
40F	20	.4139	.3894	.0235
	40	.4192	.3822	.0370
	60	.4231	.3774	.0456
	90	.4291	.3734	.0557
	150	.4359	.3674	.0685
	260	.4408	.3602	.0806
	400	.4482	.3563	.0919
	2,805	.4551	.3507	.1044
	4,605	.4525	.3483	.1042
52H	20	.4094	.3954	.0140
	40	.4109	.3924	.0185
	60	.4116	.3909	.0207
	90	.4147	.3880	.0267
	120	.4154	.3858	.0296
	180	.4177	.3822	.0355
	310	.4254	.3781	.0473
	470	.4305	.3734	.0571
	1,010	.4375	.3634	.0741
	1,430	.4408	.3589	.0819
	1,730	.4416	.3563	.0853
	2,390	.4433	.3538	.0895
	2,490	.4424	.3538	.0886
2,870	.4416	.3525	.0891	
63I	20	.4185	.3925	.0260
	40	.4223	.3872	.0351
	60	.4246	.3851	.0395
	90	.4276	.3808	.0468

TABLE 4 - (continued)

	t	C _e	C _s	Δ
63I	120	.4298	.3794	.0504
	180	.4351	.3740	.0611
	240	.4384	.3701	.0683
	330	.4424	.3668	.0756
	480	.4482	.3622	.0860
	720	.4542	.3563	.0979
	910	.4551	.3538	.1013
	1,180	.4585	.3513	.1072
	1,500	.4687	.3501	.1186
	1,810	.4668	.3482	.1186
	2,960	.4651	.3464	.1187
70J	30	.4020	.3879	.0141
	90	.4087	.3873	.0214
	200	.4147	.3822	.0325
	320	.4154	.3721	.0433
	515	.4254	.3682	.0572
	820	.4298	.3628	.0670
	1,440	.4423	.3561	.0862
	2,160	.4474	.3507	.0967
	3,380	.4525	.3465	.1060
	4,440	.4568	.3452	.1116
	5,770	.4593	.3440	.1153
	6,370	.4585	.3435	.1150
74K	20	.4124	.3865	.0259
	55	.4192	.3767	.0425
	120	.4343	.3668	.0675
	290	.4568	.3557	.1011
	600	.4635	.3477	.1158
	1,440	.4669	.3445	.1224
	1,680	.4651	.3458	.1193
	1,840	.4635	.3459	.1176
83L	50	.4072	.3865	.0207
	265	.4200	.3714	.0486
	1,260	.4525	.3564	.0961
	1,560	.4507	.3488	.1019
	1,870	.4507	.3476	.1031

TABLE 4 (continued)

	t	C _e	C _s	Δ
83L	2,610	.4626	.3506	.1120
	3,000	.4618	.3488	.1130
	3,450	.4626	.3476	.1150
	4,110	.4626	.3476	.1150
90M	40	.4124	.3836	.0288
	190	.4276	.3728	.0548
	240	.4298	.3688	.0610
	440	.4400	.3641	.0759
	820	.4542	.3570	.0972
	1,020	.4610	.3538	.1072
	1,220	.4635	.3520	.1115
	1,630	.4733	.3507	.1227
	2,190	.4762	.3494	.1268
	2,490	.4762	.3476	.1286
	3,070	.4800	.3470	.1330
	3,300	.4800	.3470	.1330
	3,480	.4800	.3470	.1330
	102N	130	.4124	.3836
360		.4238	.3774	.0464
1,180		.4384	.3642	.0742
1,820		.4482	.3570	.0912
2,930		.4568	.3507	.1061
4,210		.4643	.3470	.1173
5,600		.4669	.3458	.1211
6,830		.4687	.3470	.1217
7,330	.4687	.3454	.1233	
104O	40	.4154	.3836	.0318
	135	.4208	.3801	.0407
	335	.4276	.3741	.0535
	1,140	.4568	.3570	.0998
	1,800	.4626	.3525	.1101
	3,240	.4705	.3476	.1229
	4,155	.4743	.3476	.1267
	4,430	.4762	.3476	.1286
	4,800	.4762	.3476	.1286

TABLE 4 - (Continued)

	t	C _e	C _s	Δ	
117P	110	.4102	.3887	.0215	
	310	.4162	.3844	.0318	
	740	.4246	.3788	.0458	
	1,560	.4367	.3675	.0692	
	2,890	.4507	.3551	.0956	
	4,400	.4559	.3470	.1089	
	6,120	.4602	.3458	.1144	
	7,515	.4678	.3488	.1190	
	9,220	.4678	.3476	.1202	
	10,730	.4687	.3470	.1217	
	13,340	.4687	.3458	.1229	
	14,780	.4669	.3447	.1222	
	122Q	40	.4072	.3880	.0192
		130	.4132	.3801	.0331
360		.4283	.3741	.0542	
720		.4416	.3648	.0768	
1,410		.4602	.3538	.1064	
2,910		.4753	.3453	.1300	
4,350		.4830	.3440	.1390	
5,940		.4890	.3429	.1461	
7,440		.4910	.3417	.1493	
10,080		.4940	.3417	.1523	
11,520		.4930	.3417	.1513	
12,960		.4920	.3417	.1503	
130R		220	.4124	.3880	.0244
	520	.4208	.3829	.0379	
	1,340	.4359	.3641	.0718	
	2,820	.4576	.3488	.1088	
	4,140	.4687	.3355	.1332	
	5,610	.4743	.3263	.1480	
	7,370	.4772	.3226	.1546	
	9,000	.4791	.3195	.1596	
	10,500	.4801	.3189	.1612	
	12,700	.4840	.3179	.1661	
	15,210	.4840	.3179	.1661	
135S	480	.4109	.3898	.0211	
	1,440	.4238	.3767	.0471	

TABLE 4 - (continued)

	t	C _e	C _s	Δ
135S	3,060	.4384	.3435	.0749
	4,590	.4465	.3513	.0952
	7,140	.4602	.3361	.1241
	9,060	.4651	.3317	.1334
	11,500	.4660	.3231	.1429
	13,000	.4678	.3205	.1473
	15,900	.4696	.3169	.1527
	18,830	.4705	.3138	.1567
	23,130	.4714	.3129	.1585
	28,790	.4714	.3100	.1614
	33,000	.4724	.3100	.1624
	37,240	.4714	.3095	.1619
147T	300	.4079	.3909	.0170
	1,915	.4283	.3721	.0562
	3,240	.4400	.3589	.0811
	5,520	.4593	.3378	.1215
	9,430	.4830	.3124	.1706

TABLE 5

EXPERIMENTAL DATA FOR RATE-SEPARATION CURVES

Exp. No. and Set	σ_e	σ_s	$\frac{\sigma_e + \sigma_s}{2}$	C_e	C_s	Δ	ΔT_m
	Top Product Flow Rate	Bottom Product Flow Rate		Top Product Comp.	Bottom Product Comp.	$C_e - C_s$	Mean Temp. Diff.
	<u>Grams</u> min	<u>Grams</u> min	<u>Grams</u> min	Weight Frac. EtOH	Weight Frac. EtOH	Weight Frac. EtOH	° F
1A	0.0000	0.0000	0.0000	.6338	.4148	.2190	50.5
2A	0.0192	0.0269	0.0230	.6225	.4288	.1935	50.1
3A	0.0750	0.0931	0.0841	.5873	.4400	.1473	50.5
4A	3.55	3.87	3.71	.5085	.5070	.0015	50.5
5A	0.0974	0.0958	0.0966	.5903	.4455	.1448	50.1
6A	2.06	2.06	2.06	.5073	.5019	.0054	50.3
7A	0.286	0.311	0.298	.5491	.4727	.0764	50.3
8A	0.558	0.561	0.560	.5307	.4840	.0467	50.1
9A	1.16	1.34	1.25	.5168	.4995	.0173	50.4
10B	0.0000	0.1678	0.0839	.6472	.4725	.1747	51.3
11B	0.1870	0.0000	0.0935	.5250	.4065	.1185	49.2
12B	0.0287	0.1648	0.0967	.6357	.4706	.1651	50.8
13B	0.1458	0.0306	0.0888	.5410	.4127	.1284	48.5
14B	0.1800	0.0135	0.0973	.5164	.3924	.1240	48.2
15B	0.0000	0.1848	0.0915	.6492	.4766	.1726	51.8
16B	0.0514	0.1440	0.0977	.6280	.4660	.1620	51.0
17B	0.1260	0.0666	0.0963	.5515	.4231	.1284	49.8
18B	0.1864	0.0000	0.0932	.5127	.3856	.1271	47.8
19C	1.017	0.0000	0.508	.5081	.3993	.1088	48.9
20C	0.0000	1.234	0.617	.6594	.5058	.1536	51.2
21C	1.142	0.0000	0.571	.5144	.4172	.0972	49.6
22C	1.002	0.1365	0.569	.5136	.4533	.0603	49.9
23C	0.1601	0.941	0.551	.5693	.4981	.0712	50.5
24D	0.1048	0.0000	0.0524	.5132	.3728	.1404	48.5
25D	0.0000	0.1029	0.0515	.6757	.4857	.1900	51.9

TABLE 5 - (continued)

	σ_e	σ_s	$\frac{\sigma_e + \sigma_s}{2}$	C_e	C_s	Δ	ΔT_m
26E	0.914	0.825	0.870	.4072	.3927	.0145	47.8
27E	0.0000	0.0000	0.0000	.4947	.3404	.1543	48.0
28E	0.695	0.658	0.677	.4077	.3877	.0200	48.0
29E	0.0157	0.0317	0.0237	.4870	.3482	.1388	47.7
30E	0.304	0.327	0.315	.4200	.3772	.0428	48.9
31E	0.119	0.115	0.117	.4389	.3606	.0783	47.2
32E	0.176	0.172	0.174	.4266	.3690	.0576	47.1
33E	1.04	1.10	1.07	.4015	.3932	.0083	47.7
34E	0.0541	0.0533	0.0537	.4542	.3485	.1056	46.6
36F	0.192	0.139	0.165	.4323	.3639	.0684	47.8
37F	0.727	0.838	0.783	.4172	.3889	.0283	48.2
38F	0.0357	0.0253	0.0305	.4542	.3570	.0972	48.2
39F	0.444	0.444	0.444	.4283	.3846	.0437	47.9
40F	0.0000	0.0000	0.0000	.4538	.3495	.1043	48.3
42G	1.42	1.10	1.26	.4077	.3927	.0150	47.9
43G	0.0672	0.0533	0.0603	.4480	.3595	.0885	47.3
44G	2.47	2.37	2.42	.4017	.3997	.0020	47.5
45G	0.297	0.271	0.284	.4320	.3763	.0557	47.0
46H	0.0649	0.0571	0.0610	.4302	.3749	.0553	24.0
47H	2.05	2.10	2.08	.4025	.4023	.0002	24.1
48H	0.129	0.101	0.115	.4188	.3818	.0370	23.7
49H	0.744	0.656	0.700	.4067	.4001	.0066	23.9
50H	0.245	0.240	0.242	.4119	.3932	.0187	23.9
51H	0.420	0.431	0.426	.4079	.3976	.0103	23.9
52H	0.0000	0.0000	0.0000	.4424	.3534	.0890	24.4
53H	0.952	1.02	0.987	.4038	.4001	.0037	24.0
54H	0.0398	0.0240	0.0319	.4298	.3619	.0679	24.1
55I	0.117	0.135	0.126	.4400	.3741	.0659	46.8
56I	0.0873	0.117	0.102	.4499	.3732	.0767	47.0
57I	1.99	1.89	1.94	.4035	.3996	.0039	47.0
58I	0.425	0.337	0.381	.4177	.3860	.0317	46.8
59I	0.790	0.722	0.756	.4111	.3934	.0177	47.0
60I	0.0605	0.0420	0.0513	.4522	.3624	.0898	46.8
61I	0.229	0.261	0.245	.4303	.3860	.0443	46.6
62I	1.33	1.29	1.31	.4072	.3976	.0096	46.7
63I	0.0000	0.0000	0.0000	.4669	.3482	.1187	47.0

TABLE 5 - (continued)

	σ_e	σ_s	$\frac{\sigma_e + \sigma_s}{2}$	C_e	C_s	Δ	ΔT_m
64J	0.0365	0.0391	0.0378	.4266	.3696	.0570	23.9
65J	0.109	0.109	0.109	.4174	.3822	.0352	24.0
66J	1.40	1.35	1.37	.4023	.4016	.0007	23.4
67J	0.650	0.556	0.603	.4042	.3984	.0058	23.6
68J	0.303	0.267	0.285	.4094	.3962	.0132	23.7
69J	0.175	0.168	0.172	.4135	.3919	.0216	23.4
70J	0.0000	0.0000	0.0000	.4589	.3437	.1152	24.5
71J	0.0875	0.0905	0.0890	.4144	.3772	.0372	23.4
74K	0.0000	0.0000	0.0000	.4669	.3446	.1223	49.3
75K	0.0800	0.0519	0.0660	.4507	.3532	.0975	47.9
76K	0.828	0.811	0.820	.4094	.3858	.0236	48.6
77K	0.0278	0.0279	0.0278	.4669	.3532	.1137	48.0
78K	0.156	0.138	0.147	.4424	.3626	.0798	48.0
79K	0.594	0.571	0.583	.4134	.3801	.0330	48.3
80K	1.50	1.50	1.50	.4013	.3922	.0091	48.1
81K	0.273	0.278	0.276	.4293	.3736	.0557	47.7
82L	0.0583	0.0685	0.0634	.4334	.3745	.0589	24.4
83L	0.0000	0.0000	0.0000	.4626	.3476	.1150	24.5
84L	0.151	0.160	0.155	.4158	.3798	.0360	23.9
85L	0.239	0.305	0.272	.4072	.3902	.0170	25.3
86L	0.572	0.571	0.572	.4028	.3962	.0066	24.5
87L	1.22	1.14	1.18	.3988	.3976	.0012	24.5
88L	0.0259	0.0268	0.0264	.4381	.3637	.0744	23.5
90M	0.0000	0.0000	0.0000	.4800	.3470	.1330	48.3
91M	0.0507	0.0509	0.0508	.4460	.3613	.0847	47.7
92M	0.580	0.571	0.575	.4045	.3863	.0183	48.7
93M	0.156	0.164	0.160	.4261	.3772	.0489	48.1
94M	1.39	1.41	1.40	.3996	.3919	.0077	48.4
95M	0.321	0.288	0.305	.4144	.3836	.0308	48.3
97N	0.0246	0.0268	0.0257	.4365	.3723	.0642	24.5
98N	0.514	0.585	0.549	.4015	.3947	.0068	24.4
99N	0.326	0.306	0.316	.4055	.3944	.0110	24.6
100N	0.172	0.174	0.173	.4092	.3899	.0193	24.6
101N	0.0551	0.0602	0.0577	.4210	.3794	.0416	24.6
102N	0.0000	0.0000	0.0000	.4687	.3454	.1233	24.5

TABLE 5 - (continued)

	σ_e	σ_s	$\frac{\sigma_e + \sigma_s}{2}$	C_e	C_s	Δ	ΔT_m
104 \bar{O}	0.0000	0.0000	0.0000	.4762	.3476	.1286	48.1
106 \bar{O}	0.291	0.342	0.317	.4132	.3937	.0195	48.1
107 \bar{O}	0.0513	0.0522	0.0520	.4436	.3774	.0662	47.4
109 \bar{O}	0.0274	0.0273	0.0274	.4430	.3637	.0793	47.9
110 \bar{O}	0.157	0.156	0.157	.4251	.3874	.0377	48.1
111 \bar{O}	0.833	0.831	0.832	.4096	.3947	.0149	48.2
112P	0.0557	0.0587	0.0572	.4210	.3872	.0338	24.7
113P	0.624	0.634	0.629	.4033	.3967	.0066	24.7
114P	0.0302	0.0306	0.0304	.4238	.3801	.0437	24.8
115P	0.348	0.343	0.346	.4023	.3919	.0104	24.9
116P	0.176	0.169	0.172	.4068	.3904	.0165	24.5
117P	0.0000	0.0000	0.0000	.4669	.3452	.1226	24.3
119Q	0.0343	0.0317	0.0330	.4579	.3635	.0945	47.8
120Q	0.289	0.388	0.338	.4141	.3934	.0207	48.4
121Q	0.117	0.103	0.110	.4227	.3838	.0389	48.1
122Q	0.0000	0.0000	0.0000	.4930	.3417	.1513	48.0
123Q	0.722	0.701	0.712	.4057	.3951	.0107	48.0
124R	0.0465	0.0551	0.0508	.4346	.3817	.0529	48.7
125R	0.292	0.278	0.285	.4072	.3919	.0153	48.6
126R	0.0270	0.0313	0.0291	.4465	.3639	.0826	48.2
128R	0.813	0.596	0.704	.4018	.3969	.0049	48.1
129R	0.0826	0.0711	0.0768	.4111	.3851	.0260	48.3
130R	0.0000	0.0000	0.0000	.4840	.3179	.1661	48.2
132R	0.154	0.157	0.156	.4079	.3912	.0167	47.3
133R	0.154	0.191	0.172	.4038	.3892	.0146	47.1
135S	0.0000	0.0000	0.0000	.4728	.3106	.1622	24.1
136S	0.0788	0.0584	0.0686	.4052	.3872	.0180	24.7
137S	0.152	0.158	0.155	.4035	.3954	.0081	24.4
138S	0.0251	0.0263	0.0257	.4164	.3824	.0340	24.4
139S	0.322	0.328	0.325	.4013	.3962	.0051	24.1
140S	1.17	1.15	1.16	.4001	.3996	.0005	23.7
141S	0.0137	0.0143	0.0140	.4175	.3710	.0465	24.5
142S	0.672	0.641	0.657	.4006	.3975	.0031	24.1

TABLE 5 - (continued)

	σ_e	σ_s	$\frac{\sigma_e + \sigma_s}{2}$	C_e	C_s	Δ	ΔT_m
143T	0.132	0.0953	0.113	.4103	.3905	.0198	47.5
144T	0.589	0.507	0.548	.4109	.3999	.0020	46.4
145T	0.048	0.056	0.052	.4139	.3851	.0288	47.4
146T	0.208	0.274	0.241	.4065	.3924	.0141	47.1
147T	0.0000	0.0000	0.0000	.5378	.2855	.2523	47.2

APPENDIX C

Barrier "Drag" Factor Data

TABLE 6

BARRIER "DRAG" FACTOR DATA

A. One-Half Inch Stainless Steel Cylinder

Seconds for 1000 ml Flow	$\frac{u\eta d}{g_c} \cdot 10^8$ *	Total ΔP_f lb_f/ft^2	Plate Drag lb_f/ft^2	Cylinder Drag lb_f/ft^2
34.9	1.33	.0096	.0028	.0068
29.5	1.58	.0132	.0033	.0099
31.8	1.47	.0107	.0031	.0076
23.9	1.95	.0143	.0041	.0102
27.5	1.69	.0141	.0036	.0105

B. Five-Eighths Inch Aluminum Cylinder

Seconds for 1000 ml Flow	$\frac{u\eta d}{g_c} \cdot 10^8$ *	Total ΔP_f lb_f/ft^2	Plate Drag lb_f/ft^2	Cylinder Drag lb_f/ft^2
27.6	2.10	.0222	.0036	.0186
36.5	1.59	.0159	.0027	.0132
28.7	2.02	.0210	.0034	.0176
32.0	1.81	.0188	.0031	.0157
40.2	1.44	.0117	.0024	.0093

$$\begin{aligned}
 * \frac{u\eta d}{g_c} &= \frac{46.5 \times 10^{-8}}{\text{seconds for 1000 ml}} \quad \text{for one-half inch cylinder} \\
 &= \frac{58.0 \times 10^{-8}}{\text{seconds for 1000 ml}} \quad \text{for five-eighths inch cylinder}
 \end{aligned}$$

APPENDIX D

Estimation of Length Correction Factor (l_r)

Estimation of Length Correction Factor

As pointed out in Chapter III, the length correction factor, l_r , is composed of the sum of two effects: (1) the length of the disturbance of the linear temperature gradient between the plates caused by the barrier(s) and (2) the length necessary to re-establish the velocity distribution as the circulating fluid reverses its direction at the ends of each of the $(N + 1)$ columns created by the N horizontal barriers. These two effects will be considered separately in an attempt to determine an order of magnitude value for l_r .

1. Contribution to l_r by disturbed linear temperature gradient:

The temperature gradient between the plates has been assumed linear and is designated ΔT . Now assume that the barriers are at a uniform and constant temperature $\frac{\Delta T}{2}$. This assumption is reasonable when it is realized that the thermal conductivity of a stainless steel barrier is over forty times greater than the thermal conductivity of the surrounding alcohol-water solution. Figure 54 shows a barrier between two plates, one heated to T_H and the other cooled to T_C .

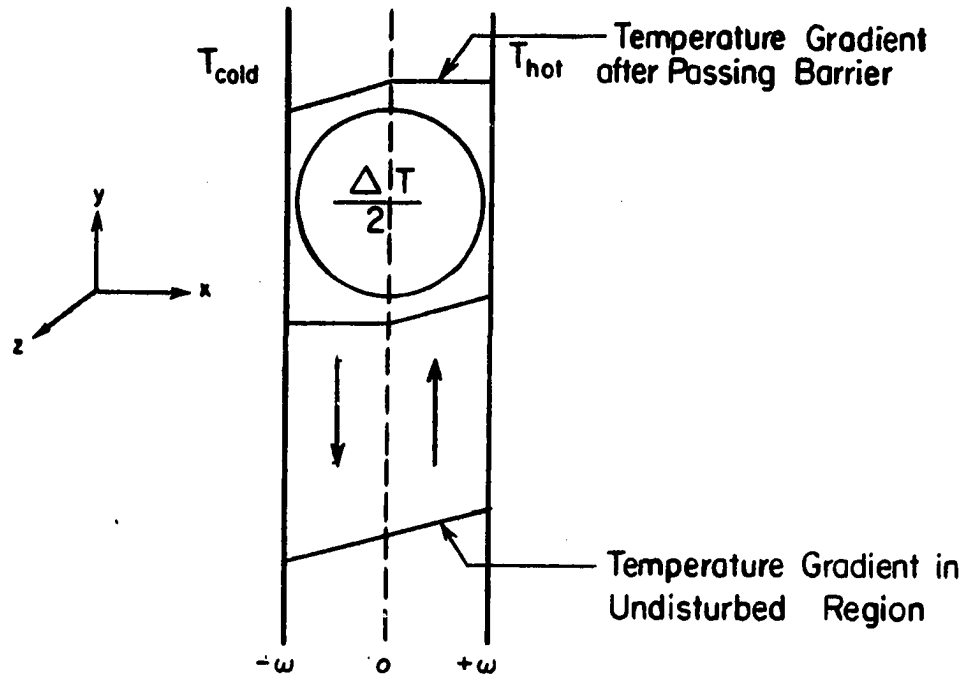


Figure 54. Disturbance of Temperature Gradient

Symmetry about the center line can be assumed; that is, the disturbance created in the stream flowing up near the hot plate will be equal to the disturbance in the stream flowing down near the cold plate since the two counter-current streams are assumed to be equal in mass flow rate. Consider the convective stream flowing up near the hot plate ($0 < x < +w$). Assuming that perfect mixing occurs around the barrier (since the flow is relatively fast past the barrier), the fluid will lose its linear temperature gradient. In fact, it is assumed that the gradient is zero after the fluid flows past the barrier. However, as soon as the fluid flows past the

barrier, the temperature gradient will begin to be re-established.

Heat will flow in from T_H by conduction and out to T_C by conduction.

Now let q be the amount of heat gained or lost by conduction:

$$q = (Bcm)(\omega cm)(\Delta y cm) \left(\frac{\rho \text{ gm}}{\text{cm}^3} \right) \left(C_p \frac{\text{cal}}{\text{gm} \cdot ^\circ\text{C}} \right) \left(\frac{\Delta T}{2} - \frac{\Delta T}{4} \right) \quad (\text{D-1})$$

For conduction,

$$q = \frac{\Delta T}{2\omega} k_t A (\Delta t) \quad (\text{D-2})$$

$$q = \frac{\Delta T}{2\omega} k_t (B\Delta y)(\Delta t) \quad (\text{D-3})$$

where k_t is the thermal conductivity. Equating q 's (where $\Delta y = \Delta l$

and $\bar{v} = \frac{\Delta y}{\Delta t}$) gives

$$\Delta l = \frac{\rho C_p \omega^2 \bar{v}}{2 k_t} \quad (\text{D-4})$$

Substituting for \bar{v} from Equation (III-119) yields

$$\Delta l = \frac{\beta_T \rho C_p g \omega^4 \Delta T}{96 k_t \eta (1 + bN)} \text{ cm} \quad (\text{D-5})$$

For the column dimensions and physical properties of the binary system studied in this work

$$\Delta l = \frac{1.6 \times 10^{-3} (\Delta T)}{(1 + bN)} \text{ cm} \quad (\text{D-6})$$

Recalling that there is an equal length of disturbance in both the

hot and cold circulating streams, the total length of the disturbance for fifty barriers ($N = 50$) at a temperature difference of 26.7°C is

$$\Delta l = 50 \times 2 \frac{(1.6 \times 10^{-3} \times 26.7)}{1 + 50 \times .035} = 1.2 \text{ cm}$$

2. Contribution to l_r by "turn-around" effect:

Near the ends of each of the $(N + 1)$ small columns formed by the N horizontal barriers, the circulating fluid divides: part of the fluid flows past the barrier and part of the fluid reverses its direction and flows back the opposite side of the column. The assumed velocity distribution given by Equation (III-44) is distorted by the turn-around, and a finite length of column is necessary to re-establish this velocity distribution. The problem is thus one of estimating the magnitude of this length of column necessary to re-establish the assumed velocity distribution.

An analogous problem was studied for several months at the University of Michigan as a possible subject for a Ph. D. thesis. However, the problem was found too difficult to handle because of the complications introduced by the corners of the column. Personal communication with Dr. C. S. Yih at the University of Michigan confirmed the difficulty of the problem. Dr. Yih stated that there is no feasible way to evaluate the magnitude of the "turn-around" length, but that, although he knew of no way to prove it, he felt

certain that the velocity distribution is re-established in two or three plate widths for low Grashof numbers.

In view of the above statement, a length correction of three plate spacings was used for the "turn-around" effect. This gives a total of six plate spacings for each barrier since two column ends are involved with each barrier.

A total length correction factor of seven plate spacings was then used ($l_r = 0.55$ cm) for each barrier. The total length correction factor can be approximated by taking the sum of the lengths for the disturbed temperature gradient and the turn-around effect. Although the length for the disturbed temperature gradient is a function of the convective velocity, it was assumed equal to one plate spacing per barrier for all runs. This gives a constant length correction factor, l_r , and is more convenient to work with.

The value of $l_r = 0.55$ cm was then used in conjunction with Equation (III-54) to give the curve in Figure 23.

APPENDIX E

**Physical Properties of
Ethyl Alcohol-Water System**

Values for the density, ρ , the viscosity, η , and the constant pressure heat capacity, C_p , for the system ethyl alcohol and water were taken from the International Critical Tables (I-2). Values of the temperature coefficient of expansion, $\beta_T = -\frac{\partial \rho}{\partial T}$, were obtained by determining the slopes of the above temperature-density data. The data presented by Franke (F3), Lemonde (L2), and Smith and Starrow (S3) were the sources of the diffusion coefficient values. Thermal conductivity values were obtained from data given by Bates, Hazzard, and Palmer (B3).

TABLE 7

PHYSICAL PROPERTIES OF ETHYL ALCOHOL-WATER SYSTEM

Comp.	\bar{T} Aver. Temp. Level	ρ Density	$\beta_T = -\frac{\partial \rho}{\partial T}$ $\beta_T \cdot 10^4$	$D \cdot 10^5$ Diff. Coef.	η Coef. of Visc.	k_t Thermal Cond.	C_p Heat Cap.
Weight Frac. EtOH	$^{\circ}\text{K}$	$\frac{\text{grams}}{\text{cm}^3}$	$\frac{\text{grams}}{\text{cm}^3 \cdot ^{\circ}\text{C}}$	$\frac{\text{cm}^2}{\text{sec}}$	centi- poise	$\frac{\text{BTU}}{\text{hr} \cdot \text{ft}^2 \cdot ^{\circ}\text{F}}$	$\frac{\text{BTU}}{\text{lb} \cdot ^{\circ}\text{F}}$
0.4000	322	0.9121	7.79	1.07	1.15	0.23	0.984
0.5095	322	0.8978	7.80	1.00	1.17	0.20	0.931

APPENDIX F

**Work of Treacy and Rich (T6) (T7)
with Horizontal Barriers**

216

Treacy (T6) and Treacy and Rich (T7) considered the use of horizontal barriers in a thermogravitational column for the separation of a binary gas mixture of nitrogen and methane. They used a concentric cylinder column with a wall spacing ($2\bar{w}$) of 1.94 cm. The barriers had inner and outer diameters such that the ratio of the barrier diameter to the wall spacing was 0.83. An optimum barrier spacing was found in that the separations increased, came to a maximum, and then decreased. Treacy and Rich attempted to explain this optimum spacing on the basis of a controlled turbulence concept. That is, as the distance between barriers was decreased, the turbulent remixing was reduced, but at the same time (for constant power input) the hot surface temperature was decreased because of the addition of conducting material. The reduction of turbulence increased the separation; the decreased temperature reduced the separation.

A similar optimum barrier spacing (or number of barriers) is predicted by Equation (III-54) in Chapter III. However, the optimum here is felt to be due to the combined effects of the reduced circulation which increases the separation, and the necessary effective length correction which tends to reduce the separation.

An attempt was made to find suitable values of b and l_r such that Equation (III-54) could be used to fit the data of Treacy (T6). It was found that a value of b of 0.12 and a value of l_r of 0.73

cm used in conjunction with Equation (III-54) gave a curve which was in good agreement with the data. (See Figure 55.) The value of b seems large perhaps, but it is within the range that might be expected.

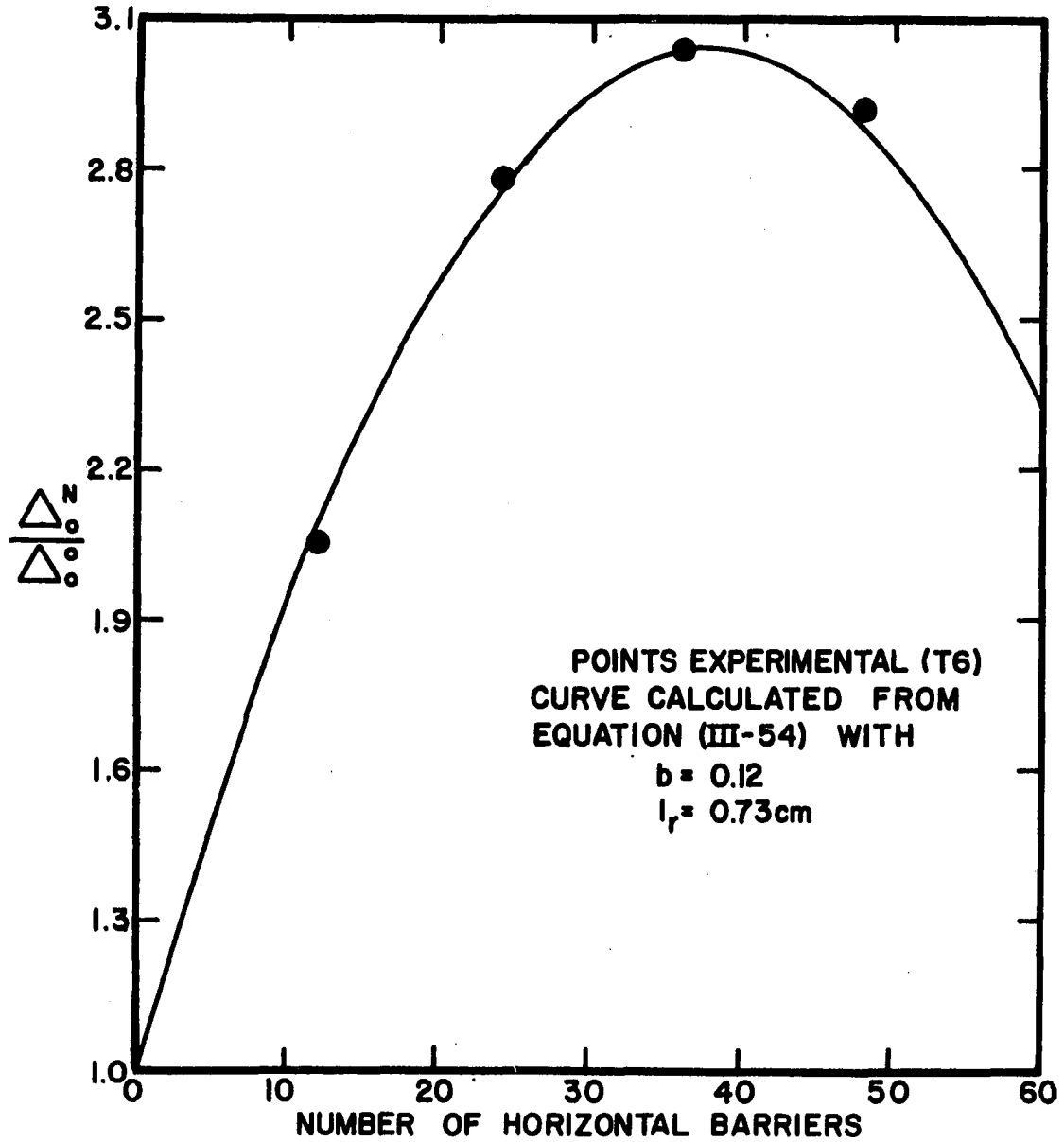
Treacy and Rich did encounter one curious fact: asbestos barriers constructed with the same dimensions as the metal barriers did not appreciably alter the separation ability of a column. A column with asbestos barriers gave essentially the same separation as a similar open column, regardless of the number of asbestos barriers used. Treacy and Rich were unable to explain this anomaly. This author as well was unsuccessful in obtaining an explanation, for Equation (III-54) is in no manner dependent on the barrier material. Asbestos barriers should alter only the magnitude of the length correction term, and it is difficult to conceive of a suitable explanation based solely on this factor.

Treacy presented transient data for one run with thirty-six horizontal barriers. However, quantitative comparison of the data with the theory of Chapter III is precluded since, with but one set of data, a value of σ_c can be found such that a fit is assured. It can be said, however, that the data are at least in qualitative agreement; that is, the time to reach the steady-state separation was increased by the addition of horizontal barriers.

One rate-separation curve was also presented for thirty-six horizontal barriers. Treacy's reported data for this case are

Figure 55

Data of Treacy and Rich (T6) Compared with
Equation (III-54)



surprising because the separations with barriers at all flow rates were equal to or greater than the separation in the open column at the same bulk flow rate. This is in direct conflict with the results obtained in this work, and hence cannot be explained, even qualitatively, from a theoretical standpoint. Several experimental techniques (sampling procedure and flow rate measurements) used by Treacy introduced experimental errors. These errors could be used as a possible basis for explanation of the above discrepancy, but the author feels that insufficient data were obtained to justify such an attempted explanation.

APPENDIX G

Summary of Equations Used to Calculate Predicted
Transient Curves for Work with Barriers

The following equations were the actual equations used to calculate the predicted transient curves for the work with horizontal barriers.

Two Barriers (special case):

$$\frac{\Delta}{\Delta N=2} = \left(\frac{1+a}{2}\right) + \left(\frac{1+2a}{4}\right) e^{-Rt} \quad (\text{G-1})$$

where a is given by Equation (III-65) with $L = 72.5$ cm, $\mu = 0.665$, and $K = 0.0102 (\Delta T)^2$.

Four Barriers:

$$\frac{\Delta}{\Delta N=4} = 0.20 + 0.80 (1 - .947e^{-0.382Rt} - .053e^{-2.618Rt}) \quad (\text{G-2})$$

Eight Barriers:

$$\frac{\Delta}{\Delta N=8} = \frac{1}{9} + \frac{8}{9} (1 - .893e^{-0.121Rt} - .085e^{-Rt}) \quad (\text{G-3})$$

Sixteen Barriers:

$$\frac{\Delta}{\Delta N=16} = \frac{1}{17} + \frac{16}{17} (1 - .96e^{-0.034Rt} - .02e^{-0.265Rt}) \quad (\text{G-4})$$

As mentioned earlier, only the roots that contributed enough to be detected on a figure were used. This is the reason that the equations for $N = 8$ and $N = 16$ do not show more terms.

APPENDIX H

Sample Calculations

Transient Behavior of a Column with Four
Equally-Spaced Horizontal Barriers

It was found in Chapter III that the transient behavior of a column with N equally-spaced horizontal barriers can be predicted by solving a system of first-order differential equations: one equation of the type

$$C_{n+1}(s) = \frac{R}{s+R} \left[C_n(s) + \frac{\Delta_{\infty}^N (s+2R)}{2Rs(N+1)} \right] + \frac{C_F}{s+R} \quad (\text{III-76})$$

$\frac{(N-2)}{2}$ equations of the type

$$C_n(s) = \frac{R}{s+2R} \left[C_{n+1}(s) + C_{n-1}(s) + \frac{\Delta_{\infty}^N}{2R(N+1)} \right] + \frac{C_F}{s+2R} \quad (\text{III-75})$$

and one equation of the type

$$C_1(s) = \frac{C_F}{s} + \frac{\Delta_{\infty}^N}{2s(N+1)} \quad (\text{III-77})$$

Now for $N = 4$, the system of equations is

$$C_3(s) = \frac{R}{s+R} \left[C_2(s) + \frac{\Delta_{\infty}^4 (s+2R)}{10Rs} \right] + \frac{C_F}{s+R} \quad (\text{H-1})$$

$$C_2(s) = \frac{R}{s+2R} \left[C_3(s) + C_1(s) + \frac{\Delta_{\infty}^4}{10R} \right] + \frac{C_F}{s+2R} \quad (\text{H-2})$$

$$C_1(s) = \frac{C_F}{s} + \frac{\Delta_{\infty}^4}{10s} \quad (\text{H-3})$$

Solving Equations (H-1) through (H-3) simultaneously yields

$$\left[C_3(s) - \frac{C_F}{s} \right] = \frac{\Delta_{\infty}^N}{10s} \frac{(s^2 + 5Rs + 5R^2)}{(s^2 + 3Rs + R^2)} \quad (\text{H-4})$$

The problem now is one of finding the inverse transform of Equation (H-4). By factoring the denominator, the inverse transform can be obtained with the aid of partial fractions:

$$\begin{aligned} \left[C_3(s) - \frac{C_F}{s} \right] &= \frac{\Delta_{\infty}^N}{10s} \frac{(s^2 + 5Rs + 5R^2)}{(s + 0.382R)(s + 2.618R)} \\ &= \frac{A}{s} + \frac{B}{s + 0.382R} + \frac{C}{s + 2.618R} \end{aligned} \quad (\text{H-5})$$

Evaluating the coefficients, A, B, and C yields

$$\left[C_3(s) - \frac{C_F}{s} \right] = \frac{\Delta_{\infty}^N}{10} \left(\frac{5}{s} - \frac{3.789}{s + 0.382R} - \frac{0.211}{s + 2.618R} \right) \quad (\text{H-6})$$

The inverse transform of Equation (H-6) is obtained easily and gives

$$\begin{aligned} (C_3 - C_F) &= \frac{\Delta_{\infty}^N}{10} (5 - 3.789e^{-0.382Rt} - 0.211e^{-2.618Rt}) \\ (C_3 - C_F) &= \frac{\Delta_{\infty}^N}{2} (1 - 0.758e^{-0.382Rt} - 0.042e^{-2.618Rt}) \end{aligned} \quad (\text{H-7})$$

$$\text{Now } R = \frac{\sigma c}{\rho v}$$

$$R = 0.070 \frac{\text{gm}}{\text{min}} \times \frac{\text{cm}^3}{0.912 \text{ gm}} \times \frac{1}{(0.0790 \text{ cm})(9.21 \text{ cm}) \frac{(145 \text{ cm})}{5}}$$

$$R = 0.00364 \text{ min}^{-1}$$

Finally, since $(C_3 - C_F) = \frac{\Delta}{2}$ (equal separation for enriching and stripping portions of the column)

$$\frac{\Delta}{2} = \frac{\Delta_{\infty}^N}{2} (1 - 0.758 e^{-.00138t} - 0.042 e^{-.0095t}) \quad (\text{H-8})$$

Rewriting Equation (H-8) yields

$$\frac{\Delta}{\Delta_{\infty}^N} = 0.20 + (0.80 - 0.758 e^{-.00138t} - 0.042 e^{-.0095t}) \quad (\text{H-9})$$

and finally

$$\frac{\Delta}{\Delta_{\infty}^N} = 0.20 + 0.80(1 - 0.947 e^{-.00138t} - 0.053 e^{-.0095t}) \quad (\text{H-10})$$

where

Δ is the total separation $(C_e - C_s)$ at time t , and

Δ_{∞}^N is the steady-state separation at infinite time with N barriers.

Equation (H-10) is shown plotted in Figure 25.

For the transient curve at the lower temperature difference, Equations (III-117) and (III-121) are utilized to calculate a new σ_c . A new R is then obtained and substituted in Equation (H-7). For four barriers at the lower temperature difference:

$$\sigma_c = 0.035 \frac{\text{gram}}{\text{min}}$$

$$R = 0.00185 \text{ min}^{-1}$$

and finally

$$\frac{\Delta}{\Delta_\infty} = 0.20 + 0.80 (1 - 0.947 e^{-.000705t} - 0.053 e^{-.0048t}) \quad (\text{H-11})$$

If an odd number of barriers is used, then the system of equations to be solved is given by $\frac{(N-1)}{2}$ equations of the type given by Equation (III-75), and one equation of the type given by (III-76). For $N = 3$:

$$C_2(s) = \frac{R}{s+R} \left[C_1(s) + \frac{\Delta_\infty^N (s+2R)}{8Rs} \right] + \frac{C_F}{s+R} \quad (\text{H-12})$$

$$C_1(s) = \frac{R}{s+2R} \left[C_2(s) + \frac{C_F}{s} + \frac{\Delta_\infty^N}{8R} \right] + \frac{C_F}{s+2R} \quad (\text{H-13})$$

and the solved system yields

$$\frac{\Delta}{\Delta_\infty} = 0.25 + 0.75 (1 - .873e^{-0.382Rt} - .127e^{-2.618Rt}) \quad (\text{H-14})$$

Determination of Thermal Diffusion Coefficient, α

Thermal diffusion coefficients are generally determined from static cell measurements, but Powers (P6) has developed a method for determining the thermal diffusion coefficient from data obtained in continuous flow thermogravitational columns.

The partial differential equation describing the behavior of the continuous flow thermogravitational column was derived

earlier, and the result was Equation (III-92):

$$\Delta = \frac{H}{2\sigma} \left(1 - e^{-\frac{\sigma L}{2K}} \right) \quad (\text{III-92})$$

where H and K are constants depending on column and system parameters. These constants can be evaluated using Equations (III-34) and (III-35) for the open column.

Powers (P3) has shown that the theory is not quantitative, but that the actual column performance can be reported by an equation similar to Equation (III-92) but with the constants H and K determined empirically:

$$\Delta = \frac{H_{\text{expt}}}{2\sigma} \left(1 - e^{-\frac{\sigma L}{2K_{\text{expt}}}} \right) \quad (\text{H-15})$$

As before, the limit as the flow rate approaches zero, $\sigma \rightarrow 0$, is

$$\Delta_0 = \frac{H_{\text{expt}} L}{4K_{\text{expt}}} \quad (\text{H-16})$$

Dividing Equation (H-15) by Equation (H-16) yields

$$\frac{\Delta}{\Delta_0} = \frac{2 K_{\text{expt}}}{\sigma L} \left(1 - e^{-\frac{\sigma L}{2K_{\text{expt}}}} \right) \quad (\text{H-17})$$

Defining

$$Z = \frac{\sigma L}{2 K_{\text{expt}}} \quad (\text{H-18})$$

Equation (H-17) becomes

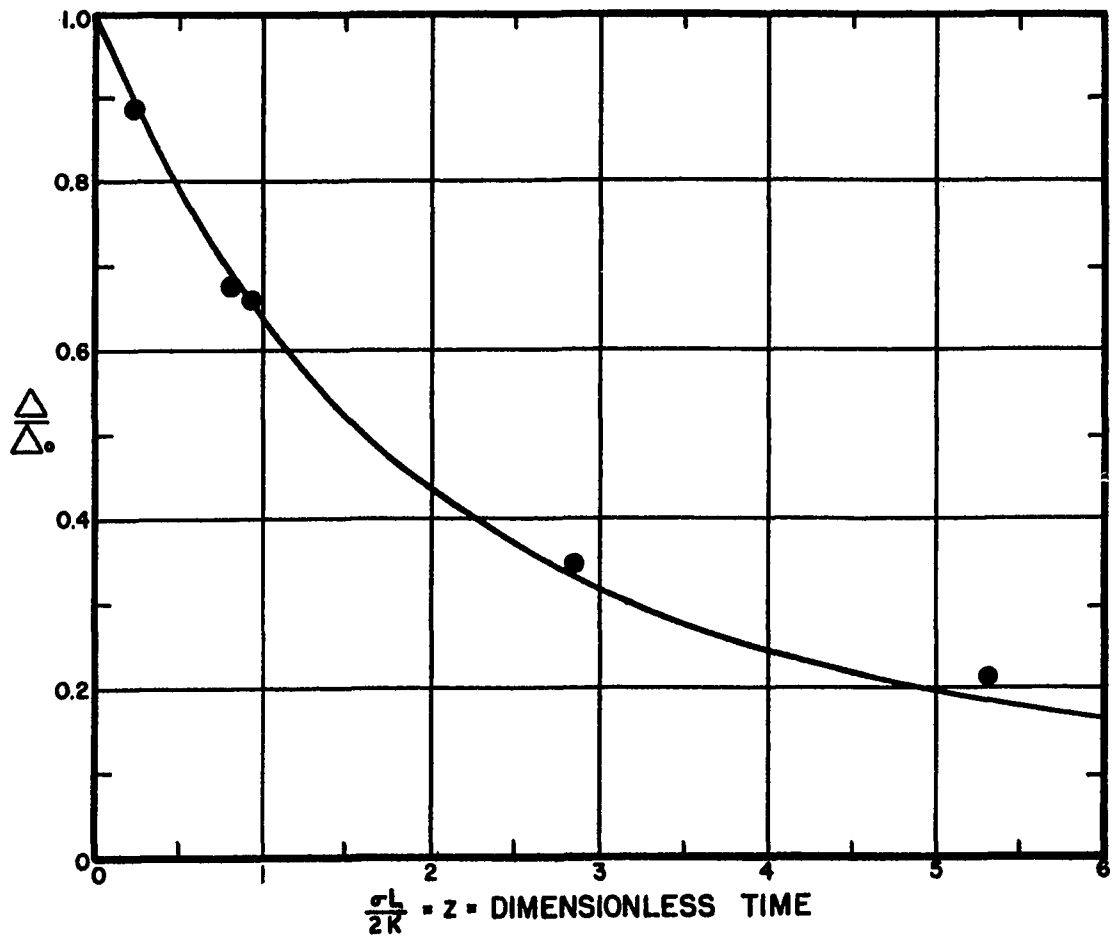
$$\frac{\Delta}{\Delta_0} = \frac{1}{Z} \left(1 - e^{-Z} \right) \quad (\text{H-19})$$

Equation (H-19) is shown plotted in Figure 56.

Now for any rate-separation curve, the only unknown in Equations (H-17) or (H-19) is K_{expt} (assuming that a point has been taken under batch conditions). Therefore, if a set of experimental data is fitted to the curve given by Equation (H-19), the best fit yields

Figure 56

Separation, Δ/Δ_0 , As a Function of Dimensionless Flow, Z



the experimental value of K_{expt} (and also Δ_0). Thus, H_{expt} can be calculated from Equation (H-16) knowing K_{expt} and Δ_0 .

Since the thermal diffusion coefficient appears only in the expression for H given by Equation (III-34), a relation must be obtained between H and H_{expt} . Powers (P3) has defined the correction factors

$$\phi_H = \frac{H_{\text{expt}}}{H} \quad (\text{H-20})$$

$$\phi_K = \frac{K_{\text{expt}}}{K} \quad (\text{H-21})$$

where ϕ_H and ϕ_K are related exponentially by

$$\phi_H = \phi_K^{0.8} \quad (\text{H-22})$$

A value for K can be obtained from Equations (III-18), (III-35), and (III-36) since every term is known. Hence, a value for ϕ_K can be obtained since a K_{expt} is obtained from the best fit of the data to the curve given by Equation (H-19). Finally, a value for ϕ_H is obtained from Equation (H-22) which relates ϕ_K to ϕ_H ; a value for H is then easily calculated from Equation (H-20). Using H and Equation (III-34), a value for the thermal diffusion coefficient, α , is then obtained. A sample calculation follows for experimental set A.

Experimental Set A

Parameter Values:

$$B = 10.16 \text{ cm}$$

$$C_F = .5095 \text{ wt. frac. EtOH}$$

$$\beta_T = 7.80 \times 10^{-4} \text{ gm}/^\circ\text{C-cm}^3$$

$$\eta = 0.0117 \text{ gm/cm-sec}$$

$$\begin{aligned}
 D &= 1.0 \times 10^{-5} \text{ cm}^2/\text{sec} & \rho &= 0.8978 \text{ gm/cm}^3 \\
 g &= 980 \text{ cm/sec}^2 & 2\omega &= 0.0792 \text{ cm} \\
 L &= 145 \text{ cm} \\
 T &= 322^\circ\text{K} \\
 \Delta T &= 27.9^\circ\text{C}
 \end{aligned}$$

In this set, a batch run was taken to obtain a value for Δ_0 .

$$\Delta_0 = .2190 \text{ wt. frac. EtOH (Run 1A)}$$

Run	Δ	σ	$\frac{\Delta}{\Delta_0}$	$Z_{\text{expt.}}$	$K_{\text{expt.}}$
	Weight Frac. EtOH	<u>grams</u> min			<u>gram-cm</u> min
2A	.1935	0.0230	.883	0.24	7.00
3A	.1473	0.0841	.673	0.87	7.00
5A	.1448	0.0966	.661	0.92	7.62
7A	.0764	0.298	.349	2.68	8.06
8A	.0467	0.560	.213	4.6	8.83
9A	.0173	1.25	.079	12.6	7.18

The average $K_{\text{expt.}}$ is 7.62 gram-cm/min. Using this value of $K_{\text{expt.}}$, a Z_{calc} can be calculated using Equation (H-18) and plotted on Figure 56 to see how well it fits the curve. The value of Δ_0 can be adjusted for a better fit if desired. Using the above average value for $K_{\text{expt.}}$

$\frac{\Delta}{\Delta_0}$	$Z_{\text{calc}} = \frac{\sigma L}{2 (K_{\text{expt.}})_{\text{avg}}}$
.883	0.218
.673	0.80
.661	0.92
.349	2.83
.213	5.32
.079	11.9

The above values of Δ/Δ_0 and Z are plotted in Figure 56; the fit seems satisfactory. Using Equation (H-16) to find H_{expt} :

$$\begin{aligned}\Delta_0 &= \frac{H_{\text{expt}} L}{4 K_{\text{expt}}} \\ H_{\text{expt}} &= \frac{4 \Delta_0 K_{\text{expt}}}{L} \\ &= \frac{4(.2190)(7.62)}{145} \\ &= .0462 \frac{\text{gram}}{\text{min}}\end{aligned}$$

Now calculate K using Equations (III-18), (III-35), and (III-36):

$$K = K_c + K_d \quad \text{(III-18)}$$

$$K_d = 2\omega\rho B D \quad \text{(III-36)}$$

$$K_d = (.0792 \text{ cm})(.8978 \frac{\text{gm}}{\text{cm}^3})(10.16 \text{ cm})(1.0 \times 10^{-5} \frac{\text{cm}^2}{\text{sec}})(60 \frac{\text{sec}}{\text{min}})$$

$$K_d = .00043 \frac{\text{gram-cm}}{\text{min}}$$

$$K_c = \frac{\beta T^2 \rho g^2 (2\omega)^7 B (\Delta T)^2}{9! D \eta^2}$$

$$= \frac{(7.8 \times 10^{-4} \frac{\text{gm}}{\text{cm}^3 \cdot ^\circ\text{C}})^2 (.8978 \frac{\text{gm}}{\text{cm}^3})(980 \frac{\text{cm}}{\text{sec}^2})^2}{9! (1.0 \times 10^{-5} \frac{\text{cm}^2}{\text{sec}})(1.17 \times 10^{-2} \frac{\text{gm}}{\text{cm-sec}})^2}$$

$$\times (.0792 \text{ cm})^7 (10.16 \text{ cm})(27.9^\circ\text{C})^2$$

$$K_c = 0.14 \frac{\text{gm-cm}}{\text{sec}}$$

$$K_c = 8.4 \frac{\text{gm-cm}}{\text{min}}$$

$$K \approx K_c \quad (K_d \ll K_c)$$

$$\phi_K = \frac{K_{\text{expt}}}{K} = \frac{7.62}{8.4} = 0.910$$

$$\phi_H = \phi_K^{0.8} = (0.910)^{0.8} = 0.928$$

$$\phi_H = \frac{H_{\text{expt}}}{H} = 0.928$$

$$H = \frac{0.0462}{0.928} = 0.0498 \frac{\text{gram}}{\text{min}}$$

$$= 0.00083 \frac{\text{gram}}{\text{sec}}$$

Finally, from Equation (III-34), the thermal diffusion coefficient is

$$\alpha = \frac{H \beta_T \rho g \eta \bar{T}}{(2\omega)^3 B (\Delta T)^2}$$

$$\alpha = \frac{(0.00083 \frac{\text{gm}}{\text{sec}})(720)(1.17 \times 10^{-2} \frac{\text{gm}}{\text{cm-sec}})(322^\circ \text{K})}{(7.8 \times 10^{-4} \frac{\text{gm}}{\text{cm}^3 \text{C}})(0.8978 \frac{\text{gm}}{\text{cm}^3})(980 \frac{\text{cm}}{\text{sec}^2})}$$

$$\times \frac{1}{(0.0792 \text{ cm})^3 (10.16 \text{ cm})(27.9^\circ \text{C})^2}$$

$$\alpha = 0.83$$

Unequal Overhead and Bottom Product Flow Rates

The following calculations were made for experimental set B, Runs 10-18:

Parameter Values:

$$\begin{aligned}
 B &= 10.16 \text{ cm} \\
 C_F &= .5070 \text{ wt. frac. EtOH} \\
 D &= 1.0 \times 10^{-5} \text{ cm}^2/\text{sec} \\
 g &= 980 \text{ cm}/\text{sec}^2 \\
 \bar{L}_f &= 145 \text{ cm} \\
 T &= 322^\circ\text{K} \\
 \Delta T &= 27.7^\circ\text{C}
 \end{aligned}$$

$$\begin{aligned}
 \beta_T &= 7.80 \times 10^{-4} \text{ gm}/^\circ\text{C-cm}^3 \\
 \eta &= 0.0117 \text{ gm}/\text{cm-sec} \\
 \rho &= 0.8978 \text{ gm}/\text{cm}^3 \\
 2\omega &= 0.0795 \text{ cm}
 \end{aligned}$$

Run	σ_e	σ_s	$\bar{\sigma}$	C_e	C_s	Δ	X
	<u>grams</u> min	<u>grams</u> min	<u>grams</u> min	Weight Frac. EtOH	Weight Frac. EtOH	Weight Frac. EtOH	
10B	0.0000	0.1678	0.0839	.6472	.4725	.1747	0.0
11 B	0.1870	0.0000	0.0935	.5250	.4065	.1185	∞
12B	0.0287	0.1648	0.0967	.6357	.4706	.1651	0.175
13B	0.1458	0.0306	0.0888	.5410	.4127	.1284	4.76
14B	0.1800	0.0135	0.0973	.5164	.3924	.1240	13.33
15B	0.0000	0.1848	0.0915	.6492	.4766	.1726	0.0
16B	0.0514	0.1440	0.0977	.6280	.4660	.1620	0.35
17B	0.1260	0.0666	0.0963	.5515	.4231	.1284	1.89
18B	0.1864	0.0000	0.0932	.5127	.3856	.1271	∞

The average flow rate, $\bar{\sigma}$, for the above nine runs is .0933 gram/min, and the K for these column conditions is 7.62 gram-cm/min from the previous part of these Sample Calculations.

Now from Equation (H-18)

$$\begin{aligned}
 Z &= \frac{\bar{\sigma} L}{2K_{\text{expt}}} \\
 &= \frac{(.0933 \frac{\text{gm}}{\text{min}}) (145 \text{ cm})}{2 (7.62 \frac{\text{gm-cm}}{\text{min}})} \\
 &= 0.887 \text{ (dimensionless)}
 \end{aligned}$$

Recall Equations (VII-2) and (VII-3) and Equations (VII-8) and (VII-9):

$$\frac{\Delta}{\Delta_0} = \frac{1+X}{4Z} \left[\left(\frac{1}{X} \right) (1 - e^{-\frac{2XZ}{1+X}}) + (1 - e^{-\frac{2Z}{1+X}}) \right] \quad (\text{VII-2})$$

$$\frac{\Delta}{\Delta_0} = 0.50 + \frac{1}{4Z} (1 - e^{-2Z}) \quad (X = 0) \quad (\text{VII-8})$$

$$\frac{\Delta}{\Delta_0} = \frac{(1+X)^2}{4XZ} \left[1 - e^{-\frac{4XZ}{(1+X)^2}} \right] \quad (\text{VII-3})$$

$$\frac{\Delta}{\Delta_0} = 1.0 \quad (\text{VII-9})$$

Since a value for Z is known, curves of Δ/Δ_0 versus X can be calculated by use of the above four equations, Equations (VII-2) and (VII-8) from conventional column theory, and Equations (VII-3) and (VII-9) from Powers' modification. The curves would be symmetrical about the point $X = 1.0$ except that the thermal diffusion coefficient, α , is a function of the average concentration in the column. Therefore, this variation in α with concentration must be taken into account. From Equations (VII-4) and (VII-7) it is known that

$$X = \frac{\sigma_e}{\sigma_s} \quad \text{and} \quad \sigma = \frac{\sigma_e + \sigma_s}{2}$$

so that

$$2\sigma = \sigma_s \left(\frac{\sigma_e}{\sigma_s} + 1 \right) = \sigma_s (X + 1)$$

$$\sigma_s = \frac{2 \sigma}{1 + X} \quad (\text{H-23})$$

and

$$\sigma_e = X \sigma_s = \frac{2 \sigma X}{1 + X} \quad (\text{H-24})$$

A material balance around the column gives

$$\sigma_e C_e + \sigma_s C_s = (\sigma_e + \sigma_s) C_F \quad (\text{H-25})$$

Substituting for C_e , where $C_e = \Delta + C_s$, yields

$$\sigma_e (\Delta + C_s) + \sigma_s C_s = (\sigma_e + \sigma_s) C_F \quad (\text{H-26})$$

$$C_s = \frac{C_F}{X} - \frac{\Delta \sigma_e}{2 \sigma} \quad (\text{H-27})$$

Now for a given X and Z , one can calculate values of $\frac{\Delta}{\Delta_0}$ from Equations (VII-2), (VII-3), (VII-8), and (VII-9). For example, for $X = 0$, $Z = 0.887$, Equation (VII-8) gives

$$\begin{aligned} \frac{\Delta}{\Delta_0} &= 0.50 + \frac{1}{4Z} (1 - e^{-2Z}) \\ &= 0.50 + (.282)(.831) \\ &= 0.734 \end{aligned}$$

Since Δ_0 is known, a value of Δ/Δ_0 yields in turn a value for Δ ,

$$\Delta = (0.734)(.2190)$$

$$\Delta = .1607 \text{ wt. frac. EtOH}$$

Then σ_e and σ_s can be obtained from Equations (H-23) and (H-24):

$$\sigma_s = \frac{2 \sigma}{1 + X} = \frac{2(.0933)}{1 + 0}$$

$$\sigma_s = .1866 \frac{\text{gram}}{\text{min}}$$

$$\sigma_s = X \sigma_s = 0$$

Finally, since C_F is known, C_s can be calculated from Equation (H-27) and then C_e follows since Δ is known

$$C_s = \bar{C}_F - \frac{\Delta \sigma_e}{2\sigma}$$

$$C_s = \bar{C}_F = .5070 \text{ wt. frac. EtOH}$$

$$\begin{aligned} C_e &= \Delta + C_s = .1607 + .5070 \\ &= .6677 \text{ wt. frac. EtOH} \end{aligned}$$

The average column concentration then is simply

$$\bar{C} = \frac{C_e + C_s}{2}$$

(H-28)

$$\bar{C} = \frac{.6677 + .5070}{2}$$

$$\bar{C} = .5874 \text{ wt. frac. EtOH}$$

and a value for α can be obtained from Figure 49. Now from Figure 49, α is found to be

$$\alpha = .825$$

For the entire set of B runs, the average feed concentration is

$$\bar{C}_F = .5070 \text{ wt. frac. EtOH}$$

and

$$\alpha = .792$$

Since the separation, Δ , is proportional to α , the ratio of the separations, Δ/Δ_0 , can be corrected for different values of α by multiplying the ratio by the α at the average concentration found above, and then dividing by the α obtained for the average feed concentration for the entire experimental set. Therefore, the ratio of the separations can be corrected for the variation in α :

$$\left(\frac{\Delta}{\Delta_0} \right)_{\text{corrected}} = 0.734 \left(\frac{.825}{.792} \right) = 0.762$$

The above corrected value is then plotted as one point (at $X = 0$) on the curve for conventional theory for a Z-value of 0.887. The remaining points are calculated from Equation (VII-2), except for $X = \infty$ which is calculated in the same manner as the above point.

A similar procedure is followed for Powers' modification using Equations (VII-3) and (VII-9).

APPENDIX I

Nomenclature

NOMENCLATURE

- a** = general constant
- b** = empirical constant; also a subscript to identify streams leaving the bottom of a column
- B** = column width
- c** = general constant
- C** = constant dependent on the relative ratio of the barrier diameter to the plate spacing
- C_p** = heat capacity at constant pressure
- C₁** = concentration of component 1
- C₂** = concentration of component 2
- C_e** = concentration of component 1 leaving the enriching section
- C_s** = concentration of component 1 leaving the stripping section
- C_F** = concentration of component 1 in the feed
- d** = barrier diameter
- D** = diffusion coefficient
- e** = subscript to identify variables in the enriching section ($y > 0$)
- F_D** = drag force by a single barrier
- g** = local acceleration of gravity
- g_c** = dimensional constant
- H** = constant defined by Equation (III-15)
- H^N** = constant given by Equation (III-45)

K = constant defined by Equation (III-18)

K_C = constant defined by Equation (III-16)

K_C^N = constant given by Equation (III-46)

K_d = constant defined by Equation (III-17)

K_p = empirical constant added to mathematical development to account for effects of parasitic remixing

k_t = thermal conductivity

l_r = length of disturbance created by a single horizontal barrier

L = total column length ($L = L_e + L_s$)

L_e = length of enriching section

L_s = length of stripping section

n = index number

N = number of horizontal barriers

o = subscript to identify streams leaving the top of a column

P = pressure; also dimensionless flow term defined by Equation (III-66)

$R = Q_c / \rho V$

s = subscript to identify variables in the stripping section ($y < 0$); also Laplace transform variable

t = time

T_H, T_C = temperature of hot and cold plates, respectively

\bar{T} = mean operating temperature

ΔT = mean temperature difference between hot and cold plates

u = bulk stream velocity

$v(x)$ = general velocity distribution function

\bar{v} = average velocity given by Equation (III-119)

x = axis normal to plates

y = axis parallel to plates in the direction of convective circulation

X = dimensionless flow defined by Equation (VII-4)

Z = dimensionless quantity defined by Equation (VII-5)

α = thermal diffusion coefficient

β_T = change in density with temperature

δ = plate spacing measurement

Δ = separation (enriching minus stripping composition)

Δ_e = separation in the enriching section of the column

Δ_s = separation in the stripping section of the column

Δ_B = separation in any column, n , defined by Equation (III-113)

Δ_L = separation in center column cut by x -axis, defined by Equation (III-114)

Δ_O^N = separation with no bulk flow and N barriers

Δ_∞ = steady-state separation (at infinite time)

ζ = dimensionless flow defined by Equation (III-112)

η = coefficient of viscosity

μ = solution per unit length of column

ξ = dimensionless time quantity defined by Equation (III-65)

ρ = density

σ = average mass flow rate

$$\bar{\sigma} = \frac{n}{\sum 1} \frac{\sigma}{n}$$

σ_c = mass flow past barriers brought about by convective circulation

σ_e = enriching section bulk flow rate

σ_F = feed bulk flow rate

σ_s = stripping section bulk flow rate

τ = amount of component one passing through a cross-section of the column normal to the plates

$\phi\left(\frac{L}{H}\right)$ = dimensionless shape ratio function

ϕ_H = correction factor defined by Equation (H-20)

ϕ_K = correction factor defined by Equation (H-21)

2ω = distance between the hot and cold plates

APPENDIX J

List of References

LIST OF REFERENCES

- A1. Abelson, P. H., Rosen, N., and Hoover, J. I., "Liquid Thermal Diffusion," TID5229 U. S. At. Energy Comm., (1958).
- A2. Alkhayov, D. G., Murin, and Ratner, A. P., Bull. Acad. Sci. U. R. S. S. Classe Sci. Chem. 1943, 3-7 (1943).
- A3. Arrhenius, S., Öfversigt Vetensk. -Akad. Förh 2, 61 (1894).
- A4. _____. Z. physik. Chem. 26, 187-8 (1898).
- B1. Bardeen, J. Phys. Rev. 57, 35-41 (1940).
- B2. _____. Phys. Rev. 58, 94-5 (1940).
- B3. Bates, O. K., Hazzard, G., and Palmer, G. Ind. Eng. Chem. (Anal. Ed.) 10, 314 (1938).
- B4. Beams, J. W., U. S. Patent 2,521,112. Sept. 5, 1950.
- B5. Becker, E. W., J. Chem. Phys. 19, 131-2 (1951).
- B6. Berchem, P. van Compt. rend. 110, 82 (1890).
- B7. Bowring, R. W. U. K. Atomic Energy Authority Report No. A. E. R. E. GP/R 2058 (1957).
- B8. Boyer, L. D. "An Experimental and Theoretical Investigation of Vertical Barriers in Liquid Thermal Diffusion Columns," University of Oklahoma Dissertation (Ph. D.), 1961.
- B9. Bramley, A., and Brewer, A. K. J. Chem. Phys. 7, 972 (1939).
- B10. _____. J. Chem. Phys. 7, 553-4 (1939).
- B11. _____. Science 90, 165-6 (1939).
- B12. Brewer, A. K., and Bramley, A. Phys. Rev. 55, 590 (1939).
- C1. Cabicar, J. and Zatka, V. Chem. Listy 48, 348-54 (1954).

- C2. Carr, H. E. Phys. Rev. 61, 726A (1942).
- C3. _____. J. Chem. Phys. 12, 349 (1944).
- C4. Chapman, S., Trans. Roy. Soc. (London) 216A, 279-348 (1916).
- C5. _____. Phil. Mag. 7, 1-16 (1929).
- C6. Chapman, and Dootson, F. W. Phil. Mag. 33, 248-53 (1917).
- C7. Chipman, J. J. Am. Chem. Soc. 48, 2577-89 (1926).
- C8. Clusius, K., and Dickel, G. Naturwissenschaften 26, 546 (1938).
- C9. _____. Naturwissenschaften 27, 148-9 (1939).
- C10. _____. Z. physik. Chem. B44, 397-450 (1939).
- C11. Corbett, J. W., and Watson, W. W. Phys. Rev. 101, 519-22 (1956).
- C12. Coulson, J. M., and Richardson, J. F. "Chemical Engineering," Pergamon Press, New York, 1954.
- C13. Crownover, C. F., and Powers, J. E. Paper presented at Tulsa, Oklahoma Meeting of A. I. Ch. E., September 1960.
- D1. Debye, P., Ann. Physik 36, 284-94 (1939).
- D2. Debye, P. J. W. U. S. Patent 2,567,765. Sept. 11, 1951.
- D3. _____. "The Collected Papers of Peter J. W. Debye," Interscience Publishers, Inc., New York, London, 1954.
- D4. Debye, P., and Bueche, A. M. "Thermal Diffusion of High Polymer Solutions," Robinson, H. A. "High-Polymer Physics," 497-527, Chem. Pub. Co., Brooklyn, 1948.
- D5. Docherty, C., and Ritchie, M. Proc. Roy. Soc. Edinburg 62A, 297-304 (1946-48).

- D6. Donaldson, J., and Watson, W. W. Phys. Rev. 82, 909-13 (1951).
- D7. Drickamer, H. G., Mellow, E. W., and Tung, L. H. J. Chem. Phys. 18, 945-9 (1950).
- D8. Dryden, H. L., Murnaghan, F. P., and Bateman, H. "Hydrodynamics," Dover Publications, Inc., New York, 1956.
- E1. Eilert, A. Z. anorg. Chem. 88, 1-37 (1914).
- E2. Emery, A. H., Jr. Ind. Eng. Chem. 51, 651-4 (1959).
- E3. Enskog, D. Physik. Zeits. 12, 56-60, 533-9 (1911); Upsala University Dissertation (Ph. D.), 1917.
- F1. Farber, M., and Libby, W. F. J. Chem. Phys. 8, 965-9 (1940).
- F2. Fleischmann, R., and Jensen, H. Ergeb. exakt. Naturwiss. 20, 121-81 (1942).
- F3. Franke, G. Ann. Physik 14, 675-82 (1932).
- F4. Frazier, D. U. S. Patent 2,743,014. April 24, 1956.
- F5. _____. U. S. Patent 2,827,171. March 18, 1958.
- F6. _____. Paper presented at New Orleans Meeting of A. I. Ch. E., February 1961.
- F7. Furry, W. H., Jones, R. C., and Onsager, L. Phys. Rev. 55, 1083-95 (1939).
- G1. Grasseli, R., Brown, G. R., and Plymale, C. E. Paper presented at Tulsa, Oklahoma Meeting of A. I. Ch. E., September 1960.
- G2. _____. Chem. Eng. Prog. 57, 59-64 (1961).
- G3. Grew, K. E., and Ibbs, T. L. "Thermal Diffusion in Gases," Cambridge University Press, Great Britain, 1952.
- G4. Grinten, W. van der. Naturwissenschaften 27, 317 (1939).
- G5. Groot, S. R. de. Physica 9, 801-16 (1942).
- G6. _____. "L'Effet Soret," Ph. D. Thesis, Amsterdam, 1945.

- G7. Groot, S. R. de, Gorter, D. J., and Hoogenstraaten, W. Physica, 10, 81-9 (1943).
- G8. Groth, W. Naturwissenschaften 27, 260-1 (1939).
- G9. Groth, W., and Harteck, P. Naturwissenschaften 27, 584 (1939).
- H1. Heines, T. S., Jr. "Operation of Continuous Thermal Diffusion Columns for Liquids," University of Michigan Thesis (Ph. D.), 1955.
- H2. Heines, T. S., Larson, O. A., and Martin, J. J. Ind. Eng. Chem. 49, 1911-20 (1957).
- H3. Henke, A. M., and Stauffer, H. C. U. S. Patent 2,936,887. May 17, 1960.
- H4. Hirota, K. and Kobayashi, Y. J. Chem. Phys. 21, 246-9 (1953).
- H5. _____. Bull. Chem. Soc. Japan 17, 42-4 (1942).
- H6. Hoff, J. H. van't. Z. phys. Chem. 1, 481-508 (1887).
- H7. Hoffman, D. T. "Thermal Diffusion in Liquids," Purdue University Thesis (Ph. D.), 1960.
- H8. Huntley, H. E. "Dimensional Analysis," Rinehart and Co., Inc., New York, 1951.
- II. Ibbs, T. L. Proc. Roy. Soc. (London) A99, 385-95 (1921).
- I2. International Critical Tables, McGraw-Hill Book Co., Inc., New York, 1928.
- J1. Jones, A. L., Pet. Proc. 6, 132-5 (1951).
- J2. _____. U. S. Patent 2,720,979. October 18, 1955.
- J3. _____. U. S. Patent 2,720,980. October 18, 1955.
- J4. _____. U. S. Patent 2,723,033. November 8, 1955.
- J5. _____. U. S. Patent 2,723,034. November 8, 1955.
- J6. _____. U. S. Patent 2,734,633. February 14, 1956.

- J7. Jones, A. L., and Foreman, R. W. Ind. Eng. Chem. 44, 2249-53 (1952).
- J8. Jones, R. C., and Furry, W. H. Rev. Mod. Phys. 18, 151-224 (1946).
- L1. Leeds and Northrup Co. "Standard Conversion Tables for Thermocouples," No. 077989, Issue 2, Philadelphia, Pa.
- L2. Lemonde, H. Compt. rend. 202, 468, 731, 1069 (1936).
- L3. Longmire, D. R. "Continuous Throughput Rectification of Organic Liquid Mixtures with Vertical Countercurrent Thermal Diffusion Columns," University of Wisconsin Thesis (Ph. D.), 1957.
- L4. Lorenz, M. G. "Thermal Diffusion in Packed Columns," Purdue University Thesis (Ph. D.), 1960.
- L5. Lorenz, M. G., and Emery, A. H. Chem. Eng. Sci. 11, 16 (1959).
- L6. Ludwig, C. Wien. Akad. Ber. 20, 539 (1856).
- M1. Milne-Thompson, L. M. "Theoretical Hydrodynamics," MacMillan and Co., Ltd., London, 1949.
- M2. Mulliken, R. S. J. Am. Chem. Soc. 44, 1033 (1927).
- N1. Nier, A. O. Phys. Rev. 56, 1009-13 (1939).
- N2. Niini, R. Suomen Kemistilehti 26B, 42-5 (1953).
- P1. Papayannopoulos, A. G., Colorado School of Mines Dissertation (M. S.), 1959.
- P2. Pierce, N. C., Duffield, R. B., and Drickamer, H. G. J. Chem. Phys. 18, 950-2 (1950).
- P3. Powers, J. E. UCRL-2168, University of California Radiation Laboratory, Berkeley, California (1954).
- P4. _____. Proceedings of the Joint Conference on Thermodynamics and Transport Properties of Fluids, published by the Institution of Mechanical Engineers, London, July 1957.
- P5. _____. Ind. Eng. Chem. 53, No. 7 (1961).

- P6. Powers, J. E. Personal Communication.
- P7. Powers, J. E., and Wilke, C. R. J. Chem. Phys. 27, 1000-1 (1957).
- P8. _____. A.I. Ch. E. Journal 3, 213-22 (1957).
- P9. Prigogine, I., and Buess, R. Physica 15, 465-6 (1949).
- R1. Ramser, J. H. Ind. Eng. Chem. 49, 155-8 (1957).
- R2. Rutherford, W. M., and Drickamer, H. G. J. Chem. Phys. 22, 1157-65 (1954).
- S1. Saxena, S. C., and Watson, W. W. Physics of Fluids 3, No. 1, 105 (Jan.-Feb. 1960).
- S2. Simon, R. Phys. Rev. 69, 596-603 (1946).
- S3. Smith, I. E., and Starrow, J. A. J. Applied Chem. (London) 2, 225-35 (1952).
- S4. Soret, C. Arch. Sci. phys. nat. (Geneva) 2, 48 (1879).
- S5. _____. Compt. rend. 91, 289 (1880).
- S6. _____. Arch. Sci. phys. nat. (Geneva) 4, 209 (1880).
- S7. _____. Ann. chim. phys. (5) 22, 293 (1881).
- S8. Sullivan, L. J., Ruppel, T. C., and Willingham, C. B. Ind. Eng. Chem. 47, 208-12 (1955).
- S9. _____. Ind. Eng. Chem. 49, 110-13 (1957).
- T1. Tanner, C. C. Trans. Faraday Soc. 23, 75-95 (1927).
- T2. Taylor, T. I., and Glockler, G. J. Chem. Phys. 7, 851-2 (1939).
- T3. Thomaes, G. J. chim. phys. 53, 407-11 (1956).
- T4. _____. J. Chem. Phys. 25, 32-3 (1956).
- T5. Tilvis, E. Soc. Sci. Fennica Commentationes Phys. - Math. 13, 1-59 (1947).

- T6. Treacy, J. C. University of Notre Dame Dissertation (M. S.) 1948.
- T7. Treacy, J. C., and Rich, R. E. Ind. Eng. Chem. 47, 1544-7 (1955).
- V1. Velden, P. F. van, Voort, H. G. P. van der, and Gorter, C. J. Physica 12, 151-62 (1946).
- V2. Vichare, G. G. University of Oklahoma Thesis (M. Ch. E.), 1961.
- V3. Von Halle, E. U. S. At. Energy, K-1420 (1959).
- W1. Waldmann, L. Naturwissenschaften 27, 230-1 (1939).
- W2. _____. Z. Physik 114, 53-81 (1939).
- W3. Watson, W. W. Phys. Rev. 56, 703 (1939).
- W4. Wereide, T. Ann. phys. 2, 55-66 (1914).
- W5. Whalley, E., and Winter, E. R. S. Trans. Faraday Soc. 45, 1091-97 (1949).